THE INFLUENCE OF PLAN GEOMETRY AND STRUCTURAL SYSTEM ON THE BEHAVIOR OF HIGH-RISE BUILDINGS

By
Muhannad Yacoub Fakhouri

Supervisor
Dr. Raed M. Samra, Prof.

This thesis was submitted in partial fulfillment of the requirements for the Master's Degree of Science in Civil Engineering

Faculty of Graduate Studies
The University of Jordan

February, 2008

This thesis (The Influence of Plan Geometry and Structural System on the Behavior of High-Rise Buildings) was successfully defended and approved on 21-2-2008

Examination Committee	**Signature**
Dr. Raed M. Samra, Chairman Dean and Professor of Civil Engineering	
Dr. Bassam Abu-Ghazaleh, Member Prof. of Civil Engineering	
Dr. Hanan Al-Nimry, Member Assist. Prof. of Civil Engineering	Feb. 25, 2008
Dr. Yahia, A. Abdel-jawad, Member Prof. of Civil Engineering (Jordan University of Science and Technology)	

تعتمد كلية الدراسات العليا
هذه النسخة من الرسالة
التوقيع.....التاريخ.....

DEDICATION

To my family who was a big asset to my achievement by creating the most supporting atmosphere.

To all who participated in creating within me the desire to pursue my dreams setting the stage for my future to reap the fruits of continuous efforts and realize the potential for success, which I pray is forthcoming.

I love you all!

Muhannad Fakhoury
Feb. 2008

ACKNOWLEDGEMENT

I would like to thank first of all almighty God for the strength he empowered me with, to be where I am today. Without God's providence and guidance, this study would have never been achieved in due time.

Sincere thanks and appreciation are also extended to my supervisor, Prof. Raed M. Samra, for his patience and streaming support in carrying out this study, taking to heart the responsibility of keeping the flow of research and presentation, avoiding obscurity and strengthening consistency in the best way possible.

Eventually, I would like to give thanks to the one who supported the modeling process, engineer Median Taha.

Table of Contents

2. CONFIGURATION CHARACTERISTICS AND PLAN IRREGULARITY

3. CASE STUDIES OF HIGH-RISE BUILDINGS AND MODELING PROCEDURES

List of Tables

List of Figures

Page

List of Photos

Notations

A	Cross-sectional area of element.
$C.M.$	Center of mass.
$C.R.$	Center of Rigidity
C_s	Seismic response coefficient.
C_T	Building period coefficient taken 0.073 for frames system, 0.049 for shear wall system and dual system.
CQC	Complete quadratic combinations.
DS	Dual system, shear wall-frame ordinary interactive systems.
E	Modulus of elasticity.
EI	Flexural rigidity.
ESD	Elastic strength demand.
$f_c^{'}$	Compressive strength of concrete.
F	Ordinary reinforced concrete moment frames.
F_y	Maximum force at yield level.
F_v and F_a	Seismic site coefficients.
F_e	Maximum elastic force.
F_M	Maximum force at demand level.
F_t	Additional lateral force applied to the top level of a structure according to the UBC 1997 to account for higher modes.
G	Shear modulus.
GA	Racking rigidity.
H	height of shear wall
h_n	Total height of the building.
I_E	Occupancy importance factor.
K_X	Building Stiffness in X-direction.

K_Y	Building Stiffness in Y-direction.
L	Length of element.
M_Y	Story moment around Y-direction.
M_X	Story moment around X-direction.
R	Response modification or force reduction.
S_1 *and* S_s	Mapped spectral acceleration for 1-sec. and short period, respectively.
S_{D1} *and* S_{DS}	Design spectral acceleration for 1-sec. and short period, respectively.
S_{M1} *and* S_{MS}	Maximum considered earthquake spectral acceleration for 1-sec. and short period, respectively.
SRSS	Square Root of Sum of Squares.
SW	Ordinary concrete shear walls.
t	thickness of wall
T	Fundamental period of the structure.
T_X	Story torsion due to E_X.
T_Y	Story torsion due to E_Y.
V	Base shear.
V_X	Story shear in X-direction.
V_Y	Story shear in Y-direction.
W	Total weight of the structure.
Δ_{Top}	Maximum top building displacement
Δ_F	Fexural deformation
Δ_S	Shear deformation
Δ_T	Total deformation

THE INFLUENCE OF PLAN GEOMETRY AND STRUCTURAL SYSTEM ON THE BEHAVIOR OF HIGH-RISE BUILDINGS

By
Muhannad Yacoub Fakhouri

Supervisor
Dr. Raed M. Samra, Prof.

ABSTRACT

This study aims to urge the structural engineer to produce creative and original designs and to have a better understanding for the manner in which a structure responds to load. That means to acquire a comprehensive knowledge about the way the structure deflects under given load combinations. Besides, the engineer should have a sense and an order of magnitude of internal forces using different structural configurations and different plan geometries.

This study focuses on the behavior of concrete structures, specifically the behavior of tall concrete structures under the effect of seismic loading. Four building shapes have been chosen in this study. Each shape has been examined using three different systems i.e. frame system, shear wall system and dual system with a total height of 120*m* and a story height of 4*m*. These building shapes include: (1) Rectangular building proposed as hypothetical model. (2) Marina City, which is an existing structure in Chicago, USA. (3)Lake Point Tower, an existing structure in Chicago, USA. and (4)Toronto City Hall, an existing structure in Toronto, Canada.

The actual deflected modes are captured and discussed for each system thoroughly. The study also shows how the overall configuration for any shape largely determines the ways in which seismic forces are distributed throughout the building, and also influences the relative magnitude of these forces as a result.

In addition, this research considers other design considerations such as the effect of torsion, due to symmetric and non-symmetric configurations, code recommendations regarding plan irregularity and some solutions to these problems, rigidity issues, and the serviceability criteria of deflection as represented by the amount of drift of the structure.

Analysis is carried out by modeling a three dimensional structure for each case with the assistance of ETABS software (Extended three dimensional analysis of building systems). The models are subjected to gravity and lateral loads. The seismic loads are the governing lateral loads and calculated using the International Building Code (IBC-2003) approach. For such buildings dynamic analysis is performed.

It is shown that good seismic design is achieved through simplicity in structural systems and structural forms.

It is apparent from the study cases that the overall deflected shape of a rigid frame structure has a shear displacement profile, shear wall system has a flexural displacement profile, and the dual system is a combination of both systems profiles. This interacting behavior is found to reduce values of drift and displacement.

The study shows also that displacement curves can serve as a good indication of structural behavior under lateral loads and also provide a clear vision about structural system performance and efficiency.

This study also emphasizes the necessity that a structural designer should understand thoroughly the importance of arranging and locating the vertical elements in any structure during the design phase.

This study demonstrates the indirect effect of the building shape on the behavior of high-rise buildings.

CHAPTER ONE

INTRODUCTION

1.1. General

"We build tall buildings of necessity; how we build them is a reflection of society. Tall buildings do not have to be beautiful, they simply must be functional; so it is the degree of our concern for their beauty that serves as a measure of our humanity." (David Fisher, 1995).

Throughout history, man has always tried to express his greatness by building monuments as high as he could practically achieve. The tremendous blossoming of reinforced concrete multistory construction in the past decades is attributed in large part to three major factors: development of high-strength materials, development of new design concepts and improving construction methods.

During the last few years, multistory structures and tall buildings have become a common feature in the Middle East, with Dubai today housing some of the highest buildings in the world. In Jordan, a number of tall buildings are emerging. Jordan Gate, now under construction, consists of two 42-story high towers and an additional 17-story podium building. The slabs are post-tensioned to reduce the required thicknesses and minimize their own weight. Also, two 12-story towers are rising between the 5th and 6th circles. Other high-rise buildings will soon follow suit in different areas in Amman.

The design of tall buildings requires a good understanding of structural behavior and design requirements. The scale of projects and the skill and engineering knowledge

required surpass anything previously encountered in Jordan. A clear vision of how the structure deforms under gravity and lateral load is essential and a proper recognition of how the various horizontal and vertical structural elements interact to resist the load is inevitable.

Today, structural engineers design structural systems, which are not only economically efficient, but also architecturally satisfying. For tall buildings, there is no single trend that dominates the architectural and structural design. Each of today's tall buildings has unique architectural and structural characteristics, which are becoming increasingly more versatile, innovative, challenging and complex.

From a structural point of view, the determination of an appropriate structural system for a tall building involves the selection and arrangement of the structural elements to resist efficiently the various combinations of lateral and gravity loads. The magnitude of the gravity loads depends on the weight of the structure and any other superimposed vertical loads. When the structure of the building is well proportioned, gravity loads introduce compressive forces on the main vertical members that carry the load to the ground; thereby creating a structure that is balanced and stable. Lateral loads whose main components are horizontal forces act on the structure with varying intensity depending on the building's geographic location, structural system, structural materials, height and shape.

Earthquake loads which are a subject of concern and consideration in this research are lateral loads. They are very complex, more uncertain than wind loads. It is quite fortunate that they do not occur frequently. When earthquake occurs, it creates ground movements and as a result, buildings respond to the accelerations transmitted from the ground through the structure's foundation. The inertia of the building can cause shearing of

the structure which can concentrate stresses on the weak walls or joints in the structure resulting in failure or perhaps total collapse.

It should be noted that for low rise buildings (short period), the higher modes pick up less forces than lower modes. On the other hand, for tall buildings (long period), higher modes pick up more forces than lower modes. Therefore, higher modes should be investigated with care in high-rise buildings.

Consequently, seismic codes include this behavior in their response spectra by lifting up the curves of the response in the long period range to accommodate the effect of higher modes in the long period range.

Other lateral loads that influence the behavior of tall buildings are the wind loads which will not be tackled in this study. However, it is worthy to mention that the average wind speed tends to increase with height and affect greatly those structures that are tall or slender. An important problem associated with wind induced motion of buildings is concerned with human response to vibration and perception of motion especially for most tall buildings.

1.2. Structural System Selection Procedures

The design of a high-rise building requires an intricate interaction between a team of creative professionals. The team usually consists of the owner, the architect, the engineers, the contractor and a project manager.

The process of structural system selection usually begins with an initial meeting between the owner and the architect to determine the programmatic requirements that need to be satisfied within a distinct budget. The next step is the creation and convening of the total team. During the team's early meetings the parameters which need to be examined are

identified. Each and every member of the team, utilizing their individual experiences, is called upon to discuss the relevant issues based on their professional understanding of the problems involved. The goal of the teamwork is to determine and analyze a number of options so that they can develop different designs for the project at hand. The evaluation criteria for the choice of a structural system can vary. However, a list can be compiled that is commonly true:

(1) Economics (time is money).

(2) Length of construction.

(3) Construction risk.

(4) Convergence of structural needs and architectural desires.

(5) Convergence of structural and mechanical needs.

(6) Local conditions (material, labor, common practice).

In high-rise structural engineering there are essentially three building materials: structural steel, reinforced concrete or variations of it, and a composite of the two. Within each material there are a very large number of options that one could choose. The design process is both a process of elimination as well as creation. Options must be eliminated so that the best value can be determined. As each system is chosen and analyzed, it is very important that a fair and honest comparison be made. Each variable can have far reaching effects and must be considered.

1.3. Concrete as a Building material

Little more than a century ago, reinforced concrete was invented. In this short period of time, reinforced concrete has gone from being a very limited material to one of the most versatile building materials available today. The first reinforced concrete

buildings were heavy and massive. Valuable floor space was taken up by the massive concrete structural systems. Today, due to our increased knowledge and improved technology, reinforced concrete buildings can be tall and elegant. Due, in part, to the use of shear walls, innovative structural systems and ultimate strength design, very little usable floor space is occupied by the structure. High strength and lightweight structural concrete allow us to use smaller member sizes and less steel reinforcement.

Because of the rapid developments of concrete construction and technology, with every passing year the use of concrete for tall buildings is becoming a constant reality. The moldability of concrete is a major factor in creating exciting building forms with elegant aesthetic expressions. Concrete is a naturally fireproof material and monolithic concrete can absorb thermal movements, shrinkage and creep, and foundation movements. Also, reinforced concrete structures are inherently stiff and have a great deal of redundancy.

Compared to steel, concrete tall buildings have larger masses and damping ratios that help in minimizing motion perception. A heavier concrete structure also provides better stability against overturning caused by lateral loads. Experts further demonstrated that either an all-concrete or a composite structural system for skyscrapers is also cost-effective. New structural systems including the composite ones that are popular now have allowed concrete high-rises to reach new heights during the last four decades. The floor erection cycle time for concrete high-rises is now almost comparable with that of steel buildings.

Although steel will continue to be the structural material of choice for many tall buildings for its strength and ductility, we may expect to see more and more concrete and

composite high-rise structures shaping the skylines of major cities of the world in the forthcoming years.

1.4. Research Significance

Since the dawn of history man has been trying to build the 'tallest building', 'tallest tower' or 'tallest structure' in the world. These buildings have become common feature in the Middle East; Amman follows distinctive development trajectories that reflect both the interactions of global forces and the local community. The primary global force affecting Amman is the competitive international environment engendered by economic globalization that makes the city an increasingly attractive location for investment.

However, the rapid growth of the urban population and the consequent pressure on the limited space have considerably influenced city residual development. The high cost of land, the desire to avoid a continuous urban sprawl, and the need to preserve important agricultural production have all contributed to drive residential buildings upward. In some cities, for example, Hong Kong and Rio de Janeiro, local topography restrictions make tall buildings the only feasible solution for housing needs.

The behavior of a tall building during an earthquake depends on several factors, including whether its shape is simple and symmetric or not? Some buildings in past earthquakes have performed poorly due to highly irregular shapes. Since the building shape is determined very early in the development of a project, it is crucial that architects and structural engineers work together during the planning stages to ensure that unfavorable features are avoided and a good building configuration is chosen.

Therefore, the design of tall buildings requires a good understanding of structural behavior and design requirements. The scale of projects and the skill and engineering knowledge required surpass anything previously encountered in Jordan. A clear vision of how the structure deforms under gravity and lateral load is essential and a proper recognition of how the various horizontal and vertical structural elements interact to resist the load is inevitable.

The study intends to draw a clear vision and offer a coherent treatment on the way tall buildings behave under earthquakes when different types of structural systems are used, realizing that the overall geometry and plan layout play a major role in determining structural response.

1.5. Research Objectives

The main purpose of this study is to acquire a comprehensive knowledge in the way which the structure deflects under seismic loads and to have a sense and an order of magnitude of internal forces using different structural configurations and different plan geometries.

This study focuses on the behavior of concrete structures; specifically the behavior of tall concrete structures under the presence of seismic loading. Four building shapes have been chosen, one hypothetical and three reflecting existing tall buildings. Each shape has been examined using three different systems: frame system, shear wall system and dual system.

The actual deflected modes have been captured and discussed for each system thoroughly. The study also shows how the overall configuration for any shape largely

determines the ways in which seismic forces are distributed throughout the building, and also influences the relative magnitude of those forces as a result. It shows also that the effect of the plan shape on the results has an indirect contribution, rather than direct bearing.

In addition, this research focuses on other design considerations such as:

(1) The effect of torsion, due to symmetric and non symmetric configurations.

(2) Code perspective to plan irregularity and some solutions to these problems.

(3) Structural rigidity issues.

(4) The serviceability criteria of deflection as represented by the amount of drift of the structure.

1.6. Research Methodology and Contents

In order to study the influence of structural system and plan geometry on the behavior of high-rise buildings, Chapter Two is first introduced to shed some light on configuration characteristics which largely determine the ways in which seismic forces are distributed throughout the building, and also influence the relative magnitude of those forces. In this chapter, plan irregularities and recommendations to solve some plan irregularity problems have been also discussed.

Chapter Three provides an outline about the structural systems used in the models, and a full description of the study cases, modeling procedures, geometric and material assumptions. In addition, loading definition and analysis criteria have been discussed.

Chapter Four illustrates and tracks the actual behavior of high-rise buildings by examining four case studies of very distinct and different plans under the presence of

seismic loads. Each plan has been studied with three different systems. These are ordinary reinforced concrete moment frames, ordinary reinforced concrete shear walls and reinforced concrete frame-wall. Also a detailed comparison is made. The comparison between these systems within the same plan geometry includes the variation in displacements, drift, base shear, base moment, base torsion and the first mode of vibration. Moreover, graphical presentation and synthesis of results are presented.

Chapter Five investigates the interaction between the building shape, overall stiffness and the structural system. A comparison of the stiffnesses of the four buildings is forthtelling, particularly when the buildings are so designed to approximately have the same mass by proportioning all four buildings to have the same floor area each.

Based on the results of this study, the last chapter draws the conclusions that have been derived during the course of this research, and recommended structural systems are proposed.

1.7. Software Overview

In general, buildings may be modeled as space frames with rigid diaphragms using standard structural analysis software. Due to the effort that is involved in dynamic analysis, experience skills in modeling are important aspects of such analysis. 3D shell elements are used to model the floor where the mass is directly applied to the surface of the elements.

Throughout this thesis ETABS (Non-Linear Version 9.07) is used. ETABS stands for “Extended 3D Analysis of Building Systems”, a product of computers and structures, Inc., CSI. Berkeley, California., USA.

For nearly 30 years, ETABS has been recognized as the industry standard for building analysis and design software. Today, continuing in the same tradition, ETABS has evolved into a completely integrated building analysis and design environment. The system built around a physical object based graphical user interface, powered by targeted new special purpose algorithms for analysis and design, with interfaces for drafting and manufacturing, is redefining standards of integration, productivity and technical innovation.

ETABS is a three dimensional finite element program that has been developed specifically for multi-story building structures. It uses object-based modeling. A building is modeled as a collection of structural objects such as columns, beams, braces and walls rather than nodes and finite elements.

CHAPTER TWO

CONFIGURATION CHARACTERISTICS AND PLAN IRREGULARITY

2.1. General

While the provision of earthquake resistance is accomplished through structural means, the architectural decisions also play a major role in determining the building's seismic performance through the proposed building shape. Therefore, the building architecture must permit an effective seismic design as much as possible. At the same time the structural engineer must permit the functional and aesthetic aims of the building to be realized.

In other words, the architect who has some understanding of these seismic forces and their sources can respond with a reasonable layout in the early design stage and can communicate with the structural engineer because he talks his language. That is, an architect having a basic understanding of engineering principles can truly collaborate with the structure's specialist to achieve the optimum design of tall buildings.

The building configuration and geometry properties can be defined as the size, shape and proportions of the three-dimensional form of the building as well as the type of structural elements and their locations.

Configuration largely determines the ways in which seismic forces are distributed throughout the building, and also influences the relative magnitude of those forces. For a given ground motion, the major determinant of the total inertial force in the building is the building mass, while the size and shape of the building (together with the choice of

materials), establish its weight.

For a given structural plan, an almost infinite variety of configurations can provide a solution, and it is the variables in these configurations that affect the distribution of inertial forces due to ground shaking.

Thus the discussion of configuration influence on seismic performance translates into the identification of configuration variables that affect the distribution of forces. These variables represent irregularities or deviations from a "regular" configuration.

Some factors that attribute to harmony of structural behavior under seismic loading are elaborated in the following paragraphs.

2.2. Configuration Characteristics and their Effects

Configuration characteristics are issues relating to the building configuration such as:

(1) Proportions and symmetry.

(2) Plan Density, Perimeter Resistance, and Redundancy.

These characteristics are discussed in the subsequent paragraphs.

2.2.1 Proportions and Symmetry

2.2.1.1. Building Proportions: Height-to-Depth Ratio

In seismic design, the proportions of a building may be more important than its absolute size. For tall buildings, the slenderness ratio (height/least depth) of a building, calculated in the same way as for an individual member, is a more important consideration than just height alone. The more slender a building, the worse the overturning effects of an earthquake and the greater the earthquake stresses in the outer columns, particularly the overturning compressive forces which can be very difficult to deal with.

As urban land becomes more expensive, there is a trend towards designing buildings which, although not necessarily very high, may have a large height/depth ratio. In looking at the influence of building size on seismic performance, the influence of both the dynamic environment and the characteristics of ground motion result in more complexity than does the influence of size on vertical forces. Increasing the height of a building may be equivalent to increasing the span of a cantilever beam. The problem with the analogy is that as a building grows taller its period will tend to increase, and a change in period means a change in the building response.

2.2.1.2. Symmetrical Plan Shape

The term symmetry denotes a geometrical property of building plan configuration. Structural symmetry means that the center of mass (*C.M.*) and center of resistance *(C.R.)* are located at, or close to, the same point.

However, a building with reentrant corners is not necessarily asymmetrical (a cruciform building may be symmetrical) but it is irregular, as defined in the IBC code. Thus symmetry is not sufficient on its own, and only when it is combined with simplicity it becomes beneficial. Nevertheless, it is true that as the building becomes more symmetrical, its tendency to suffer torsion and stress concentration will be reduced, and performance under seismic forces will tend to be less difficult to analyze. This suggests that when good seismic performance must be achieved with maximum economy of design and construction, the symmetrical, simple shapes are much preferred. But these tendencies must not be mistaken for an axiom that a symmetrical building will not suffer torsion.

The effects of symmetry refer not only to the overall building shape, but to its details of design and construction. Study of building performance in past earthquakes indicates that performance is sensitive to quite small variations in symmetry within the overall form. This is particularly true in relation to shear-wall design and where service cores are designed to act as major lateral resistant elements. It is possible to have a building which is geometrically symmetrical in exterior form, but highly asymmetrical in the arrangement of its structural systems. The most common form of this condition (sometimes termed “false symmetry”) is the building with interior structural cores that, for planning reasons, are asymmetrically arranged. This can be a major source of undesirable torsional response.

Finally, it must be recognized that architectural requirements will often make the symmetrical design impossible. In these circumstances, it may be necessary, depending on the size of the building and the type of asymmetry, to subdivide the building into simple elements.

2.2.2. Plan Density, Perimeter Resistance, and Redundancy

Other configuration characteristics that have an impact on seismic performance are density of structural elements, perimeter resistance and its effect on torsional resistance, and redundancy. These factors are presented in the next paragraphs.

2.2.2.1. Plan Density

The size and density of structural elements in the buildings of former centuries is strikingly greater than in today's buildings as structural technology has allowed us to develop this trend further.

Earthquake forces are generally greater at the base of the building. The bottom story is required to carry its own lateral load in addition to the shear forces of all the stories above, which is analogous to the downward build-up of vertical gravity loads. At this same lowest level, programmatic and aesthetic criteria are often imposed on the buildings that demand the removal of as much solid material as possible. This requirement is the opposite of the most efficient seismic configuration, which would provide the greatest intensity of vertical resistant elements at the base, where they are most needed.

An interesting statistical measure in this regard is the ground level vertical plan density, defined as the total area of all vertical structural elements divided by the gross floor area. The most striking characteristic of the modern framed building is the tremendous reduction of structural plan density compared to historic buildings.

The densely filled-in "footprints" of buildings of previous eras present a striking contrast: the structural plan density can go as high as 50%, in the case of the Tag Mahal, in India, and the ratio for St. Peter's in Rome is about 25%, while the proposed models in this study for example which reflect today's buildings have plan density ratios for moment resisting frames type in the range between (2.5 to 5.0) %.

2.2.2.2. Perimeter Resistance:

The walls in Figure (2.1.b) below form greater lever arms for resisting overturning and torsional moments than those in Figure (2.1.a).

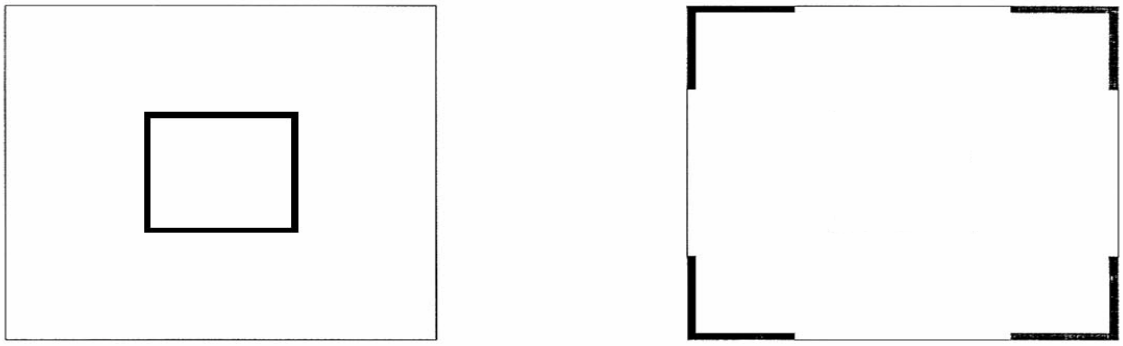

(a) Small Torsional Resistance (b) Large Torsional Resistance

Figure (2.1): Perimeter Resistance

In resisting torsion, with the center of twist of a symmetrical building located at or near the geometrical center, the further the resisting element is placed from the center, the greater the lever arm through which it acts, and hence the greater the resisting moment that can be generated. Placing resisting members on the exterior perimeter whenever possible is always desirable, whether the elements are walls, frames, or braced frames, and whether they have to resist direct lateral forces, torsion or both.

2.2.2.3. Redundancy

The design characteristic of redundancy plays an important role in seismic performance, and is significant in several aspects, most especially because the redundant design will almost certainly offer alternative load paths and in doing this it tends to result in higher plan density as discussed above. In addition, historic buildings tended to be highly redundant, because short spans required many points of support, and thus each

supporting member held much lower stresses, often even within the capability of unreinforced masonry. Thus, the very limitations of traditional materials forced the designers into good design practices such as redundancy, direct load paths and high plan density.

The detailing of connections is often cited as a key factor in seismic performance, since the more integrated and interconnected a structure is, the more load distribution possibilities there are. Redundancy can be stated as the tolerance to failure of some members, by providing excess capacity and multiple load paths.

2.3. Plan Irregularity of Structures

Irregular structures should involve extra analysis and dynamic consideration rather than use of the equivalent static lateral force method. These irregularities vary in the importance of their effects, and their influence also varies in accordance with the particular geometry or dimensional basis of the condition.

Irregularity in the horizontal direction may exist due to displacement, geometry, and discontinuity. The international building code (IBC 2003) defined these irregularities as one of these types listed below:

(1) Torsional irregularity in rigid diaphragms, when the maximum displacement of one corner of the diaphragm exceeds 1.2 times the average displacement of both corners in each direction. Also when the maximum displacement of one corner of the diaphragm exceeds 1.4 times the average displacement of both corners in each direction, it is said to be an extreme torsional irregularity.

(2) Reentrant corners, when the projection of both ends of reentrant corners exceeds 15% of the structure's dimension.

(3) Diaphragm discontinuity is considered when openings in the diaphragms exceed 50% of its area. Also 50% difference in effective diaphragms stiffness from one story to the next is considered.

(4) Out-of-Plane offsets, represents discontinuities in a lateral-force-resistance path, such as out-of-plane offsets of the vertical elements.

(5) Nonparallel Systems, when the vertical lateral-force-resisting elements are not parallel to or symmetric about the major orthogonal axes of the structure.

2.4. Solutions to Some Problems of Configurations

2.4.1. Reentrant Corners

There are two related problems created by reentrant corner plans. The first is that they tend to produce variations of rigidity, and hence differential motions, between different parts of the building, resulting in a local stress concentration at the "notch" of the reentrant corner. In Figure (2.2 b), if the ground motion occurs with a north-south emphasis at the L-shaped building shown, the wing oriented north-south will, for geometrical reasons, tend to be stiffer than the wing oriented east-west. The north-south wing, if it were a separate building, as shown in Figure (2.2.a), would tend to deflect less than the east-west wing, but the two wings in the L-shape are tied together and attempt to move differentially at their notch, pulling and pushing each other.

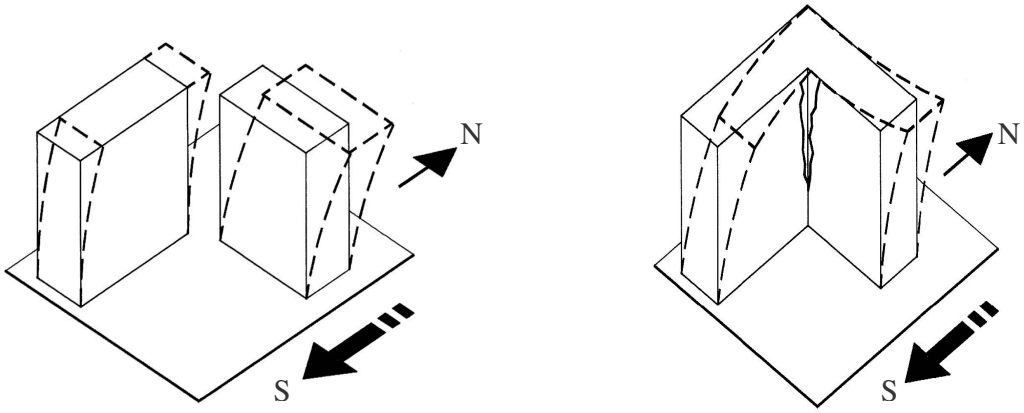

(a) Separated Building (b) L-shaped Building

Figure (2.2): Effect of Reentrant Corner

This action creates high stress concentration in addition to the torsional effect that results due to the differences between *C.M.* and *C.R.* These stresses depend mainly on the mass of the building, the structural system, and the length and height of wings relative to their aspect ratio.

The remedy for this problem can be achieved by three basic means:

- Separate the building wings structurally with seismic joints as shown in Figure (2.3 a)
- Provide effective connection to tie the building elements together at lines of stress concentration and introduce resistance elements at appropriate locations to reduce torsion. These connection elements may be collector beams well designed to transfer forces across intersection areas. Walls at the same location may even be more efficient than collector beams, if they are accepted by the architect as shown in Figure (2.3.b).
- Create splay corners which reduce stress concentrations using the same concept of a haunch beam as shown in Figure (2.3.c).

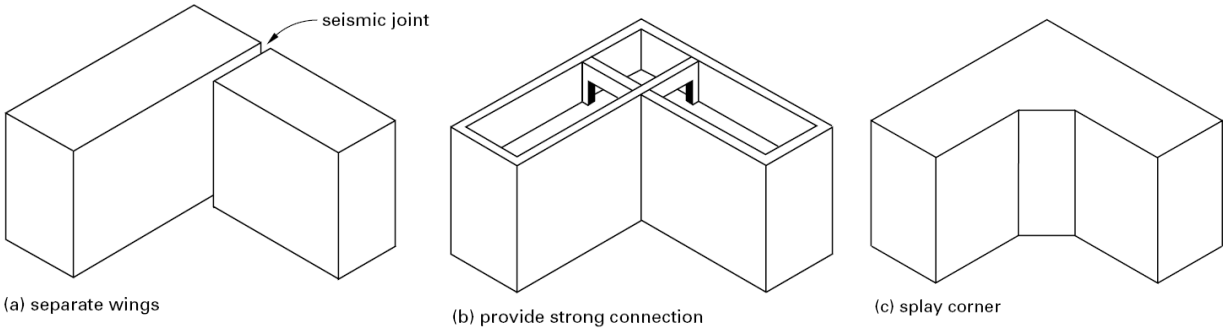

Figure (2.3): Solutions to Reentrant Corners

2.4.2. Variation in Perimeter Strength and Stiffness

This problem may occur in buildings whose configuration is geometrically symmetrical and simple, but nonetheless irregular for seismic design purposes. If there is wide variation in strength and stiffness around the perimeter, the centers of mass and resistance will not coincide, and torsional forces will tend to cause the building to rotate around the center of resistance.

Some solutions can be suggested as follows:

- Distribute the shear walls in an efficient way to produce the minimum eccentricity between *C.M.* and *C.R.* and minimize the torsional moment that may develop.
- Increase the stiffness of the open facades by adding shear walls at or near the open face. This solution is, of course, dependent on a design which permits this solution.
- When the torsional moment magnitude is reasonable and acceptable, structure should be designed to resist it.

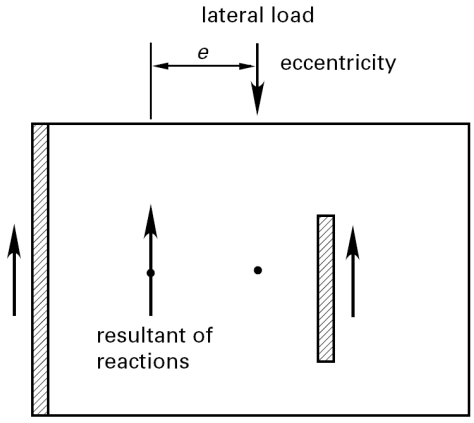

Figure (2.4): Torsional Eccentricity

2.4.3. Non Parallel Systems

This condition results in a high probability of torsional forces under a ground motion, because the centers of mass and resistance cannot coincide for all directions of ground motion. Moreover, the narrower portions of the building tend to be more flexible than the wider ones, which increase the tendency to torsion. Non-rectilinear forms have become increasingly fashionable in the last few years as a reaction to the rectangular "box"-buildings. Forms that are triangular, polygonal, or curved have become commonplace, even in very large buildings.

To alleviate this problem non-structural façades may be used as external cladding to give the shapes their needed curved edges. Otherwise, special care may be undertaken during the design stage to reduce the torsional effect as much as possible by increasing the stiffness in the narrow part of the building, for example.

2.4.4. Diaphragm Discontinuity

A diaphragm configuration is the arrangement of horizontal resistance elements that transfer forces between vertical resistance elements. The diaphragm acts as a horizontal beam, and its edges act as flanges. The following must be observed:

- Ensure that the openings do not interfere with diaphragm attachment to walls or frames.
- Ensure that multiple openings are spaced sufficiently far from one another to allow reinforcing elements to develop their required capacity
- Ensure that collectors and drag struts are uninterrupted by openings, leading to torsion and stress concentrations.

CHAPTER THREE

CASE STUDIES OF HIGH-RISE BUILDINGS AND MODELING PROCEDURES

3.1. General

Examining the behavior of high-rise buildings under the effect of seismic loads will be carried out using four different plan geometries with different structural systems. These plans are:

(1) Rectangular building proposed as a hypothetical model.

(2) Marina City which is a twin tower in Chicago, USA.

(3) Lake Point Tower which is an existing building in Chicago, USA.

(4) Toronto City Hall which is an existing structure composed of two curved buildings in Toronto, Canada.

All detailed information, properties and governing parameters are provided in this chapter.

3.2. Structural Systems Used in the Models

Three major systems have been used in all models. These are:

(1) Rigid frame systems *(F)*

(2) Shear wall systems *(SW)*

(3) Dual wall-frame systems *(DS)*

3.2.1. Rigid Frame System

Rigid frames connect the columns and girders via moment-resistant connections. The lateral stiffness of a rigid frame depends on the bending stiffness of the columns,

girders and connections to the frame, Figure (3.1). A major advantage of the rigid frame is the open rectangular spaces which allow greater planning for windows and doors. When used as the sole lateral load resisting system, rigid frames are economical only up to about 25 stories. Above that height they are too flexible. Increasing the member sizes would call for uneconomical solutions. Rigid frames are ideal for reinforced concrete, because of the inherent rigidity of the joints. Steel frames are more costly to stiffen the moment-resistant connections.

The size of the columns and girders at any level are directly a function of the external shear at that level. Therefore, they increase in size towards the base. Floor designs are not repetitive as in braced frames. Ceiling height also increases towards the base because of the larger girders, so story heights vary.

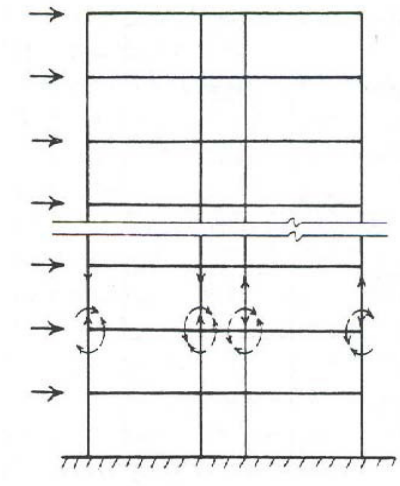

Figure (3.1): Rigid Frame of a High-Rise Building
(Coull, A. and Smith, B., 1991)

3.2.2. Shear Wall Systems

Shear walls, made from reinforced concrete, may serve as both architectural and structural partitions, capable of carrying gravity and lateral loads. Their very high in-plane stiffness and strength make them ideal for bracing tall buildings. In a shear wall building as

shown in Figure (3.2), the shear walls provide the primary lateral load resistance. Shear walls act as vertical cantilevers in the form of separate planar walls and non-planar assemblies, typically around elevators, stairs and service shafts. Shear walls are stiffer than rigid frames, and are economical to about 35 stories. The restrictions in planning when using shear walls means that they are mostly suited to hotels and residential buildings. They provide repetitive floor by floor planning, with continuous vertical walls that serve simultaneously as acoustical and fire insulation between units.

When shear walls are combined with frames, the walls attract all the lateral loads, so the frame is designed only for gravity. The wall layout must be planned so that the lateral load tensile stresses are suppressed by the gravity load compressive stresses. Shear walls behave well in seismic events because of their planned ductility.

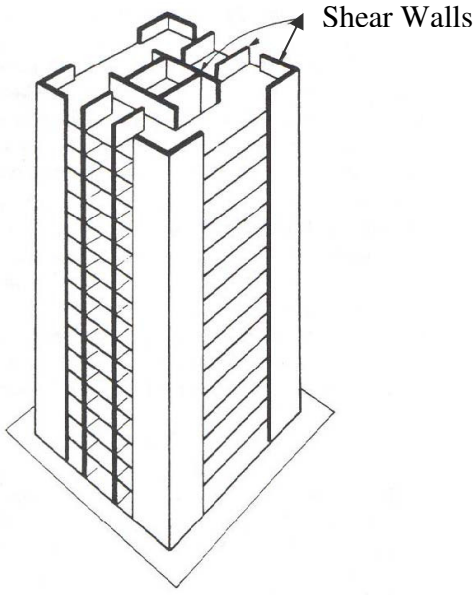

Figure (3.2): Interior and Corner Shear Walls
(Coull, A. and Smith, B., 1991)

3.2.3. Wall-Frame Systems

The combination of shear walls and rigid frames is called a wall-frame system. The structure is constrained to adopt a common deflected shape to both systems through the horizontal rigidity of the girders and slab. The walls and frame interact horizontally, especially at the top, to produce a stiffer and stronger structure. The interacting wall-frame combination is appropriate for buildings in the 40-65 story range, well above the range of rigid frames or shear walls alone as shown in Table [3.1]. Most wall-frames are made of reinforced concrete.

Steel buildings may use the braced frame to offer similar benefits of horizontal interaction. The braced frames behave with an overall flexural tendency that interacts with the shear mode of the rigid frame.

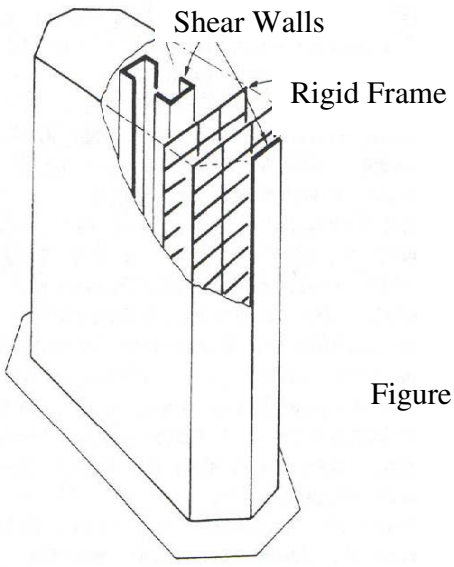

Figure (3.3): Wall-Frame

Table [3.1]: Structural System vs. Number of Stories
According to (Coull, A. and Smith, B., 1991)

Structural System	Number of Stories (Range of Practical Application)
Frame	25
Shear Wall	35
Wall-Frame	40-60

3.3. Geometric and Material Assumptions for all Models

The generated 3D models will be those of reinforced concrete buildings with a total height each of 120*m* having the following characteristics and governing parameters:

(1) The number of stories is taken as 30, with a typical floor height of 4*m*.

(2) All models have a floor area approximately equal to 1800m^2.

(3) Material: Concrete with unit weight = 24 kN/m^3, a compressive strength $f_c^{'}$ = 50 MPa for walls and columns and with $f_c^{'}$ = 30 MPa for beams and slabs.

(4) Cross-section of frame elements as listed in Table [3.2].

Table [3.2]: Dimensions of Beams and Columns

Section - Location	Depth (mm)	Width (mm)
Columns – Story (1 to 10) and all the exterior columns	1000	1000
Columns – Story (11 to 20)	800	800
Columns – Story (21 to 30)	600	600
Edge Beams all Stories	1000	500

Flat plates, in which the columns are cast integrally with the floor slabs, behave under horizontal loading similarly to rigid frames. The response of the structure with regular columns grid can be studied by considering each bay-width replaced by an equivalent rigid frame bent. The flexural stiffness of the equivalent beam depends mainly on the width-to-length spacing of the columns and on the dimensions of the columns.

The design strip of equivalent frame according to the ACI 318-05 is shown in Figure (3.4).

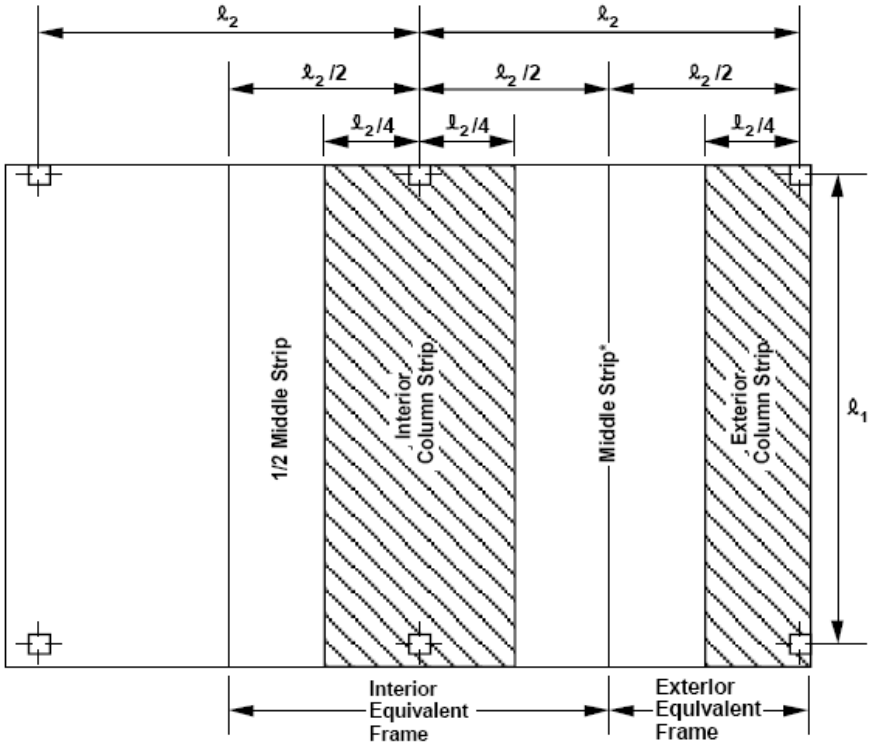

(a) Column Strip for $l2 \leq l1$

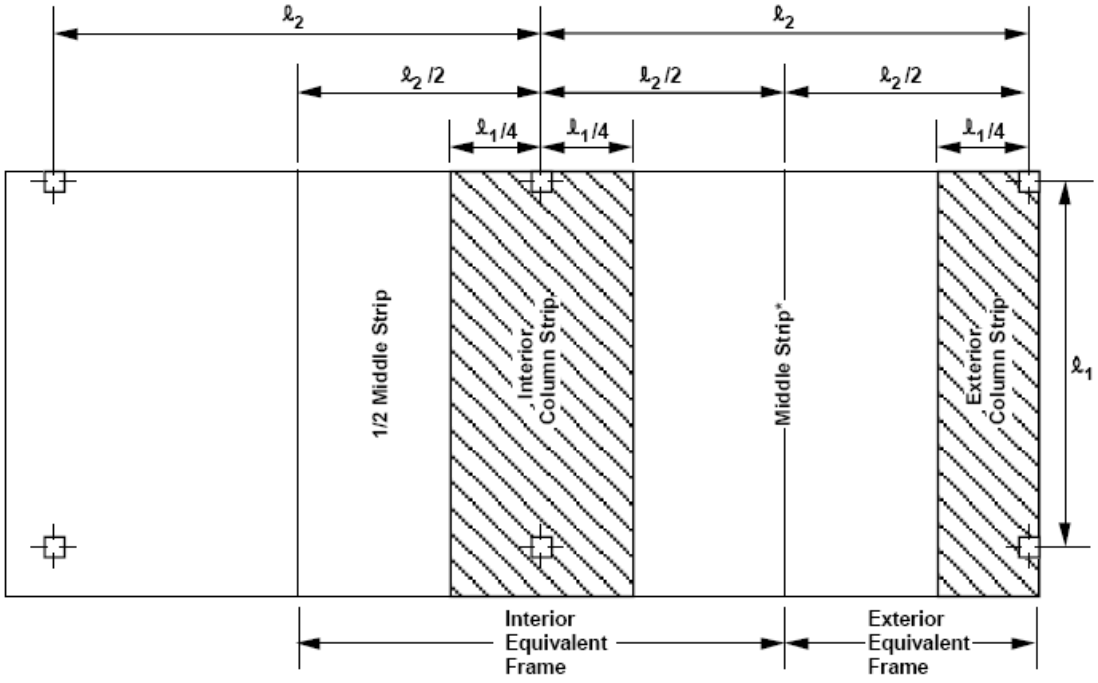

(b) Column Strip for $l2 > l1$

Figure (3.4): Definition of Design Strip of Equivalent Frame According to the ACI Code

(5) Shell elements, which include all walls and slabs, are listed in Table [3.3].

Table [3.3]: Modeling Element Thicknesses

Section - Story	Thickness *(mm)*	Story
Slab - All	300	All
Wall	1000	1 to 10
	800	11 to 20
	600	21 to 30

3.3.1. Loading Definition

3.3.1.1. Gravity Loads

(1) Dead load represents the own weight of the structure.

(2) Superimposed Dead load has been taken uniformly = 2.5 kN/m^2

3.3.1.2. Lateral Loads

These include equivalent static earthquake loading or dynamic earthquake loading based on the International Building Code (IBC 2003), for the two directions X and Y.

Torsion has proven to be one of the major causes of failures in previous earthquakes, hence the effect of torsion must be carefully considered in design. The IBC 2003 requires an additional torsional moment which is accounted for by assuming an accidental eccentricity equal to 5% of the structure's dimension. This 5% additional eccentricity has been taken into consideration.

3.3.1.2.1. Equivalent Static Lateral Force Loading

The equivalent static force procedure in the International Building Code (IBC 1617.4) specifies the following formula for calculating base shear (V):

$$V = C_s W \qquad (3.1)$$

where the seismic response coefficient, C_s, is defined as:

$$C_s = \frac{S_{D1}\, I_E}{RT} = \begin{pmatrix} \leq & S_{DS}\, I_E / R \\ \geq & 0.044\, S_{DS}\, I_E \end{pmatrix} \quad (3.2)$$

and

$$S_{DS} = 2/3\, S_{MS} \quad (3.3)$$

$$S_{D1} = 2/3\, S_{M1} \quad (3.4)$$

$$S_{MS} = F_a\, S_s \quad (3.5)$$

$$S_{M1} = F_v\, S_1 \quad (3.6)$$

Where;

W= the total weight of the structure and may include other loads as listed in the IBC which are (1) In areas used for storage, a minimum of 25 % of the reduced floor live load .(2) Where an allowance for partition load is included in the floor load design, the actual partition weight or a minimum weight of 0.479 kN/m^2 of floor area, which ever is greater. (3) Total operating weight of permanent equipment. (4) 20 % of flat roof snow load where flat roof snow load exceeds 1.44 kN/m^2.

F_v and F_a = site coefficients.

S_1 and S_s = the mapped spectral acceleration for 1-sec. and short period, respectively.

S_{D1} and S_{DS} = the design spectral acceleration for 1-sec. and short period, respectively.

S_{M1} and S_{MS} = the maximum considered earthquake spectral acceleration for 1-sec. and short period respectively.

I_E = Occupancy importance factor.

R = the response modification factor.

T = fundamental period of the structure (seconds).

The upper bound value for C_s tends to govern for relatively stiff structures that exhibit a small (short) fundamental period of vibration (T). The lower bound value for C_s

tends to govern for relatively flexible structures that exhibit a large (long) fundamental period of vibration (T).

For all four case studies considered in this thesis, the values are taken for the structural models as follows:

(1) The mapped spectral acceleration for short period assumed to be S_s=0.5.

(2) The mapped spectral acceleration for 1-second period assumed to be S_1= 0.2.

(3) The site is classified as class C, very dense soil and soft rock, the seismic site coefficient for short and one second period F_a=1.2 and F_v=1.6, respectively.

(4) Occupancy importance factor, I_E = 1 and seismic use group I.

(5) The fundamental (natural) period has been calculated using the following IBC 2003 expression based on the height of the structure:

$$T_a = C_T (h_n)^{3/4} \tag{3.5}$$

Where; h_n= total height of the building.

C_T = building period coefficient taken as:

= 0.073 for concrete moment frames systems *(F)*.

= 0.049 for both shear wall system *(SW)* and dual system *(DS)*.

(6) Response modification or force reduction (R) coefficient which is the ratio of the elastic strength demand to the actual yield level of the structure is taken according to the IBC 2003 as (3) for ordinary reinforced concrete moment frames - *F*, (4.5) for ordinary reinforced concrete shear walls - *SW* and (5.5) for dual system – *DS*, consisting of shear wall-frame ordinary interactive system.

The *R* factor is intended to account for inelastic structural behavior and the ability of a structure to displace/deform and dissipate energy without failing. Since all R

coefficients specified are greater than unity ($R > 1.0$), the R coefficient effectively reduces the calculated base shear (V) by varying amounts depending on the ductility of a structure. In general, ductile structural systems should have higher R coefficients than brittle structural systems.

3.3.1.2.2. Dynamic Analysis

In the civil engineering field, two design philosophies are basically distinguished, elastic design and inelastic design. In the elastic design philosophy, structures are designed for the elastic strength demand (F_e) to remain elastic and no internal force redistribution is permitted during the life time of the structure. This behavior implies the recovery of work done by the external loads after their removal. However, in the inelastic design, a structure is only designed to the yield level of the structure (F_y); refer to Figure (3.5). Therefore, the force reduction coefficient that was discussed previously is equal to $R = F_e/F_y$ i.e. the ratio of the elastic strength demand to the actual yield level of the structure.

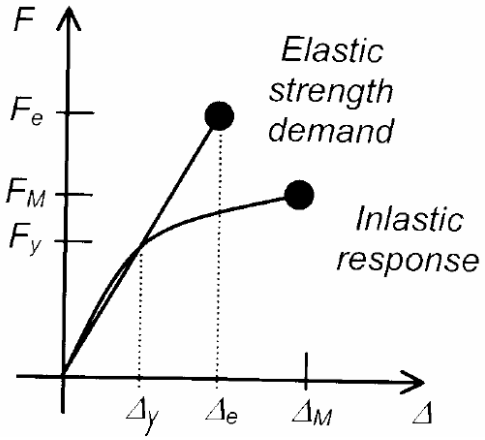

Figure (3.5): Force Reduction Value, (Armouti, 2004).

where, F_e: maximum elastic force demand

F_y: maximum force at yield level

F_M: maximum force at demand level

This implies that designing structures with strength less than their elastic strength demand imposes requirements in structural design. These requirements include good ductility and good energy dissipation of the structure.

Design of earthquake-resistant structures to remain elastic under a strong earthquake is achievable, however, it requires high strength and, in turn, high cost which might not be economically feasible. As a result, indirect inelastic analysis will be used in all the models.

In order to do that the elastic analysis based on the IBC 2003 design Spectrum, Figure (3.6), will be transformed to inelastic values. The elastic response spectrum is scaled to match the equivalent lateral force analysis procedure (approximate inelastic analysis). Therefore, a factor is used to scale the elastic response spectrum base shear to match with the equivalent lateral force procedure.

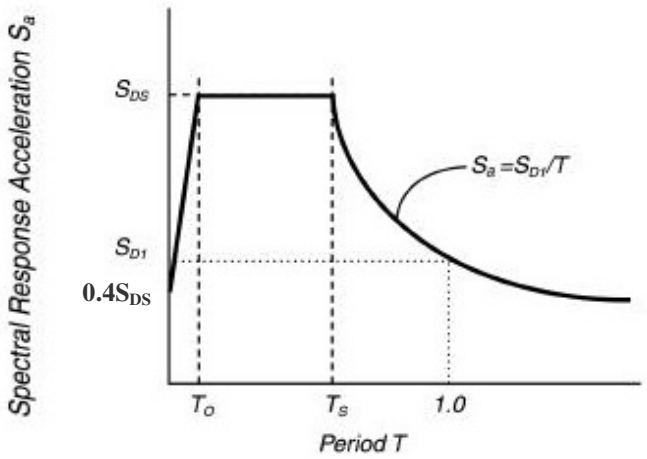

Figure (3.6): IBC 2003 Design Response Spectrum

Two cases are defined in the X and Y directions with an assumed 5% structural damping. Also the complete quadratic combination (*CQC*) is used for modal analysis which is based on the probabilistic correlation of the periods of the mode shapes and requires statistical analysis.

3.3.2. Other Issues

(1) All vertical elements are assigned at the base as fixed supports.

(2) Only two major directions have been considered in the comparison, along the X and Y axes.

(3) All Tables and plotted graphs are based on dynamic analysis.

(4) Bays throughout all systems range from 5m to 10m.

(5) All shell element slabs are joined with a horizontal rigid diaphragm, which does not change its plan shape when subjected to lateral load due to its rigidity, in order to distribute story shear to the resisting vertical elements.

CHAPTER FOUR

IMPACT OF STRUCTURAL SYSTEM ON THE BEHAVIOR OF HIGH-RISE BUILDING

4.1. General

This chapter intends to illustrate and track the actual behavior of high-rise buildings by examining four case studies of distinct and very different plans under the presence of seismic loads. Each plan has been studied with three different systems. These are ordinary reinforced concrete moment frames, ordinary reinforced concrete shear walls and reinforced concrete frame-wall. Also a detailed comparison is made.

The comparison between these systems within the same plan geometry includes the variation in displacements, drift, base shear, base moment, base torsion and the first mode of vibration. In addition, a graphical presentation and synthesis of results is presented.

Three of the four diverse layout plans have been chosen to reflect existing high-rise buildings. These plans are shown in Figure (4.1); a complete description of these plans will be discussed later.

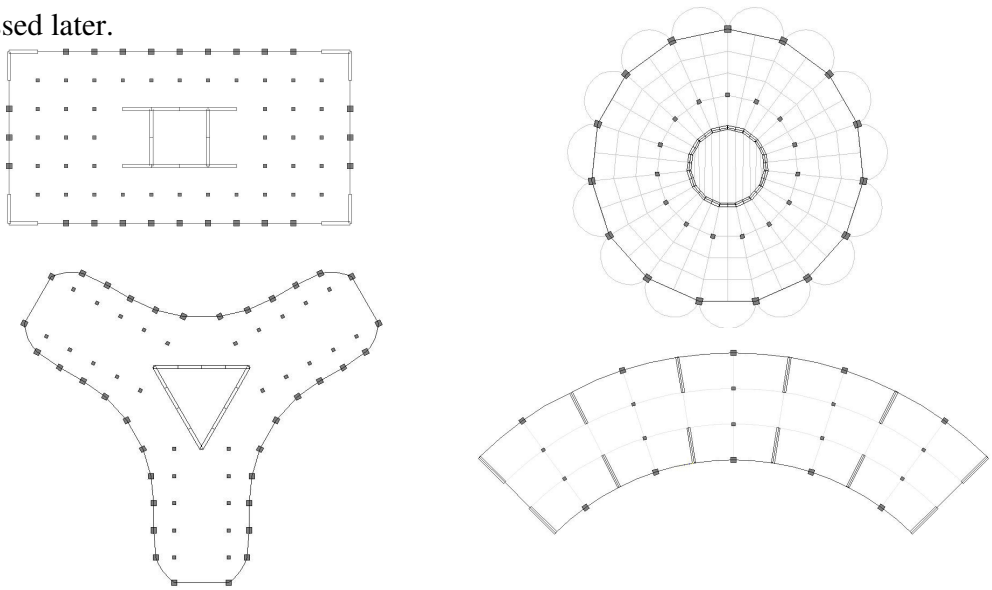

Figure (4.1): High-Rise Building Proposed Plans

4.2. Case Study (1): Rectangular Shape

This section deals with the first case study of a rectangular shaped structure which is a typical high-rise building. A complete set of analysis tables and graphs is provided.

4.2.1. Rectangular Layout Plans - (60*m* x 30*m*) with grid spacing of 5*m*

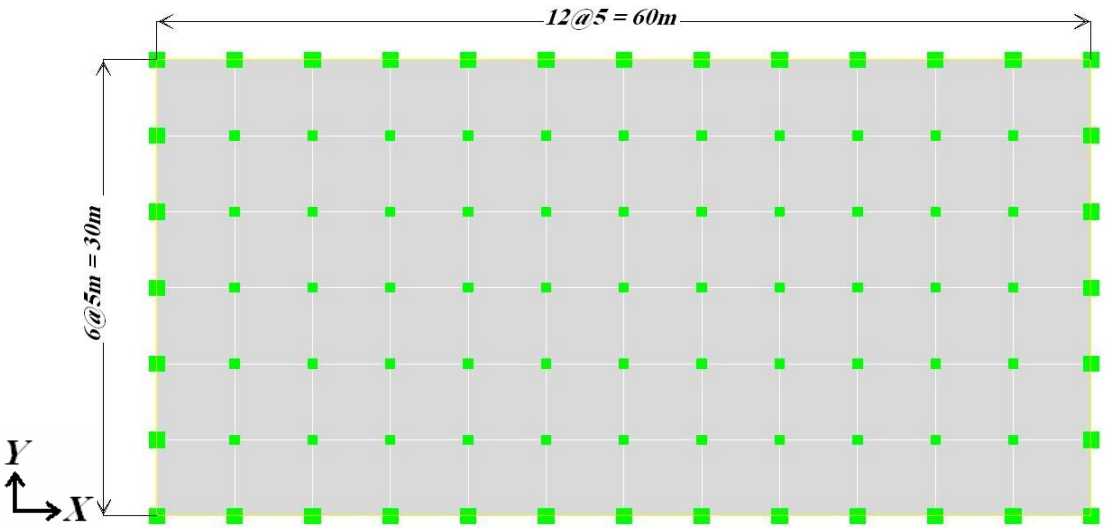

(a) Frame system

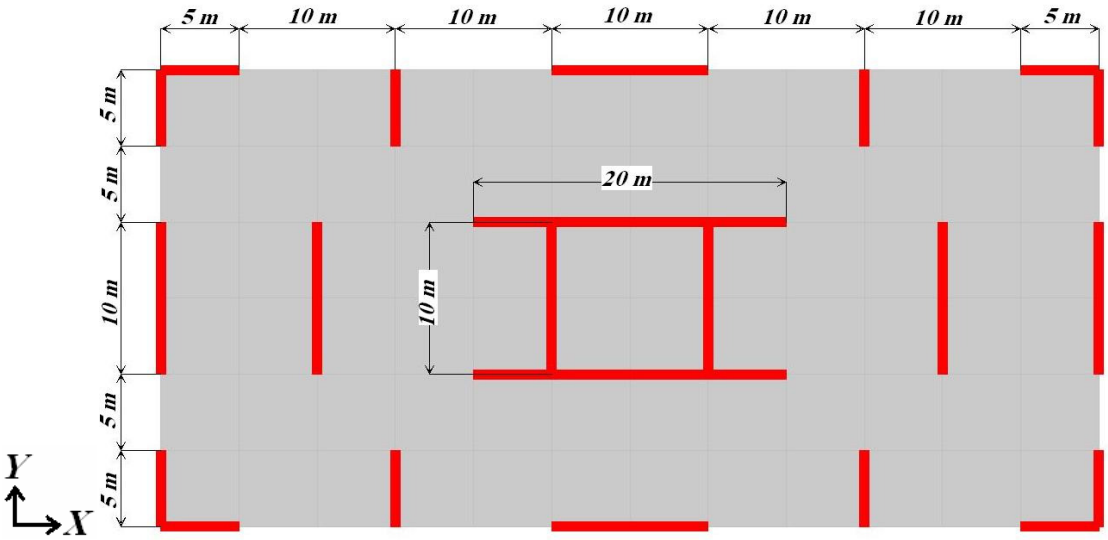

(b) Shear Wall System

Figure (4.2 a, b): High-Rise Building with Rectangular Plan Geometry

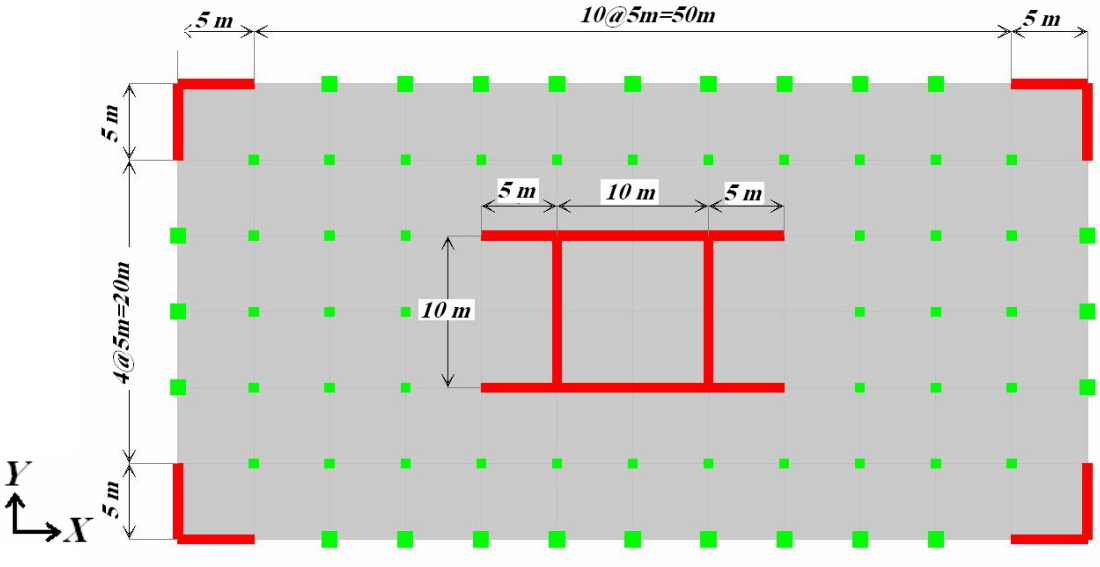

(c) Wall-Frame System

Figure (4.2 c): High-Rise Building with Rectangular Plan Geometry

Using ETABS software, 3D models have been generated as shown in Figure (3.3). Buildings are idealized as an assemblage of area, line and point objects. Those objects are used to represent walls, floors, columns and beams. The basic frame geometry is defined with reference to a simple three-dimensional grid system.

Torsional behavior of the floors and interstory compatibility of the floors are accurately reflected in the results.

As mentioned before all elements i.e. slabs and walls are assigned as full shell-type elements, which combine both in-plane and out-of-plane stiffness. Meshing for these elements have been carried out at each beam and intersected line with maximum size of 1m.

All data extracted from the models has been summarized and arranged in tables given in the next section.

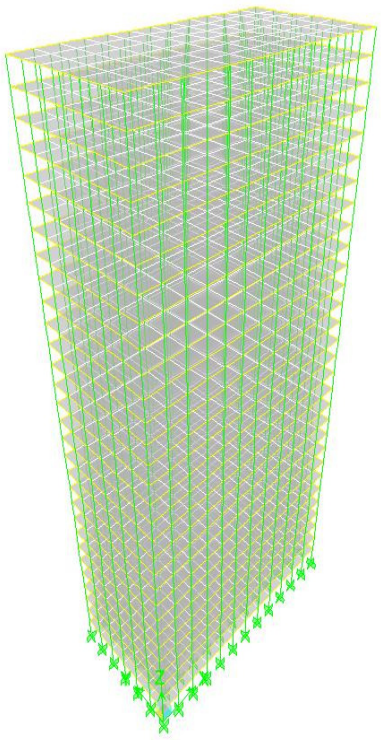

(a) 3D Rectangular Shape Tower, *F*

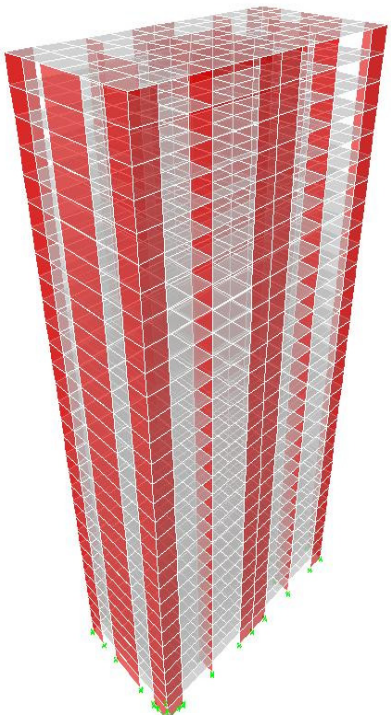

(b) 3D Rectangular Shape Tower, *SW*

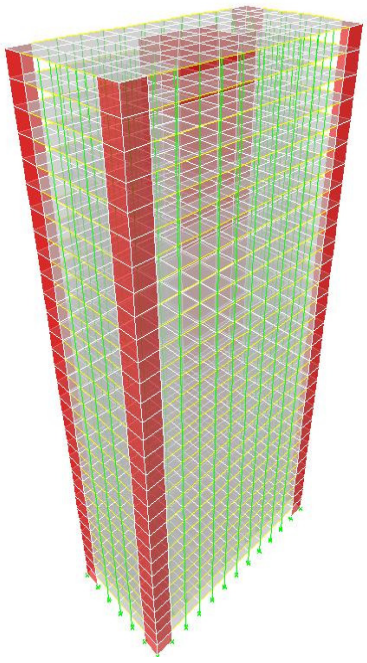

(c) 3D Rectangular Shape Tower, *DS*

Figure (4.3): 3D-ETABS Generated Profiles of Rectangular High-Rise Buildings

4.2.2. Comparison Tables

4.2.2.1. Maximum Diaphragm Drift Ratio Due to Earthquake in X-direction

Table [4.1]: Maximum Diaphragm Drift Ratio Due to E_X

Frame (*F*)			Shear Wall (*SW*)		Wall-Frame (*DS*)	
Story	**Point No.**	**Drift X (%)**	**Point No.**	**Drift X (%)**	**Point No.**	**Drift X (%)**
1	91	0.0445	85	0.0047	91	0.0052
2	85	0.0797		0.0100		0.0102
3		0.0879		0.0143		0.0138
4	91	0.0891		0.0180		0.0168
5		0.0884	91	0.0211		0.0192
6	85	0.0870		0.0239		0.0213
7	91	0.0855		0.0262		0.0230
8	85	0.0839		0.0283		0.0244
9	91	0.0823	85	0.0301		0.0255
10	85	0.0805		0.0317		0.0265
11	91	0.0825		0.0335		0.0278
12	85	0.0806	91	0.0350		0.0285
13		0.0789		0.0363		0.0291
14	91	0.0771		0.0374		0.0295
15		0.0753		0.0384		0.0297
16		0.0733		0.0393		0.0299
17	85	0.0712		0.0400		0.0300
18		0.0689		0.0407		0.0300
19	91	0.0666		0.0413		0.0300
20		0.0641		0.0417		0.0298
21		0.0663		0.0426		0.0301
22		0.0637		0.0430		0.0297
23	85	0.0604		0.0432		0.0293
24		0.0567		0.0432		0.0287
25	91	0.0525		0.0430		0.0280
26	85	0.0476	85	0.0427		0.0273
27	91	0.0419		0.0423		0.0264
28		0.0353		0.0417		0.0256
29	85	0.0279		0.0411		0.0247
30		0.0207		0.0404		0.0237

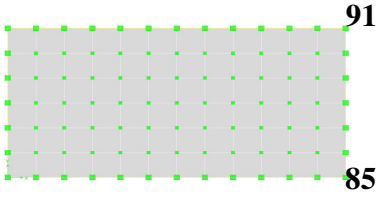

4.2.2.2. Maximum Diaphragm Drift Ratio Due to Earthquake in Y-direction

Table [4.2]: Maximum Diaphragm Drift Ratio Due to E_Y

Frame (*F*)			Shear Wall (*SW*)		Wall-Frame (*DS*)	
Story	**Point No.**	**Drift Y (%)**	**Point No.**	**Drift Y (%)**	**Point No.**	**Drift Y (%)**
1	7	0.0545	7	0.0061	7	0.0074
2		0.1019		0.0133		0.0145
3	91	0.1151		0.0189		0.0193
4	7	0.118	91	0.0234		0.0232
5	91	0.1177	7	0.0271		0.0263
6		0.1163		0.0302		0.0287
7	7	0.1146	91	0.0327		0.0306
8	91	0.1129		0.0347		0.0321
9	7	0.1112	7	0.0364		0.0333
10		0.1094	91	0.0377		0.0342
11		0.1126		0.0394		0.0357
12	91	0.1108	7	0.0405		0.0364
13		0.1089		0.0413		0.0369
14	7	0.1069		0.0420		0.0372
15		0.1047		0.0425		0.0374
16	91	0.1023	91	0.0429		0.0375
17		0.0998		0.0431		0.0376
18	7	0.0971		0.0432		0.0376
19		0.0944		0.0433		0.0375
20	91	0.0918	7	0.0432		0.0374
21	7	0.096	91	0.0436		0.0379
22	91	0.0934		0.0433		0.0376
23		0.0895		0.0428		0.0372
24	7	0.0850		0.0422		0.0366
25		0.0798		0.0415		0.0358
26		0.0737		0.0406		0.0348
27		0.0666	7	0.0396		0.0338
28	91	0.0583		0.0386		0.0326
29		0.0489		0.0375		0.0315
30	7	0.0402		0.0366		0.0302

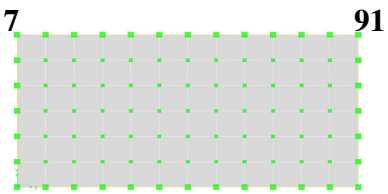

4.2.2.3. Diaphragm Center of Mass (*C.M.*) Displacement X Due to E_X

The relation between center of mass and center of rigidity is very important especially in seismic design due to the eccentricity that exists between them, which produces large torsional moment. Torsion has proven to be one of the major causes of failures in previous earthquakes, hence the effect of torsion must be carefully considered in the design.

Building's center of mass is a point through which the base shear can be assumed to act. This base shear is resisted by the vertical members; each member may have a different rigidity and thus provides a different lateral resisting force in the opposite direction of the base shear. On the other hand, building's center of rigidity is a point through which the resultant of all the resisting forces acts.

If the building's center of mass does not coincide with its center of rigidity, the building will tend to act as if it is "pinned" at its center of rigidity. This topic will be discussed thoroughly in Chapter 5.

The next two Tables [4.3] and [4.4] represent the displacements in X and Y directions for the rigid diaphragm at center of mass (*C.M.*).

Table [4.3]: Diaphragm *C.M.* Displacement X Due to E_X

X - Displacement (*cm*)			
Story	**Frame *(F)***	**Shear Wall *(SW)***	**Wall-Frame *(DS)***
1	0.16	0.02	0.02
2	0.45	0.05	0.05
3	0.78	0.11	0.10
4	1.1	0.17	0.16
5	1.43	0.25	0.23
6	1.74	0.34	0.31
7	2.06	0.44	0.39
8	2.36	0.55	0.48
9	2.65	0.66	0.57
10	2.94	0.78	0.67
11	3.23	0.90	0.77
12	3.51	1.04	0.87
13	3.78	1.17	0.98
14	4.04	1.31	1.09
15	4.3	1.45	1.19
16	4.54	1.60	1.30
17	4.78	1.74	1.41
18	5.01	1.89	1.52
19	5.22	2.04	1.62
20	5.43	2.20	1.73
21	5.64	2.35	1.84
22	5.83	2.50	1.94
23	6.02	2.66	2.04
24	6.19	2.82	2.15
25	6.34	2.97	2.24
26	6.49	3.13	2.34
27	6.61	3.28	2.43
28	6.72	3.43	2.53
29	6.8	3.58	2.61
30	6.87	3.73	2.70

4.2.2.4. Diaphragm *C.M.* Displacement Y Due to E_Y

Table [4.4]: Diaphragm *C.M.* Displacement Y Due to E_Y

Y - Displacement (*cm*)			
Story	**Frame (*F*)**	**Shear Wall (*SW*)**	**Wall-Frame (*DS*)**
1	0.16	0.02	0.02
2	0.47	0.06	0.06
3	0.82	0.12	0.12
4	1.19	0.19	0.19
5	1.56	0.28	0.27
6	1.92	0.37	0.35
7	2.28	0.48	0.44
8	2.63	0.59	0.54
9	2.98	0.70	0.64
10	3.32	0.83	0.75
11	3.66	0.95	0.86
12	4	1.08	0.98
13	4.34	1.22	1.09
14	4.67	1.35	1.21
15	4.98	1.49	1.33
16	5.3	1.63	1.45
17	5.6	1.77	1.56
18	5.89	1.91	1.68
19	6.18	2.05	1.80
20	6.45	2.20	1.92
21	6.74	2.34	2.04
22	7.01	2.48	2.16
23	7.28	2.62	2.28
24	7.53	2.76	2.40
25	7.76	2.89	2.51
26	7.98	3.03	2.63
27	8.17	3.16	2.74
28	8.35	3.29	2.85
29	8.51	3.41	2.95
30	8.64	3.54	3.06

4.2.2.5. Story Forces Due to E_X

Table [4.5]: Story Forces Due to E_X

Story	Frame (*F*)			Shear Wall (*SW*)			Wall-Frame (*DS*)		
	V_X*10^3 (kN)	T_X*10^6 (kN.m)	M_Y*10^6 (kN.m)	V_X*10^3 (kN)	T_X*10^6 (kN.m)	M_Y*10^6 (kN.m)	V_X*10^3 (kN)	T_X*10^6 (kN.m)	M_Y*10^6 (kN.m)
1	23.0	0.424	1.610	22.9	0.418	1.270	23	0.415	1.490
2	22.8	0.420	1.530	22.7	0.415	1.200	22.8	0.413	1.410
3	22.5	0.412	1.450	22.4	0.409	1.130	22.6	0.407	1.340
4	22.0	0.401	1.380	22	0.400	1.070	22.2	0.399	1.270
5	21.4	0.390	1.300	21.3	0.389	1.000	21.6	0.389	1.200
6	20.8	0.378	1.230	20.6	0.375	0.940	21	0.378	1.130
7	20.2	0.367	1.160	19.7	0.360	0.890	20.3	0.365	1.070
8	19.7	0.355	1.100	18.8	0.343	0.840	19.6	0.351	1.010
9	19.1	0.344	1.030	17.8	0.325	0.790	18.8	0.337	0.950
10	18.6	0.333	0.960	16.7	0.306	0.750	18	0.322	0.890
11	18.2	0.323	0.900	15.8	0.289	0.710	17.2	0.308	0.840
12	17.7	0.314	0.840	14.9	0.273	0.670	16.6	0.295	0.790
13	17.2	0.304	0.780	14.1	0.258	0.640	15.9	0.283	0.740
14	16.7	0.294	0.720	13.4	0.244	0.600	15.3	0.271	0.690
15	16.2	0.283	0.660	12.7	0.232	0.570	14.7	0.260	0.640
16	15.6	0.272	0.600	12.2	0.221	0.530	14.2	0.250	0.590
17	15.1	0.261	0.550	11.9	0.213	0.500	13.8	0.241	0.550
18	14.5	0.250	0.490	11.6	0.206	0.460	13.4	0.232	0.500
19	13.9	0.239	0.440	11.4	0.200	0.420	13	0.224	0.450
20	13.3	0.227	0.390	11.3	0.196	0.380	12.6	0.216	0.400
21	12.7	0.216	0.340	11.2	0.192	0.340	12.3	0.208	0.360
22	12.1	0.204	0.290	11.1	0.188	0.300	11.8	0.200	0.310
23	11.4	0.191	0.250	10.8	0.183	0.260	11.3	0.190	0.260
24	10.6	0.177	0.200	10.5	0.176	0.220	10.7	0.179	0.220
25	9.7	0.161	0.160	9.9	0.165	0.170	9.9	0.165	0.170
26	8.6	0.143	0.120	9.1	0.152	0.130	9	0.149	0.130
27	7.3	0.121	0.080	8.1	0.133	0.100	7.8	0.128	0.090
28	5.8	0.096	0.050	6.6	0.109	0.060	6.3	0.104	0.060
29	4.1	0.067	0.030	4.7	0.078	0.030	4.4	0.073	0.030
30	2.1	0.034	0.010	2.4	0.039	0.010	2.2	0.037	0.010

*Where M_Y: moment around Y-axis, V_X: shear in X-direction and T_X: torsion due to E_X.

4.2.2.6. Story Forces Due to E_Y

Table [4.6]: Story Forces Due to E_Y

	Frame (*F*)			Shear Wall (*SW*)			Wall-Frame (*DS*)		
Story	V_Y*10^3 (kN)	T_Y*10^6 (kN.m)	M_X*10^6 (kN.m)	V_Y*10^3 (kN)	T_Y*10^6 (kN.m)	M_X*10^6 (kN.m)	V_Y*10^3 (kN)	T_Y*10^6 (kN.m)	M_X*10^6 (kN.m)
1	18.5	0.699	1.240	25.8	0.938	1.570	18.4	0.677	1.080
2	18.3	0.690	1.180	25.6	0.931	1.480	18.3	0.672	1.020
3	17.9	0.675	1.120	25.3	0.919	1.400	18	0.661	0.960
4	17.5	0.656	1.070	24.9	0.901	1.330	17.6	0.646	0.910
5	17.0	0.635	1.010	24.2	0.878	1.250	17.1	0.626	0.860
6	16.5	0.614	0.950	23.5	0.850	1.180	16.5	0.604	0.810
7	16.0	0.593	0.900	22.6	0.818	1.110	15.8	0.579	0.770
8	15.5	0.574	0.850	21.6	0.783	1.050	15.1	0.553	0.720
9	15.1	0.555	0.800	20.6	0.746	0.990	14.4	0.526	0.690
10	14.7	0.538	0.750	19.6	0.709	0.940	13.6	0.499	0.650
11	14.3	0.522	0.700	18.7	0.674	0.880	12.9	0.473	0.610
12	14.0	0.506	0.650	17.8	0.642	0.830	12.3	0.450	0.580
13	13.6	0.490	0.610	17	0.611	0.780	11.7	0.428	0.550
14	13.2	0.474	0.560	16.2	0.582	0.740	11.3	0.409	0.520
15	12.8	0.457	0.520	15.6	0.557	0.690	10.8	0.391	0.480
16	12.4	0.440	0.480	15	0.534	0.640	10.5	0.376	0.450
17	11.9	0.422	0.430	14.6	0.515	0.590	10.2	0.364	0.420
18	11.5	0.404	0.390	14.2	0.498	0.540	10	0.353	0.390
19	11.1	0.386	0.350	13.9	0.483	0.500	9.8	0.344	0.350
20	10.6	0.368	0.310	13.6	0.469	0.450	9.7	0.335	0.320
21	10.2	0.351	0.280	13.4	0.455	0.400	9.5	0.327	0.280
22	9.7	0.333	0.240	13	0.440	0.350	9.4	0.318	0.250
23	9.3	0.315	0.200	12.6	0.423	0.290	9.1	0.307	0.210
24	8.7	0.294	0.170	12	0.401	0.240	8.7	0.292	0.180
25	8.1	0.270	0.130	11.2	0.373	0.200	8.2	0.273	0.140
26	7.3	0.243	0.100	10.2	0.338	0.150	7.5	0.248	0.110
27	6.3	0.210	0.070	8.9	0.294	0.110	6.6	0.217	0.080
28	5.1	0.170	0.050	7.2	0.238	0.070	5.4	0.177	0.050
29	3.7	0.121	0.020	5.1	0.169	0.040	3.8	0.127	0.030
30	1.9	0.063	0.010	2.6	0.084	0.010	1.9	0.064	0.010

*Where M_X: moment around X-axis, V_Y: shear in Y-direction and T_Y: torsion due to E_Y.

4.2.3. Graphical Presentation

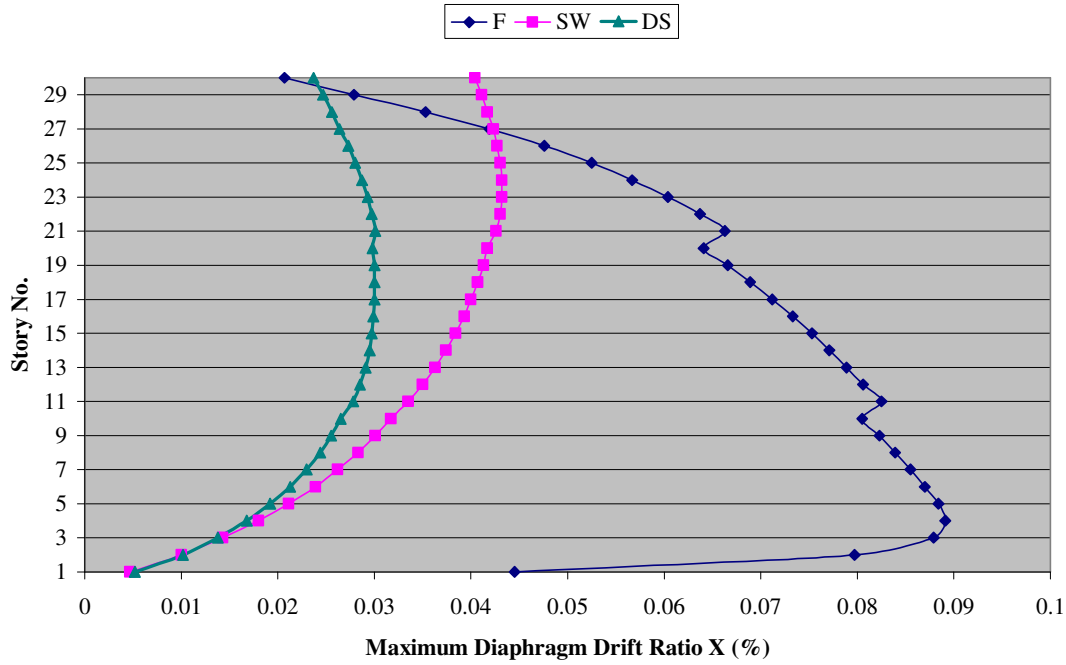

Figure (4.4): Rectangular Shape – Maximum Diaphragm Drift Ratio Due to E_X

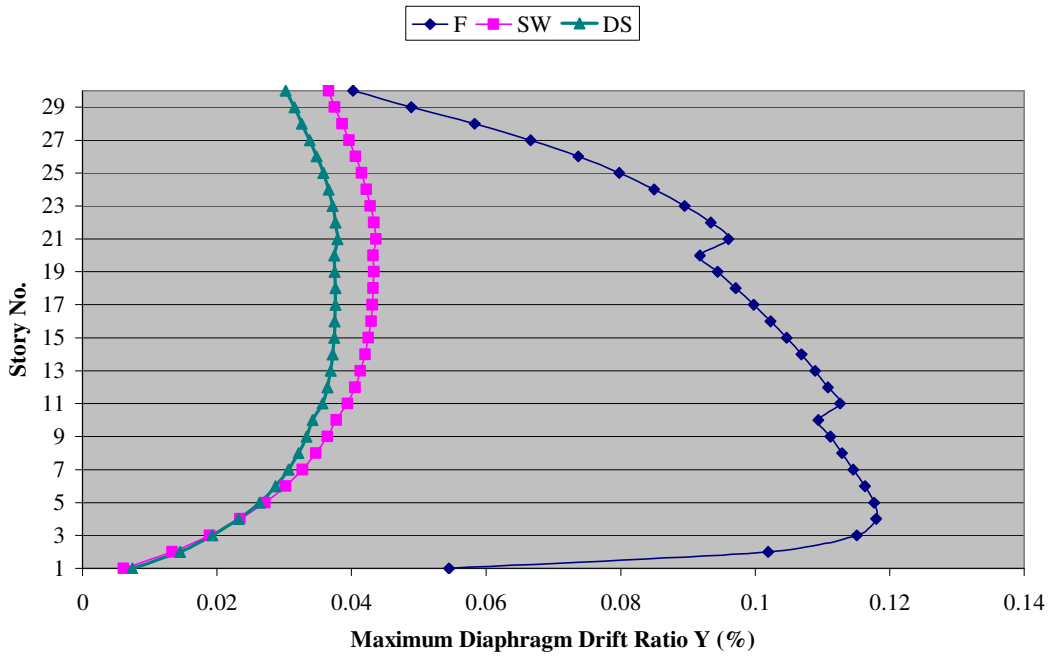

Figure (4.5): Rectangular Shape – Maximum Diaphragm Drift Ratio Due to E_Y

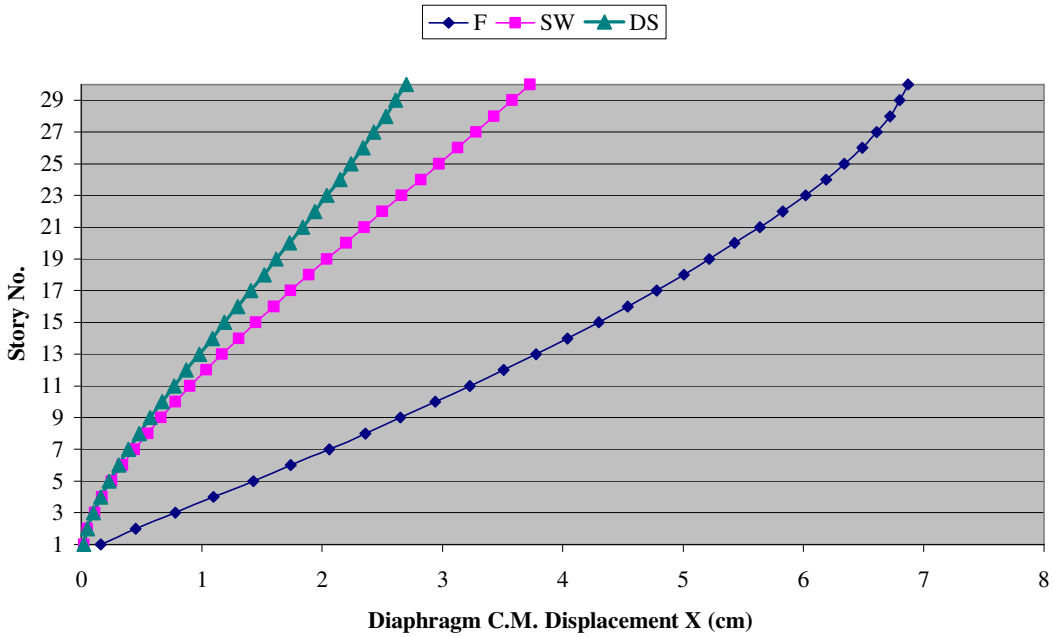

Figure (4.6): Rectangular Shape – Diaphragm *C.M.* Displacement X Due to E_X

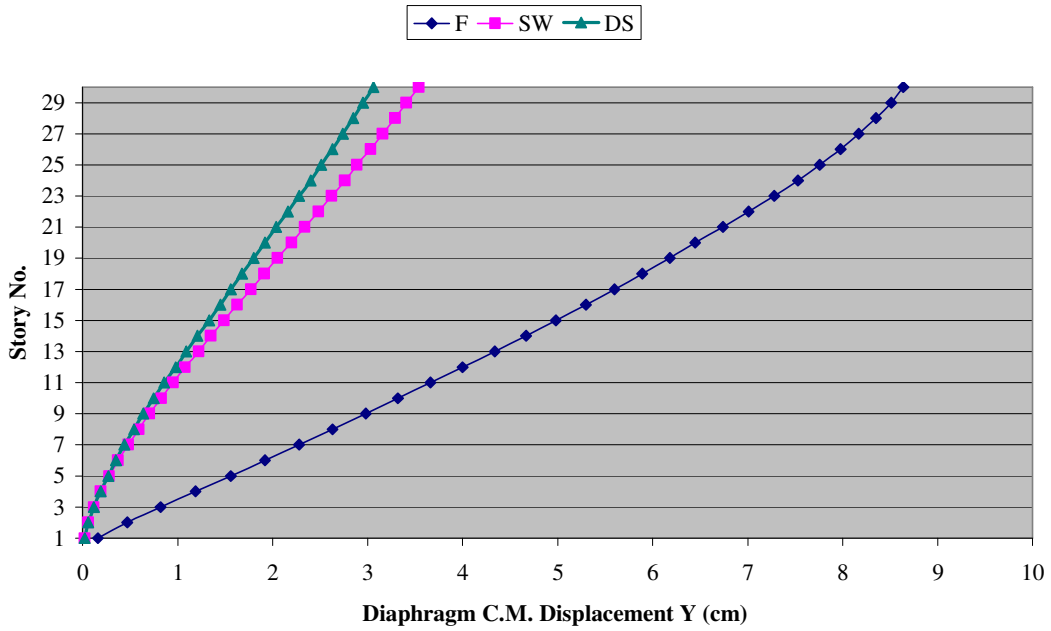

Figure (4.7): Rectangular Shape – Diaphragm *C.M.* Displacement Y Due to E_Y

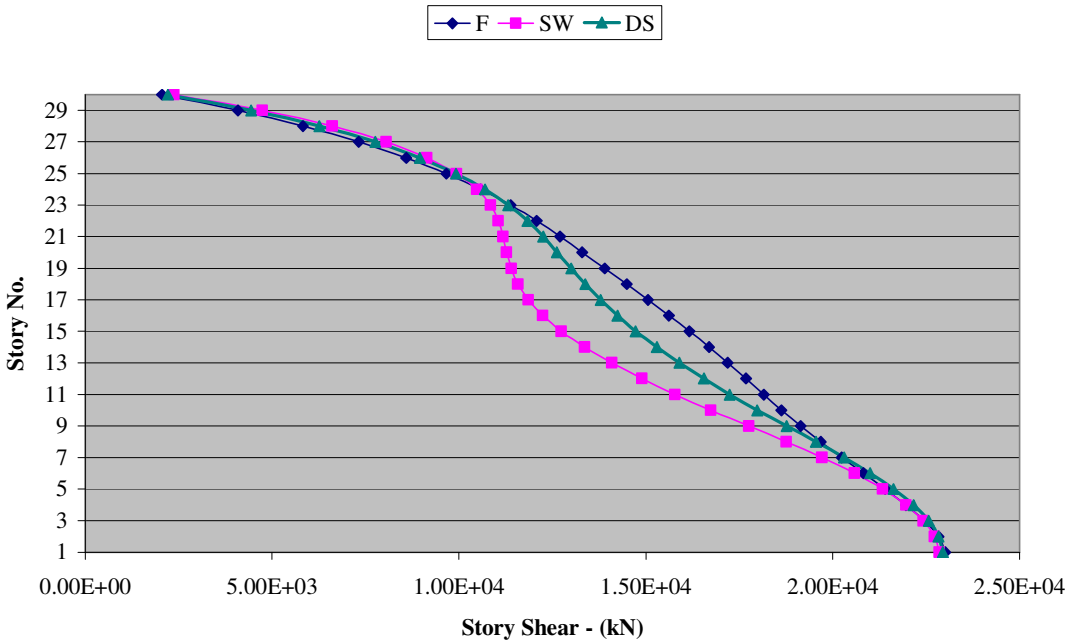

Figure (4.8): Rectangular Shape – Story Shear V_X Due to E_X

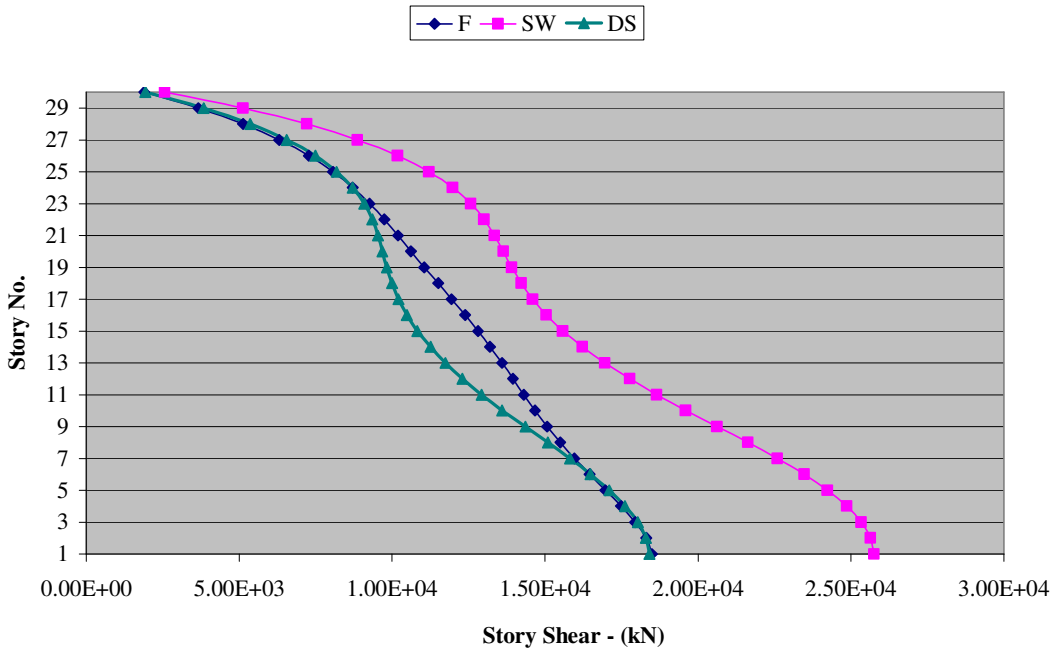

Figure (4.9): Rectangular Shape – Story Shear V_Y Due to E_Y

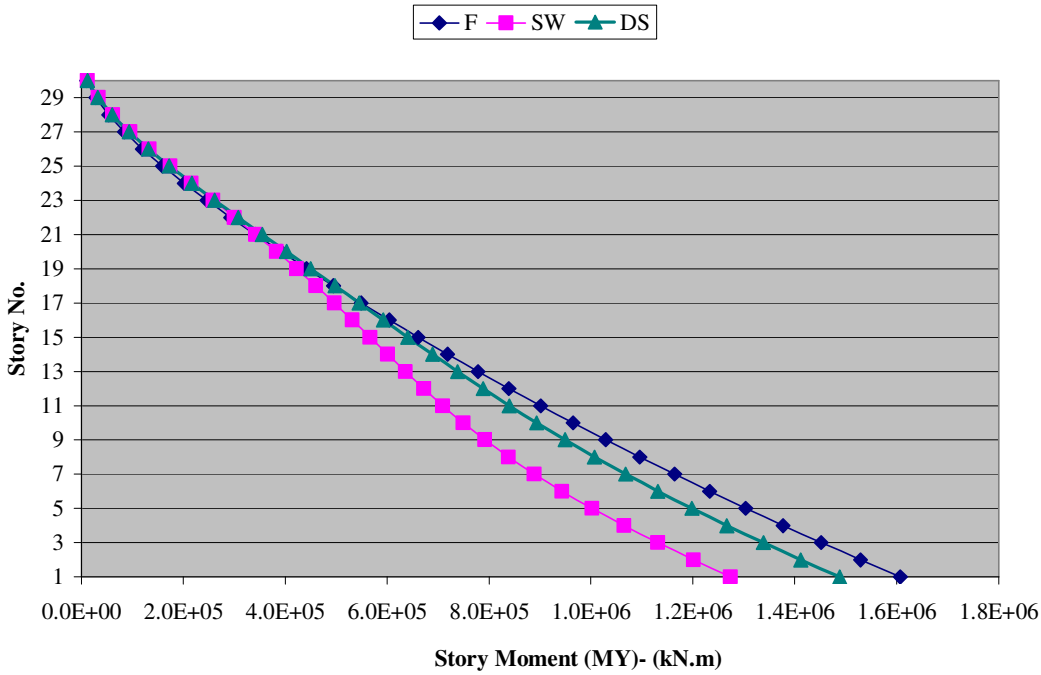

Figure (4.10): Rectangular Shape – Story Moment M_Y Due to E_X

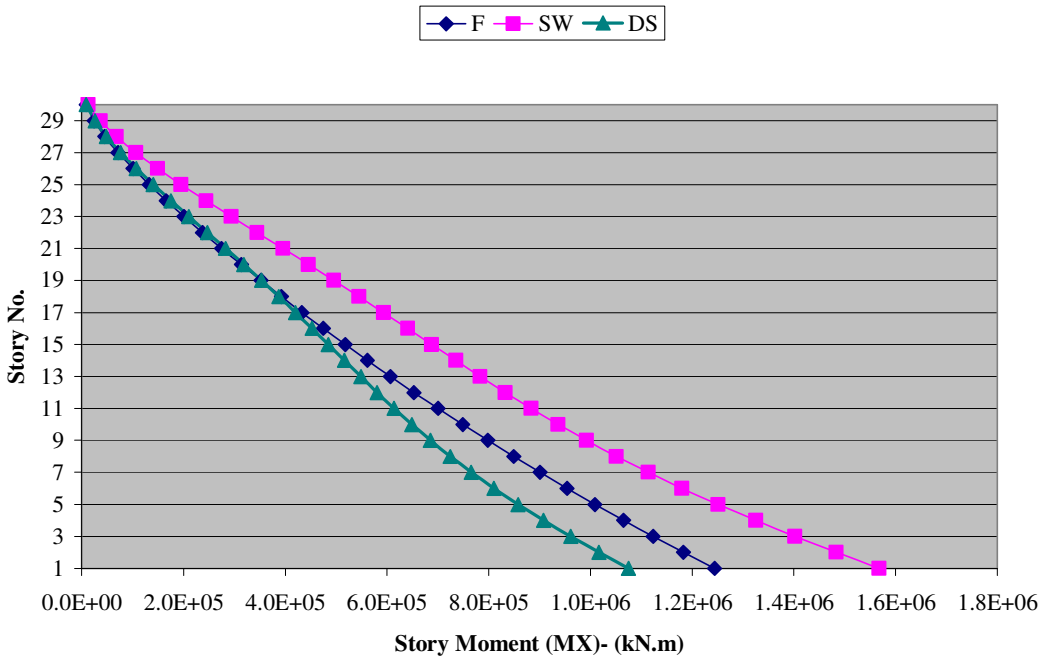

Figure (4.11): Rectangular Shape – Story Moment M_X Due to E_Y

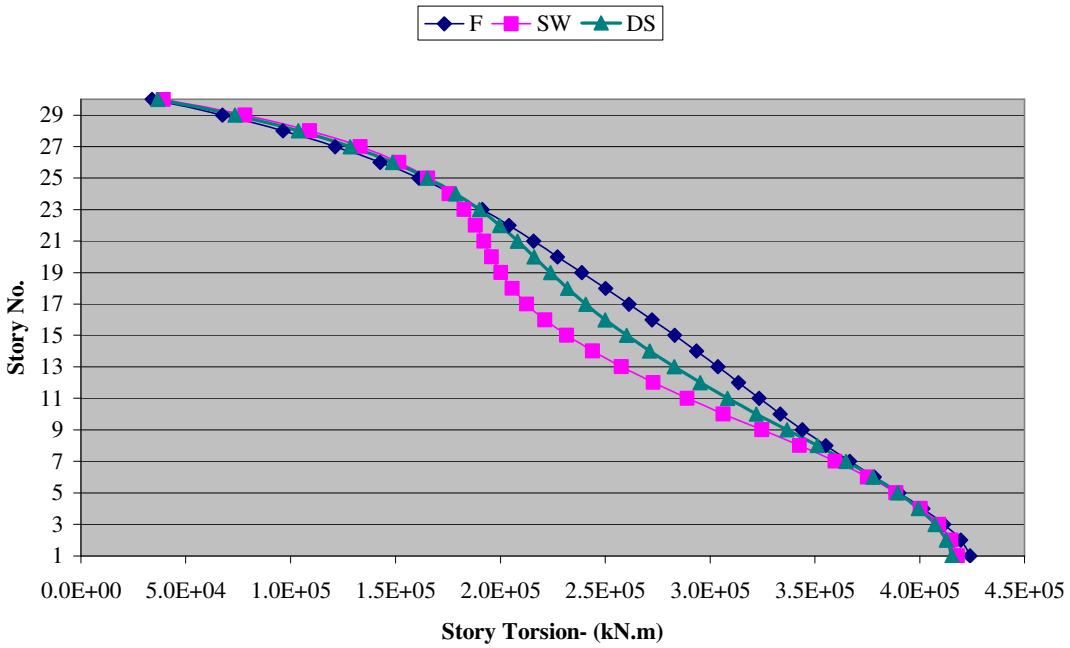

Figure (4.12): Rectangular Shape – Story Torsion (T_X) Due to E_X

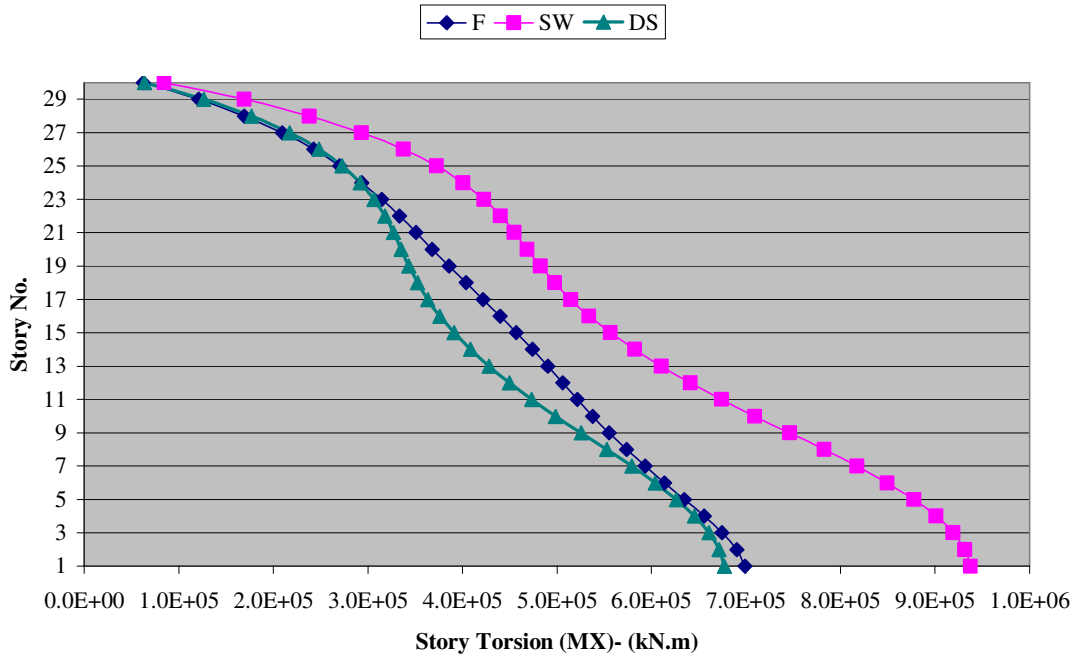

Figure (4.13): Rectangular Shape – Story Torsion (T_Y) Due to E_Y

4.2.4. Summary of Results for Rectangular Shape

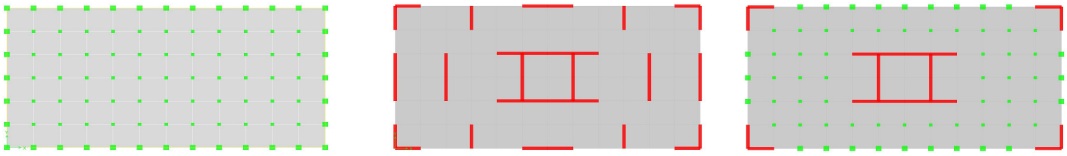

Figure (4.14): Rectangular Shape with Three Structural Systems

Table [4.7]: Summary of Results- Rectangular Shape

	F	***SW***	***DS***
Max. drift Ratio X- %	0.089	0.043	0.030
Max. drift Ratio Y- %	0.118	0.044	0.038
C.M. Absolute Max. displacement X-cm	6.9	3.7	2.7
C.M. Absolute Max. displacement Y-cm	8.6	3.5	3.1
Base shear-*VX*- kN (10^3)	23	22.9	23
Base shear –*VY*- kN (10^3)	18.5	25.8	18.4
Base moment-*MY*- kN (10^6)	1.61	1.27	1.49
Base moment –*MX*- kN.m (10^6)	1.24	1.57	1.08
Base torsion-*TX*- kN.m (10^6)	0.424	0.418	0.415
Base torsion-*TY*- kN.m (10^6)	0.70	0.94	0.68
First mode shape period – sec.	3.15	2.04	2.02

The building stiffness has been calculated for comparison purposes by placing the static seismic forces according to the IBC equivalent force procedure at the center of mass (*C.M.*) for each story distributed vertically in a power distribution applied in the two directions X and Y. Then the stiffness is simply calculated by dividing the total base shear force over the calculated maximum top displacement in each direction.

To illustrate this method the overall building stiffness in the X- direction has been calculated using the equivalent static force procedure for the frame system by dividing the base shear which is equal $V = 23000$ kN over the maximum top displacement which is $\Delta_{Top} = 0.09$ *cm* caused by the distributed story forces placed at *C.M.* This distribution follows an exponential curve with $K = 2$ as the period T of this structure > 2.5.

Therefore, the overall building stiffness in the X-direction can be approximated as follows:

$K = V/\Delta_{Top} = 23000/0.09 = 2.5 \times 10^5$ kN/m.

The concept employed in the equivalent static lateral force method is to place static loads on a structure with magnitudes and direction that closely approximate the effects of dynamic loading caused by earthquakes. Concentrated lateral forces due to dynamic loading tend to occur at floor and ceiling/roof levels in buildings, where concentration of mass is the highest. Furthermore, concentrated lateral forces tend to be larger at higher elevations in a structure. Thus, the greatest lateral displacements and the largest lateral forces often occur at the top level of a structure (particularly for tall buildings).

In general, the distribution of lateral story forces is associated with the first (fundamental) mode of vibration of a cantilevered structure. (In this case, a typical structure is idealized as a vertical cantilever rigidly attached to the ground.) The effects of higher modes of vibration differ from UBC 1997 to IBC 2003.

In the UBC this effect is implemented by considering an additional lateral force, F_t, applied to the top level of a structure equal to $(0.07\ T\ V)$, and this is only when the building period > 0.7 sec.. But in the case of this study the IBC 2003 addresses the effects of higher modes of vibration when calculating story forces, F_x, by utilizing an exponential distribution, $1 < k < 2$, that can vary based on the natural (fundamental) period of vibration of the structure. On the contrary, the distribution of the UBC 1997 assumes the structure responds in first mode of vibration only which is a linear distribution.

Consequently, the vertical distribution of the base shear is expressed in the UBC 1997 and for a building period $T > 0.7$ sec. as follows:

For top force $F_t = 0.07\ T\ V \leq 0.25\ V$

The rest of the base shear, i.e. *(V- F_t),* is given as,

$$F_x = \frac{w_x\ h_x}{\sum w_i\ h_i}(V - F_t\ ) \tag{4.1}$$

This distribution is given in Figure (4.15) with the force F_t. Note that the top floor force equals both F_t and F_n.

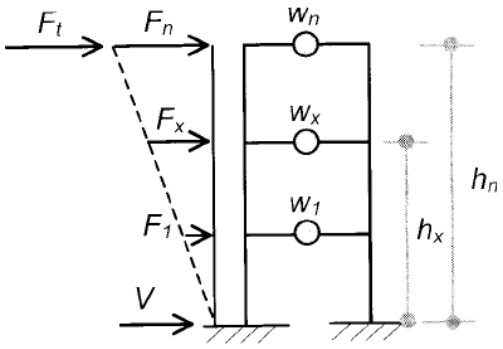

Figure (4.15): Vertical Seismic Force Distribution According to the UBC 1997, (Armouti , 2004).

In the IBC 2003 this distribution also assumes that the structure responds in the first mode only. The floor forces, F_x, are given by:

$$F_x = C_{vx}\ V \tag{4.2}$$

where, $C_{Vx} = \frac{w_x\ h_x^{\ k}}{\sum w_i\ h_i^{\ k}}$, the power k is taken as follows :

k = 1, for $T \leq 0.5$ sec.

k = 2, for $T \geq 2.5$ sec.

Interpolation can be used to calculate k values for periods in between.

The above values of k indicate that for long period structures, the value of k increases the degree of curvature which transfers more forces to the upper stories as illustrated in Figure (4.16). This action is meant to include the effect of higher modes of long period structures which is analogous to the addition of the force F_t in the UBC code.

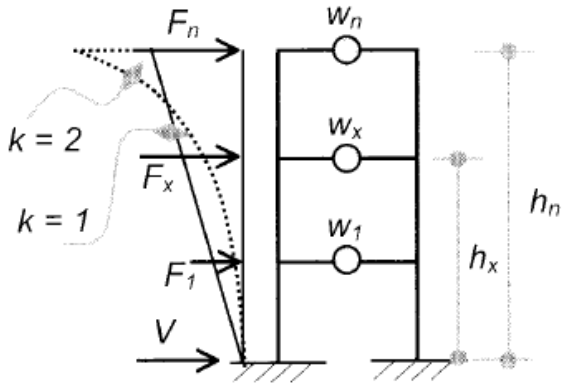

Figure (4.16): Vertical Seismic Force Distribution According to IBC 2003

Table [4.8]: Rectangular Shaped Building Stiffness

	$K_X^{(1)}$*10 ^{6}	$K_Y^{(2)}$ *10 ^{6}	K_X/K_Y
F	0.253	0.156	1.63
SW	0.535	0.810	0.66
DS	0.630	0.389	1.62

(1) K_X: Building Stiffness in X-direction, kN/m
(2) K_Y: Building Stiffness in Y-direction, kN/m

4.2.5. Synthesis of Results: Remarks and Comments

- **Drift Ratio Curves:** Refer to Figures (4.4) and (4.5)

  (1) The reduction of column and wall sizes every 10 stories affects the drift more in the case of frame system (*F*) than in the cases of shear wall system (*SW*) or dual system (*DS*). This can be explained by the way walls and columns have been reduced and by the direct relation between drift and stiffness. In walls, the reduction has been carried out only by reducing their thicknesses while keeping their lengths the same; hence the change in stiffness is insignificant because inertia, which is the primary function of stiffness, is proportioned by the cube of the length. While in columns, the change affects directly the whole gross section area, the inertia and in turn the stiffness. The stiffer the structure, the less drift can be observed.

(2) The *(F)* system drift curves have a steep positive slope in the first 3 stories, then a decreasing negative slope all the way up. This can be explained by the shear mode behavior of the *(F)* system. This behavior forces the relative displacement between adjacent floors to decrease while ascending to top of the building, which means a decrease in drift values (defined as the relative displacement of the adjacent story over height). However, the reason for the steep curves in the first stories is the presence of the assigned fixed supports at the bottom which counteracts the actual shear-mode behavior and injects in some way flexural behavior. If the supports have been assigned as pinned, the steep positive slope at the first stories will vanish as shown in Figure (4.17).

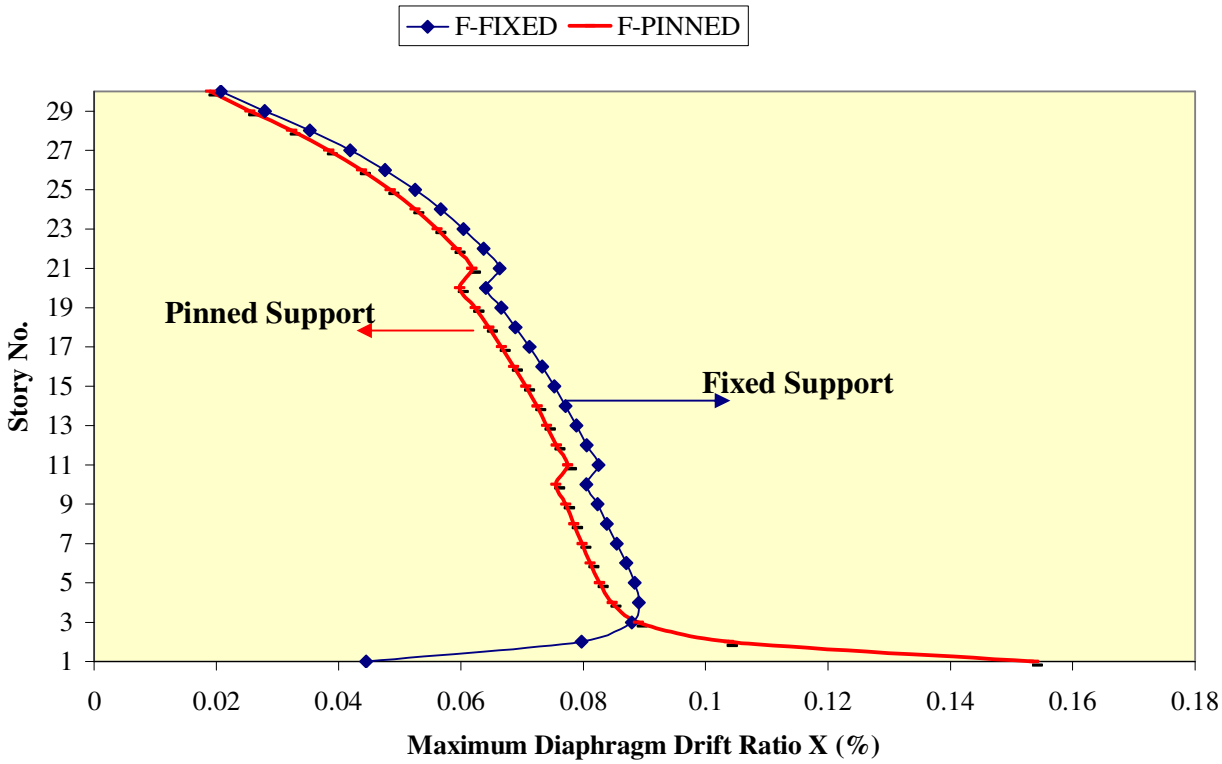

Figure (4.17): Effect of Support Type on Drift Calculations

(3) Maximum drift ratio in (*F)* system is 0.09% which is almost (2-3) times the other systems as noticed from Figures (4.4) and (4.5).

(4) The least drift values are observed in the (*DS)* system followed by the (*SW)* system then the (*F)* system, that leads us to say that the (*DS*) displays better behavior under lateral seismic loads in this case and provides a sense of human comfort during these motions because of the interaction between the deflected shapes of both, the frame and the shear wall systems.

(5) The curves in both the *(SW)* and *(DS)* systems rise smoothly in the lower two-thirds of the building height, then slightly decrease and converge to the inside in the last 10 stories. In contrast, the *(F)* system curve has a positive steep slope in the first 3 stories, then a negative slope in the last top stories. The trends displayed in the *(SW)* and *(DS)* systems are some what similar, but they are obviously different from that of *(F)* system.

- **Displacement Curves:** Refer to Figures (4.6) and (4.7)

(1) The curve for each system shows how the system behaves under lateral load. As can be seen the (*F)* system tends to behave in a shear mode with maximum slope at the top and (*SW)* system behaves in a distinct flexural mode with maximum slope at the bottom while the (*DS)* system has a flexural profile in the lower part and a shear profile in the upper part. This causes the walls to push back the frames near the base and the frames to pull back the walls at the top.

(2) Maximum displacement for the (*F)* system is 7cm in the long direction which is 2 times more than that of the (*SW)* system and 3 times that of the (*DS)* system in the

same direction. This shows that the (*DS)* system provides more rigidity than the other two systems, which is also indicated in Table [4.8].

(3) In the rectangular shape configuration the short direction displacement is more than long direction because it has lower stiffness.

- **Story Forces Curves:**

(1) The story shear curves rise smoothly throughout the height in the case of the (*F)* system and in an oscillating manner in the (*SW)* and (*DS*) systems. Refer to Figures (4.8) and (4.9).

(2) As can be noticed from Table [4.8], the stiffness ratio i.e. K_X/K_Y, which is almost identical of both the *(F)* and (*DS)* systems, is the result of both having the same base shear magnitude, refer to Table [4.7]. This leads us to say that it is not merely the stiffness of building in one direction which contributes to the behavior of a high-rise building under seismic loads, but it is the overall stiffness in the two directions which makes the difference.

(3) Contrary to the (*F)* and (*DS)* systems, the *(SW)* system has a base shear force in the short direction greater in value than the long direction as shown in Table [4.7]. That can be explained by the nature of the structural configuration of shear wall elements chosen which, in this case, produces a stiffness in the long direction equal to 0.66 that of the short one, i.e. the short direction is no longer the weak direction.

(4) The moment curves are methodically drawn without any inflection points as they are only a function of the story shear multiplied by the height. Refer to Figures (4.10) and (4.11).

(5) The shear force curve of the (*SW)* system shown in Figure (4.9) indicates the large forces that have been attracted by the shear walls due to the large inertia of these walls in this direction. In addition, (*SW)* masses add more weight than the other systems which influences base shear force magnitude, bearing in mind that earthquake loading is a function of the structure's weight. Resistance to lateral load is provided by shear walls or braced. Therefore, the *(DS)* system has been clearly introduced to reduce the number of shear wall elements in any structural layout plan by creating an interactive sharing system of story shear forces between frames and walls which also to help in reducing the economical issues. This system can be noted for example in the UBC 1997, that defines the system so that the moment-resisting frames to be designed to independently resist at least 25 percent of the design base shear and the whole system shall be designed to resist the total design base shear in proportion to their relative rigidities considering the interaction of the dual system at all levels.

(6) The torsional curves display the same pattern as the shear force curves in both directions, as the torsional moment is derived from the shear force multiplied by the eccentricity. Therefore, torsion and shear forces are interrelated. Refer to Figures (4.12) and (4.13).

(7) The torsional moment is larger in the Y-direction because of the minimum eccentricity of 5% which depends on the building width perpendicular to the earthquake direction i.e. 60*m* used for E_Y. The accidental 5% eccentricity need not be amplified according to the IBC because the maximum story drift, computed by

including accidental torsion at one end of the structure transverse to an axis, is not more than 1.2 times the average of the story drifts at the two ends of the structure.

(8) The *(DS)* system has the lowest fundamental period which is a good indication of its structural stiffness.

(9) The first mode of vibration tends to deflect in the direction that has less stiffness, as indicated in Figure (4.18). It can be noted also the period for the first mode displayed in the *(SW)* and *(DS)* systems are some what similar and obviously different from that of *(F)* system.

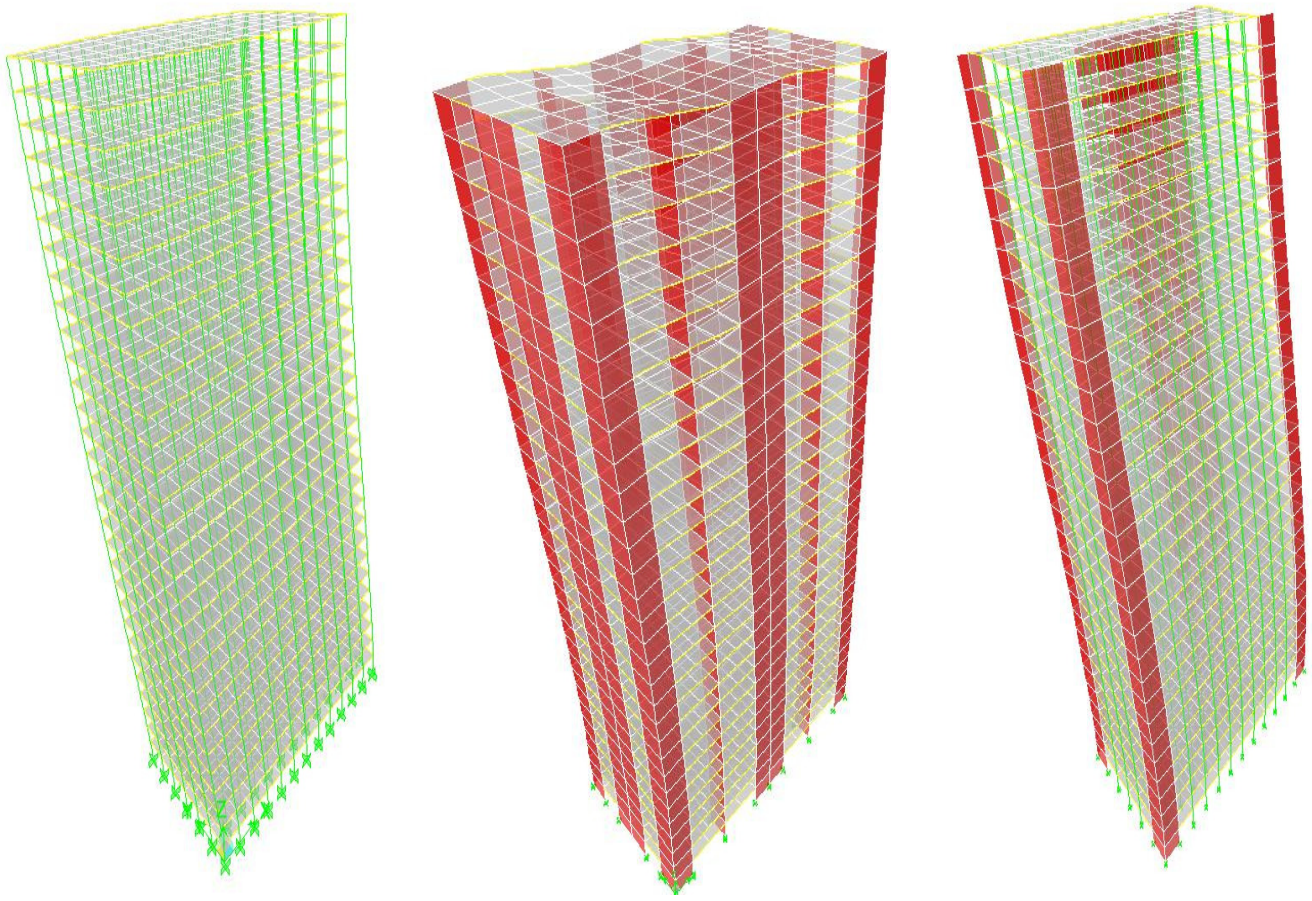

(a) *F* with *T*=3.15 sec. (b) *SW* with *T*=2.04 sec. (c) *DS* with *T*=2.02 sec.

Figure (4.18): Rectangular High-Rise Building -First Mode of Vibration (Natural Period)

4.3. Tracing the Trend – Examining curves for the Frame System

The original rectangular frame system *(F)* has been modified by reducing its stiffness to trace the effect of configuration on the overall results. Therefore, all columns along column lines A, B, C, D, E, and F have been removed as shown in Figure (4.19).

Using the same method outlined before for stiffness calculation, the stiffness for the new configuration is found to be equal to the following:

$K_{X\ modified} = 35\ \%\ K_{X\ original}$ and $K_{Y\ modified} = 56\ \%\ K_{Y\ original}$

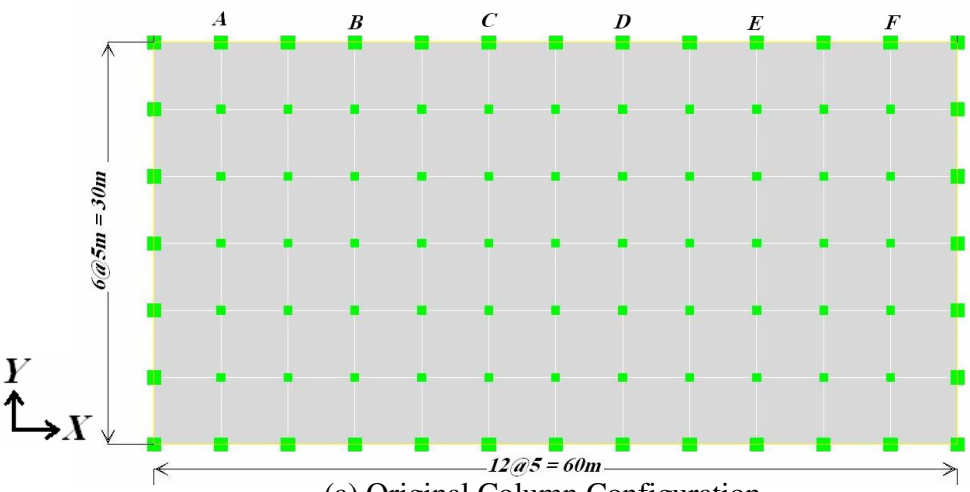

(a) Original Column Configuration

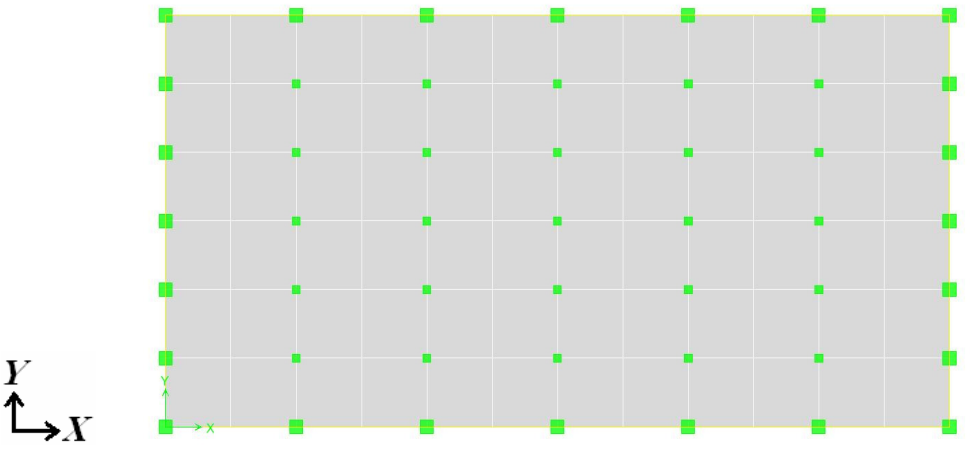

(b) New Column Configuration

Figure (4.19): Two Types of Frame System *(F)* Configurations

4.3.1. Graphical Presentation

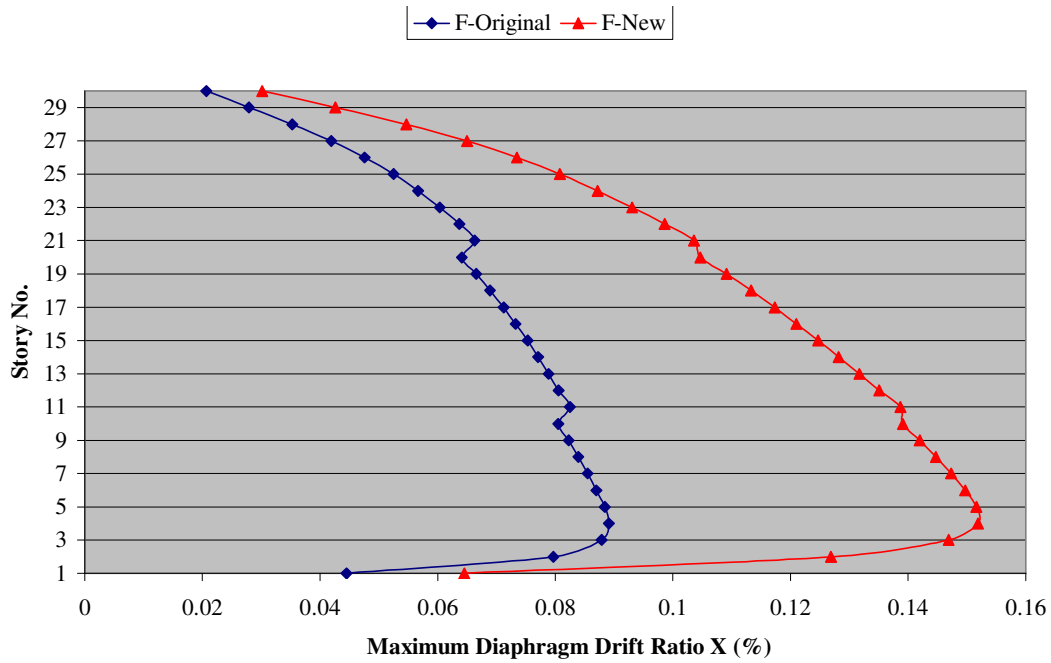

Figure (4.20): Rect. Shape – Max. Diaphragm Drift Ratio Due to E_X-Different *F* Systems

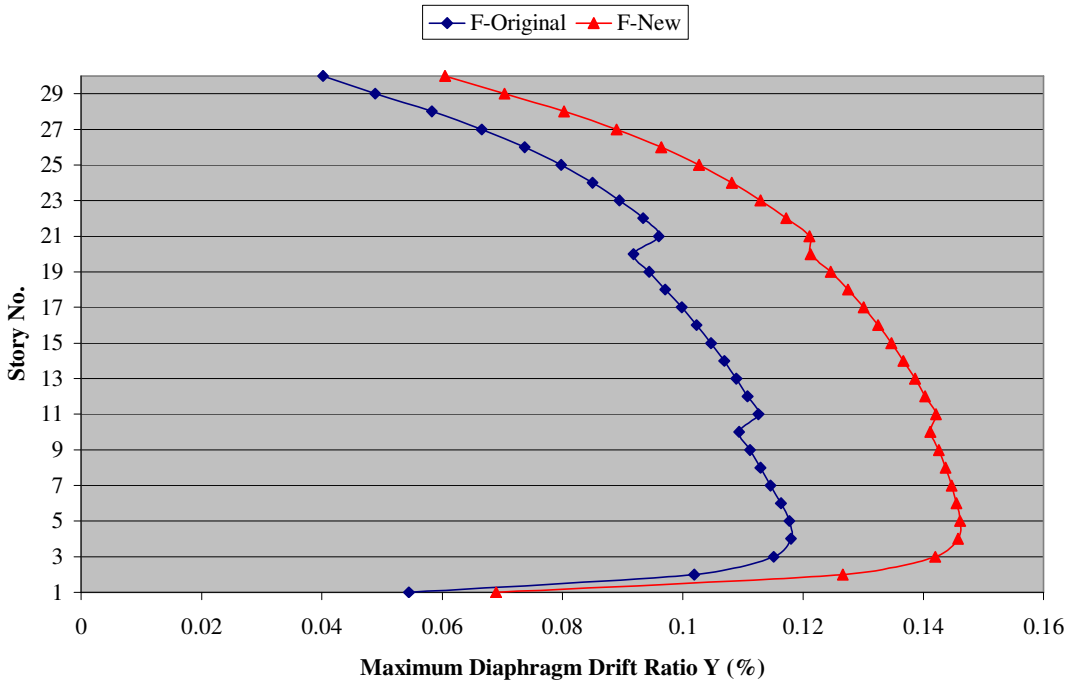

Figure (4.21): Rect. Shape– Max. Diaphragm Drift Ratio Due to E_Y-Different *F* Systems

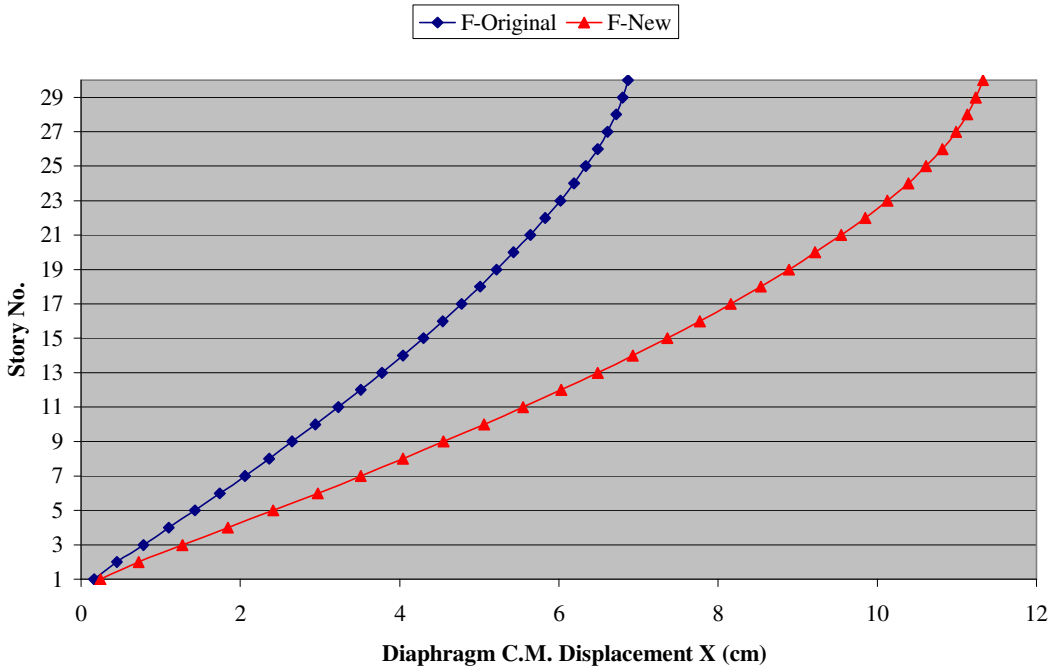

Figure (4.22): Rect. Shape – Max. Displacement X Due to E_X –Different *F* Systems

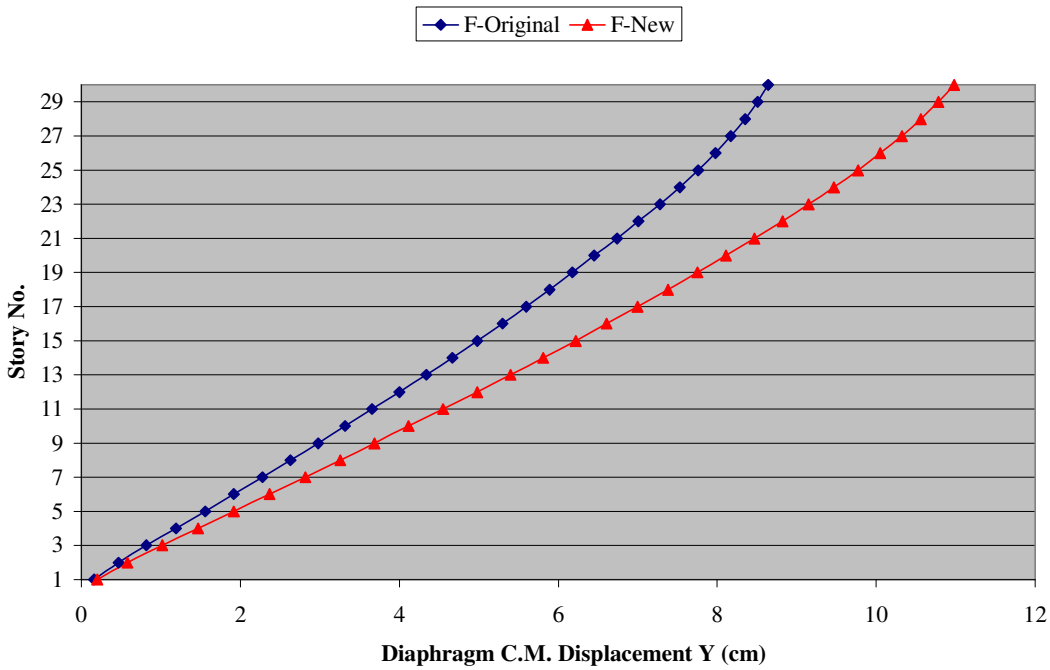

Figure (4.23): Rect. Shape – Max. Displacement Y Due to E_Y –Different *F* Systems

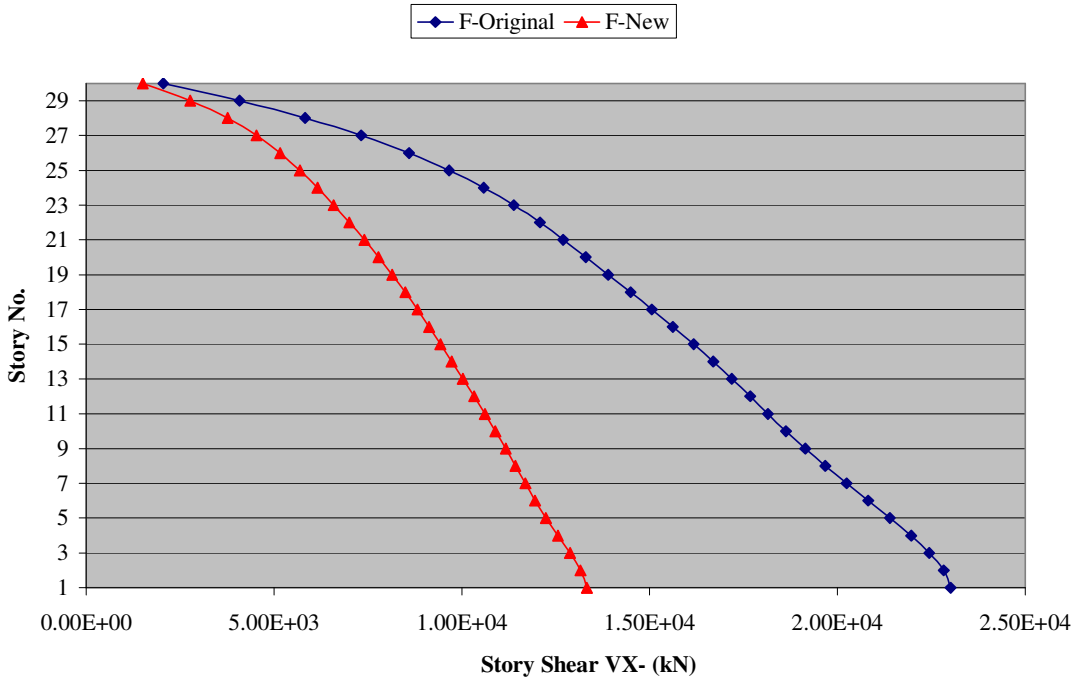

Figure (4.24): Rect. Shape – Story Shear X Due to E_X for Different *F* Systems

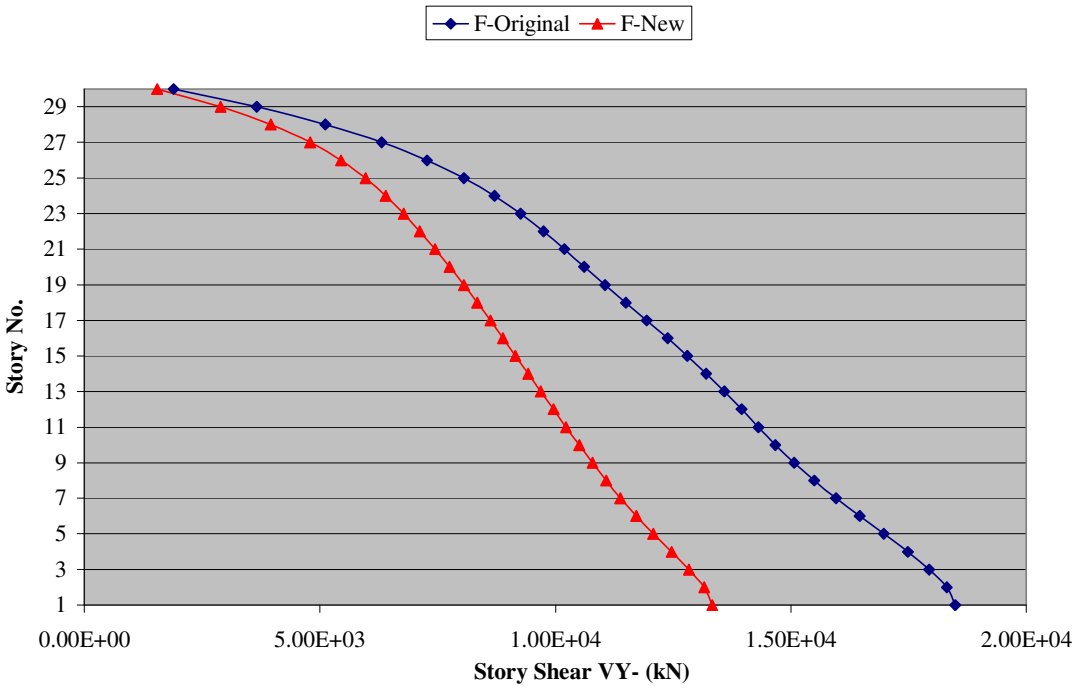

Figure (4.25): Rect. Shape – Story Shear Y Due to E_Y for Different *F* Systems

4.3.2. Comparing Results for Different Frame Systems

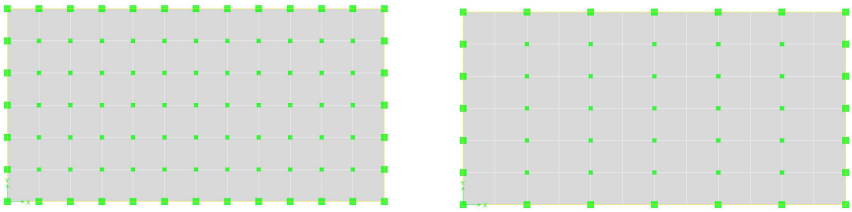

Figure (4.26): Rectangular Shape with Two Frame Systems Configuration

Table [4.9]: Summary of Results- Rectangular Shaped Building for Different (*F*) Systems

	$F_{ORIGINAL}$	$F_{MODIFIED}$	% Change
Maximum drift Ratio X- %	0.089	0.152	+70%
Maximum drift Ratio Y- %	0.118	0.146	+24%
C.M. Absolute Max. displacement X-cm	6.9	11.3	+64%
C.M. Absolute Max. displacement Y-cm	8.6	11.0	+28%
Base shear-V_X- kN (10^3)	23	13.3	-42%
Base shear –V_Y- kN (10^3)	18.5	13.3	-28%
First mode shape period – sec.	3.15	4.15	+32%

Table [4.10]: Rectangular Shaped Building Stiffness for Different Frame Systems

	$K_X^{(1)}*10^6$	$K_Y^{(2)}*10^6$	K_X/K_Y
$F_{Original}$	0.253	0.156	1.63
$F_{Modified}$	0.089	0.087	1.02
% Change	-65%	-44%	

(1) K_X: Building Stiffness in X-direction, kN /m
(2) K_Y: Building Stiffness in Y-direction, kN /m

4.3.3. Discussing the Effects of Different Frame systems

(1) The magnitude of the modified configuration drift values curves has increased as shown in Figures (4.20) and (4.21), because of the reduction in stiffness in both directions. This shows how the stiffness plays a significant role with regard to drift values; the more reduction of stiffness in any direction, the more increase in drifts and displacements there is.

(2) The steep slopes in the first stories shown in the drift curves, Figures (4.20) and (4.21), consolidate our understanding of how the frame behaves under lateral load i.e. the shear mode behavior. Shear mode produces minimum slope at the bottom of the building and a maximum one upward, which means large drifts in the lower stories and small in the upper ones.

(3) As observed, the new calculated base shears in both directions are the same, refer to Table [4.10], because the stiffness ratio $K_X/K_Y = 1.0$. Consequently, forces are distributed evenly to both directions. Also, this applies to both displacement and drift values which are close in magnitude.

(4) The displacement curves, Figures (4.22) and (4.23), indicate that the reduction in building stiffness affects clearly the higher stories more than the lower ones. In addition, the difference from the original curve is augmented while moving up the height of building.

(5) The reduction in stiffness produces a more flexible which is reflected in higher displacement values. This can be spotted from the first mode period which has increased from 3.15 to 4.15 sec. as shown in Table [4.9].

(6) The more flexible the structure becomes, the less ground acceleration absorbed by the structure, which in turn decreases the base shear force, see Figures (4.24) and (4.25). This reduction in forces happens at the account of increasing the displacement values. However, the structure can survive earthquake excitation as long as the maximum displacement demand doesn't reach the ultimate displacement capacity of the structure. Therefore, such displacements impose additional structural requirements in term of ductility and energy dissipation.

4.4. Case Study (2): Marina City, Chicago, USA

Photo (4.1): Marina City, Chicago, USA
(1959-1964)

Marina City is a mixed-use residential /commercial building complex occupying an entire city block on State Street in Chicago, Illinois. The complex consists of two corncob-shaped 61-story, 179*m* tall residential towers. It was designed in 1959 by architect Bertrand Goldberg and completed in 1964. Marina City was the first urban post-war high-rise residential complex in the United States.

For many years Goldberg had felt there were advantages in the use of circular forms: the aerodynamic properties in a cylindrical high-rise structure; the structural equidistance from the center, and therefore uniform function of all parts; the absence of special corner conditions; and the creation of centrifugal or 'kinetic' spaces resulting from non-parallel walls. The towers derive much of their rigidity from the cylindrical core.

Applied aerodynamics is the science of improving man-made objects such as airplanes. The solution of an aerodynamic problem normally involves calculating various properties of the flow, such as velocity, pressure, density, and temperature, as a function of space and time. Understanding the flow pattern makes it possible to calculate or approximate the forces and moments acting on bodies in the flow. Structural engineers also use the advantages of cylindrical buildings in aerodynamics as it offers less surface area perpendicular to lateral load direction, thus the magnitude of load pressure is greatly reduced.

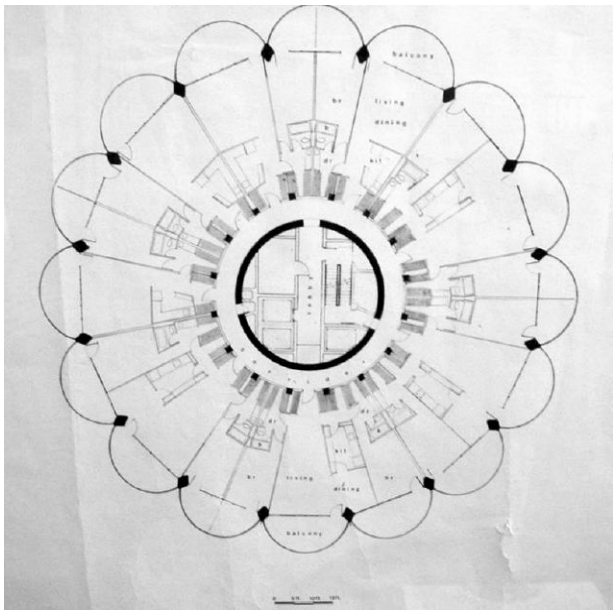

Figure (4.27): Actual Marina City Plan (Chicago),
(1959-1964)

4.4.1. Marina Layout Plans

The second case study to be considered is the Marina City, a cylindrical building form which provides true tubular geometry and true-three dimensional response to lateral loads. In this study three different structural systems have been used, one represents the actual Marina case system and two other hypothetical systems, as shown in Figure (4.28).

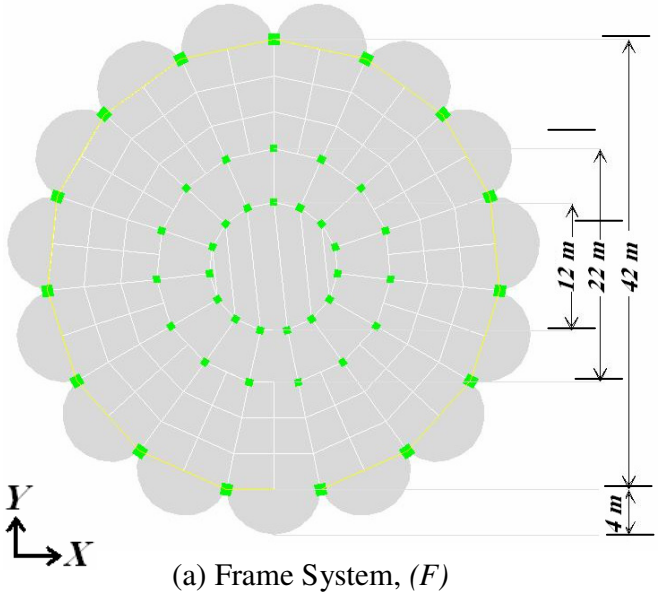

(a) Frame System, *(F)*

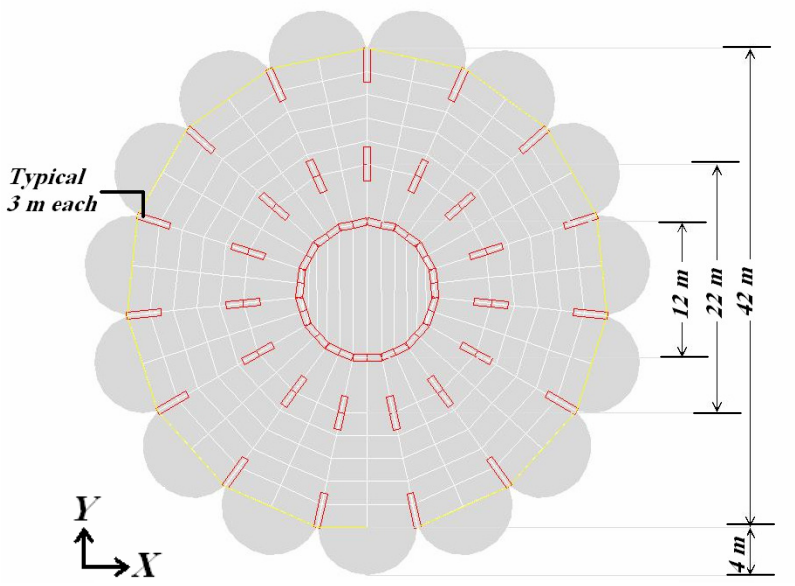

(b) Shear Wall System, *(SW)*

Figure (4.28 a, b): Marina Tower Plan Geometry

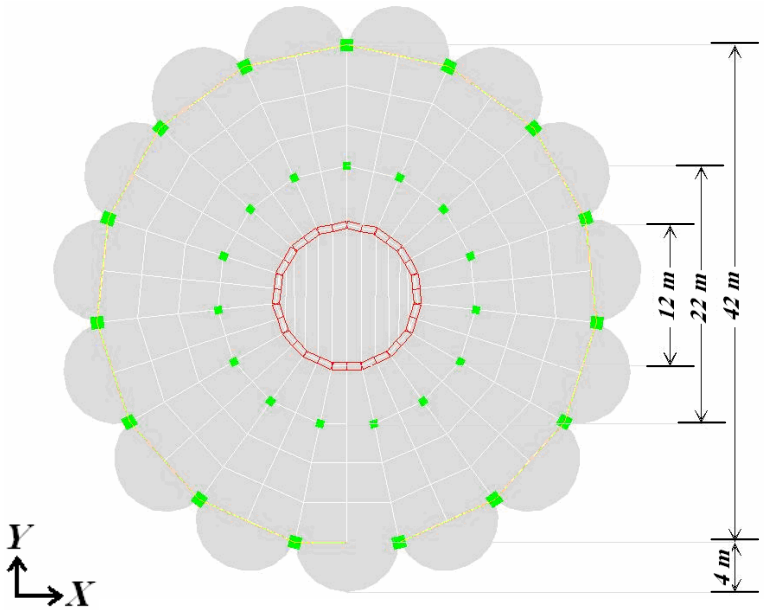

(c) Wall-Frame System, Same as Actual, *(DS)*

Figure (4.28 c): Marina Tower Plan Geometry

The 3D models have been generated using ETABS for all three structural systems as shown in Figure (4.29).

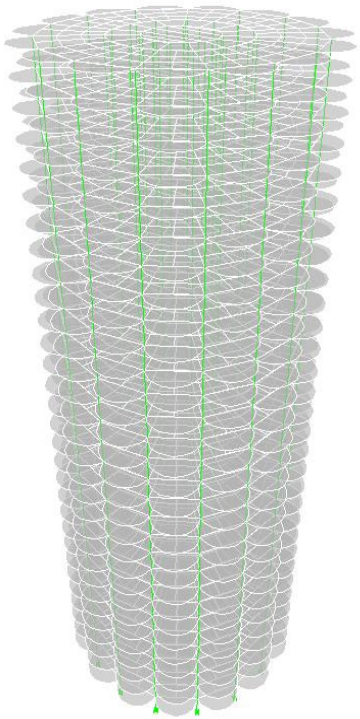

(a) 3D Marina Tower, (*F*)

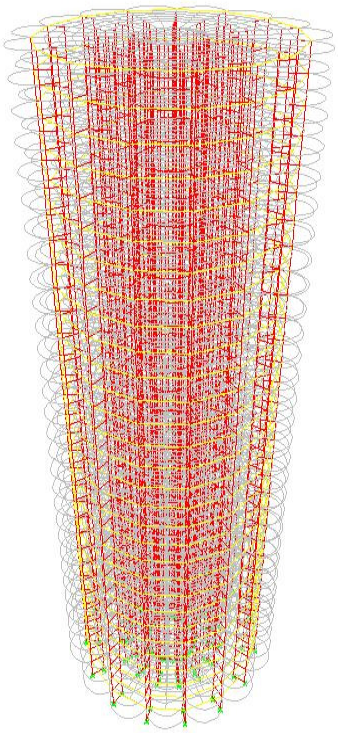

(b) 3D Marina Tower, *(SW)*

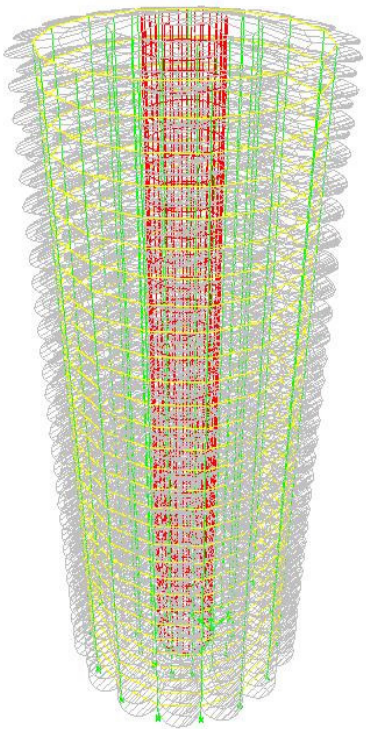

(c) 3D Marina Tower, *(DS)*

Figure (4.29): 3D-ETABS Generated Profiles of Marina Tower

4.4.2. Comparison Tables

The comparison tables that follow consider only the X-direction, representing any typical radial direction due to symmetry.

4.4.2.1. Maximum Diaphragm Drift Ratio Due to Earthquake in X-direction

Table [4.11]: Maximum Diaphragm Drift Ratio Due to E_X

Frame (*F*)			Shear Wall (*SW*)		Wall-Frame (*DS*)	
Story	**Point No.**	**Drift X (%)**	**Point No.**	**Drift X (%)**	**Point No.**	**Drift X (%)**
1	35	0.0820	35	0.0129	35	0.0131
2		0.1583		0.0239		0.022
3		0.1762		0.0270		0.0271
4		0.1788		0.0293		0.0316
5		0.1769		0.0312		0.0355
6		0.1738		0.0327		0.0388
7		0.1705		0.0339		0.0416
8		0.1672		0.0348		0.0440
9		0.1639		0.0356		0.0460
10		0.1609		0.0365		0.0477
11		0.1657		0.0394		0.0509
12		0.1627		0.0403		0.0524
13		0.1591		0.0406		0.0537
14		0.1552		0.0409		0.0547
15		0.1512		0.0411		0.0556
16	174	0.1471	174	0.0412	174	0.0563
17		0.1429		0.0413		0.0569
18		0.1386		0.0413		0.0574
19		0.1341		0.0412		0.0578
20		0.13		0.0413		0.0581
21		0.1358		0.0434		0.0596
22		0.1316		0.0433		0.0597
23		0.1251		0.0428		0.0596
24		0.1178		0.042		0.0593
25		0.1097		0.0411		0.0588
26		0.1007		0.04		0.0581
27		0.0902		0.0387		0.0571
28		0.0778		0.0371		0.056
29		0.0632		0.0353		0.0548
30		0.0479		0.0332		0.0530

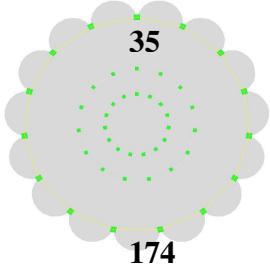

4.4.2.2. Diaphragm Center of Mass (*C.M.*) Displacement X Due to E_X

Table [4.12]: Diaphragm *C.M.* Displacement X Due to E_X

X- Displacement (*cm*)			
Story	**Frame (*F*)**	**Shear Wall (*SW*)**	**Wall-Frame (*DS*)**
1	0.22	0.02	0.03
2	0.64	0.07	0.08
3	1.13	0.13	0.16
4	1.63	0.20	0.25
5	2.13	0.28	0.36
6	2.62	0.37	0.49
7	3.1	0.47	0.62
8	3.58	0.56	0.77
9	4.04	0.67	0.92
10	4.5	0.77	1.09
11	4.97	0.89	1.26
12	5.44	1.00	1.44
13	5.9	1.12	1.62
14	6.34	1.25	1.81
15	6.78	1.37	2.00
16	7.2	1.50	2.19
17	7.61	1.63	2.39
18	8.00	1.76	2.59
19	8.39	1.89	2.78
20	8.76	2.02	2.99
21	9.14	2.15	3.19
22	9.51	2.29	3.39
23	9.87	2.42	3.59
24	10.2	2.56	3.80
25	10.5	2.69	4.00
26	10.78	2.83	4.20
27	11.03	2.96	4.40
28	11.25	3.09	4.60
29	11.44	3.21	4.80
30	11.59	3.33	4.99

4.4.2.3. Story Forces Due to E_X

Table [4.13]: Story Forces Due to E_X

Story	Frame (*F*)			Shear Wall (*SW*)			Wall-Frame (*DS*)		
	V_X*10^3 (kN)	T_X*10^6 (kN.m)	M_Y*10^6 (kN.m)	V_X*10^3 (kN)	T_X*10^6 (kN.m)	M_Y*10^6 (kN.m)	V_X*10^3 (kN)	T_X*10^6 (kN.m)	M_Y*10^6 (kN.m)
1	12.5	0.144	0.850	22.8	0.213	1.350	12.6	0.133	0.670
2	12.3	0.141	0.800	22.7	0.211	1.280	12.5	0.131	0.630
3	12.1	0.136	0.760	22.4	0.208	1.210	12.3	0.128	0.590
4	11.7	0.131	0.730	21.9	0.203	1.140	11.9	0.125	0.560
5	11.4	0.126	0.690	21.3	0.197	1.070	11.5	0.120	0.520
6	11.1	0.121	0.650	20.5	0.190	1.010	11	0.116	0.490
7	10.8	0.117	0.610	19.7	0.182	0.960	10.5	0.111	0.470
8	10.6	0.112	0.580	18.8	0.174	0.900	10	0.106	0.440
9	10.3	0.108	0.540	17.9	0.166	0.850	9.5	0.100	0.420
10	10.0	0.103	0.510	17	0.157	0.810	8.9	0.095	0.400
11	9.8	0.099	0.480	16.1	0.149	0.760	8.5	0.090	0.380
12	9.5	0.095	0.440	15.3	0.141	0.720	8	0.085	0.360
13	9.2	0.090	0.410	14.6	0.134	0.680	7.6	0.080	0.340
14	9.0	0.086	0.380	13.9	0.126	0.640	7.3	0.076	0.330
15	8.7	0.082	0.350	13.3	0.119	0.600	7	0.072	0.310
16	8.4	0.078	0.320	12.9	0.113	0.560	6.7	0.068	0.290
17	8.2	0.074	0.290	12.5	0.107	0.520	6.6	0.064	0.270
18	7.9	0.070	0.260	12.2	0.101	0.480	6.4	0.061	0.250
19	7.6	0.066	0.240	11.9	0.096	0.440	6.3	0.058	0.240
20	7.3	0.062	0.210	11.7	0.091	0.390	6.2	0.055	0.210
21	7.0	0.058	0.190	11.5	0.087	0.350	6.2	0.052	0.190
22	6.6	0.053	0.160	11.3	0.082	0.300	6.1	0.049	0.170
23	6.3	0.049	0.140	10.9	0.078	0.260	6	0.047	0.150
24	5.9	0.045	0.110	10.4	0.073	0.220	5.9	0.044	0.130
25	5.4	0.040	0.090	9.8	0.067	0.170	5.7	0.041	0.100
26	5.0	0.036	0.070	8.9	0.060	0.130	5.3	0.037	0.080
27	4.4	0.031	0.050	7.7	0.052	0.090	4.8	0.033	0.060
28	3.6	0.025	0.030	6.3	0.042	0.060	4.1	0.027	0.040
29	2.7	0.018	0.020	4.4	0.030	0.030	3.1	0.020	0.020
30	1.5	0.010	0.010	2.2	0.015	0.010	1.7	0.011	0.010

*Where M_Y: moment around Y-axis, V_X: shear in X-direction and T_X: torsion due to E_X

4.4.3 Graphical Presentation

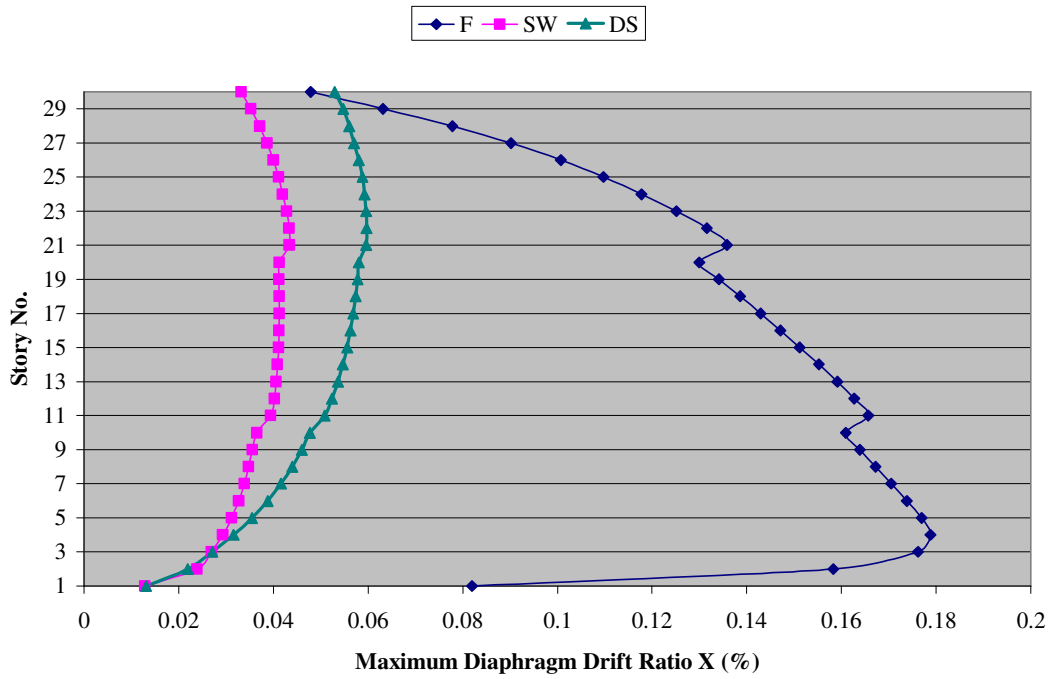

Figure (4.30): Marina Tower – Maximum Diaphragm Drift Ratio Due to E_X

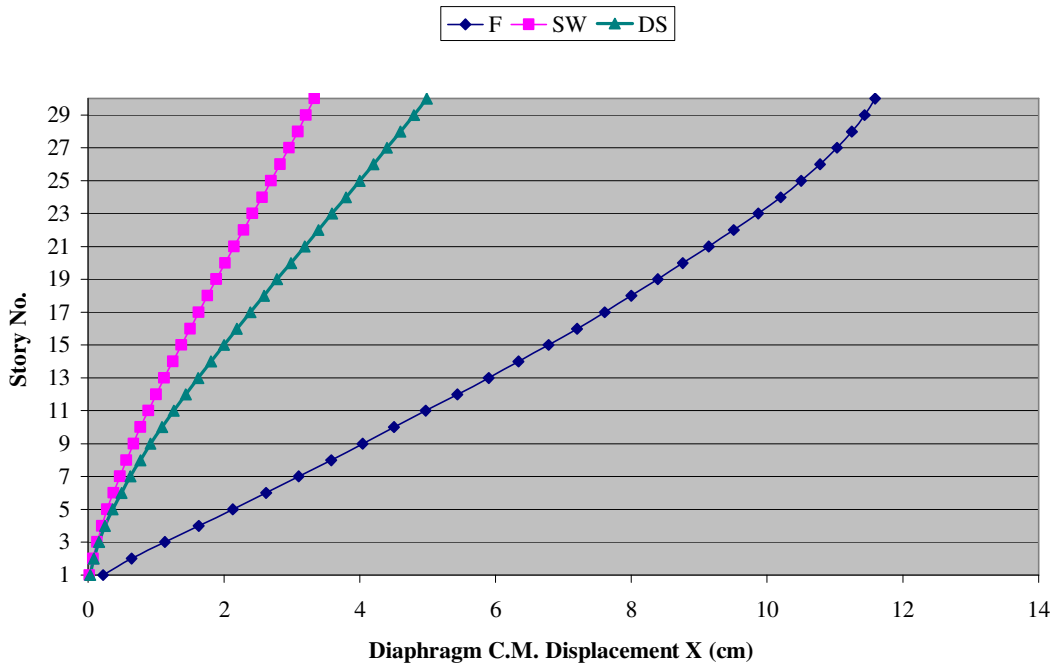

Figure (4.31): Marina Tower – Diaphragm *C.M.* Displacement X Due to E_X

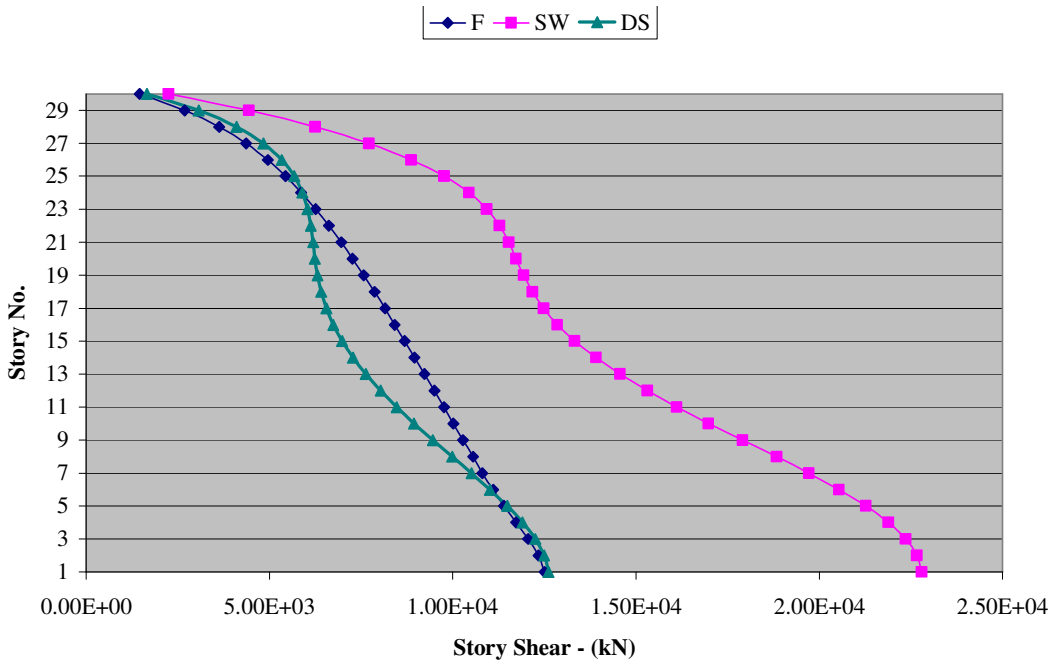

Figure (4.32): Marina Tower – Story Shear V_X Due to E_X

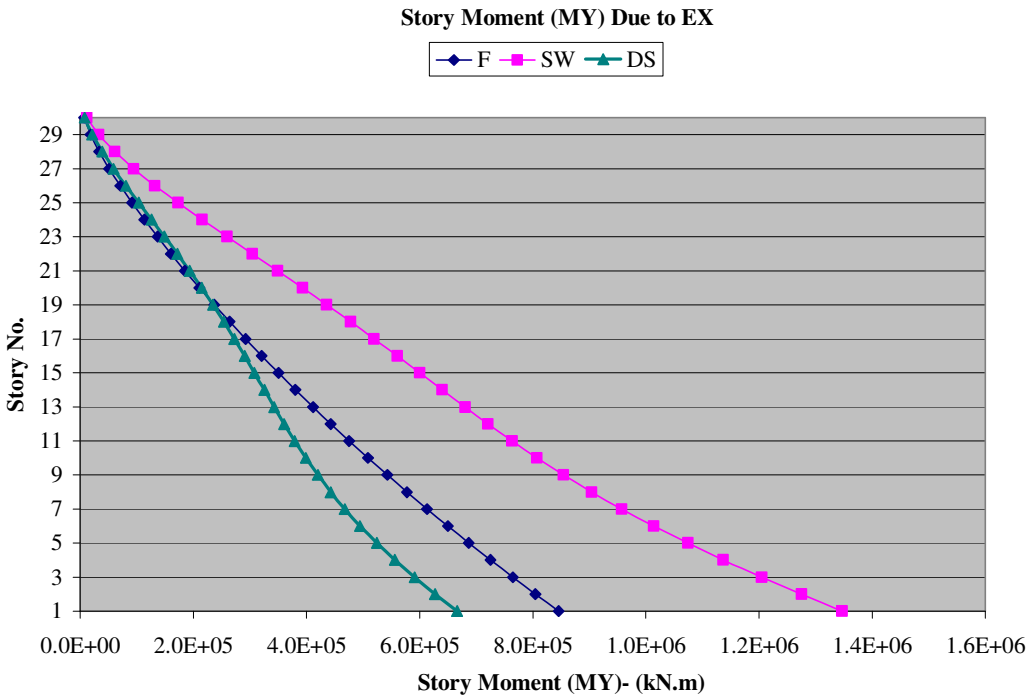

Figure (4.33): Marina Tower – Story Moment M_Y Due to E_X

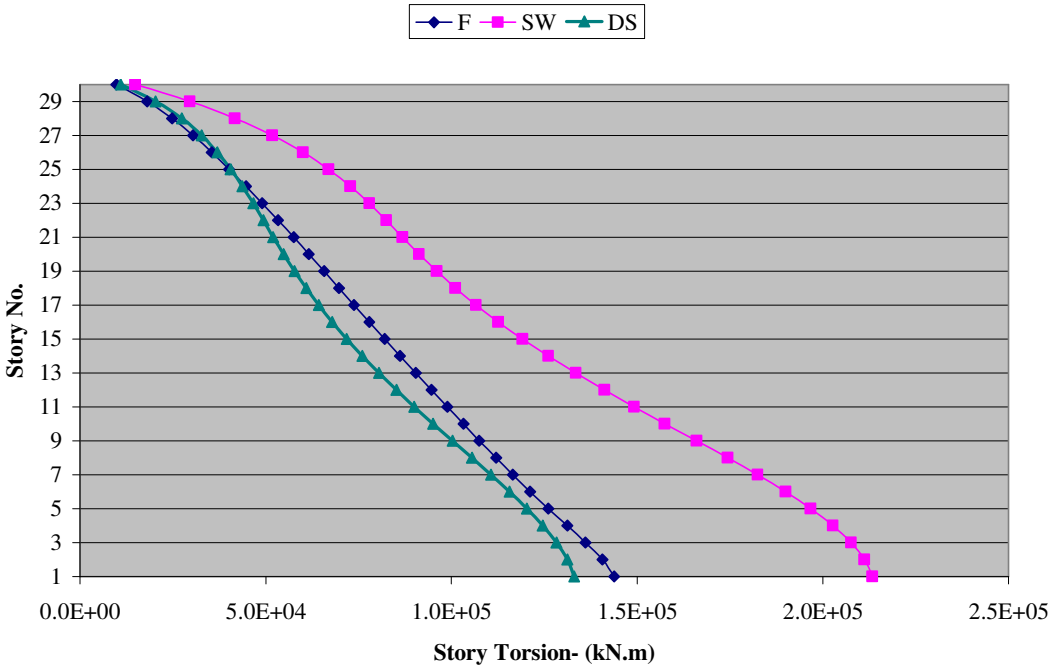

Figure (4.34): Marina Tower – Story Torsion (T_X) Due to E_X

4.4.4. Summary of Results for Marina Tower

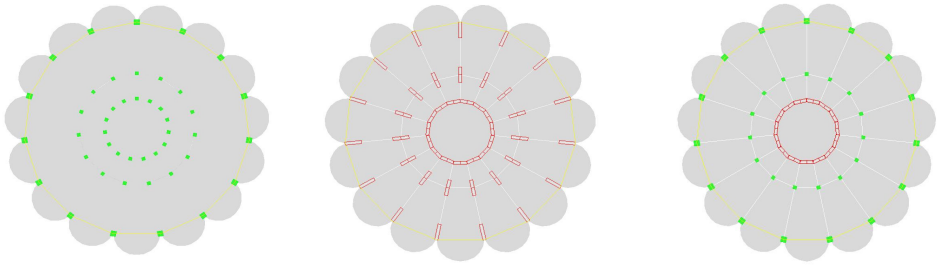

Figure (4.35): Marina Tower with Three Structural Systems

Table [4.14]: Summary of Results- Marina Tower

	F	***SW***	***DS***
Max. drift Ratio X- %	0.180	0.043	0.056
C.M. Absolute Max. displacement X-cm	11.6	3.33	5.0
Base shear-V_X- kN (10^3)	12.5	22.8	12.6
Base moment –M_Y- kN.m (10^6)	0.85	1.35	0.67
Base torsion-T_X- kN.m (10^6)	0.14	0.21	0.13
First mode shape period – sec.	4.24	1.73	2.90

Table [4.15]: Marina Tower Stiffness

	K_X (1)*10^6
F	0.079
SW	0.453
DS	0.250

(1)K_X: Building Stiffness in X-direction, kN/m

4.4.5. Synthesis of Results: Remarks and Comments

- **Drift Ratio and Displacement Curves:** Refer to Figures (4.30) and (3.31)

  (1) Maximum drift ratio and displacement for the three systems can be arranged in a descending manner as follows: (*F*), (*DS*) and (*SW*). This arrangement is inversely proportional to the calculated stiffness values shown in Table [4.15]. Thus, the

(*SW)* system in this case study provides more comfort and rigidity in the presence of seismic oscillating motion.

(2) The Displacement for (*F)* system is 4 times that for (*SW)* system and 2.5 times the displacement for (*DS*) system which shows how flexible this system is.

(3) The displacement curves trend remains the same for each system. While the frame system deflects in shear mode, the shear wall system deflects in flexural mode and the dual system deflects with both curvatures i.e. shear and flexural mode.

- **Story Forces Curves:** Refer to Figures (4.32) to (4.34)

(1) It should be noted that (*DS)* system has the least base moment value even in the previous case of rectangular shape, among the three systems. This is due to the nature of the deflected shape which exhibits two different curvatures and due to the horizontal interaction between the walls and frames which causes increased lateral stiffness of the structure and reduced moments in the walls and in the overall base moment.

(2) The stiffness Table [4.15] is still a good indication and also reflects those results. It shows that the (*SW)* system with the largest stiffness produces the largest base shear and the least displacement.

(3) The first mode of vibration for the (*F)* system gives the longer period and the largest displacement, i.e. the most flexible system.

(4) The larger the structure stiffness the more it attracts seismic forces, which explains the right shift in the shear force curve in shear wall system, Figure (4.32). In addition, the overall mass in the (*SW)* system exceeds the other two systems, which adds more inertia forces when it accelerates.

(5) Core systems, which are felt to be an especially appropriate structural system for tall buildings, provide stiffness and stability against lateral loads. This influence can be noticed clearly when tracking how the stiffness and displacement values changed dramatically in this case study when the circular core in the *(DS)* system is replaced by a group of columns in the *(F)* system.

(6) The circular core inherently holds in its shape an important influence on the overall stability. The more compact the plan, the more stability it is. At the University of Kassel, a simple test method was developed within a doctorate thesis in order to show the influence of wall shape on resistance to seismic shocks. A weight of 40 kg at the end of 5.5m long pendulum was dropped against the models. The rammed mold with square plan showed the first large cracks after the second strokes, Figure (4.36 a). After three strokes, one part of the wall separated Figure (4.36 b), and after four strokes the mold collapsed, Figure (4.36 c). On the other hand, the circular plan mold showed the first cracks only after three strokes, Figure (4.36 d), and only after six strokes did one small part of the wall separate, Figure (4.36 e). (Mink, Gernot, 2001).

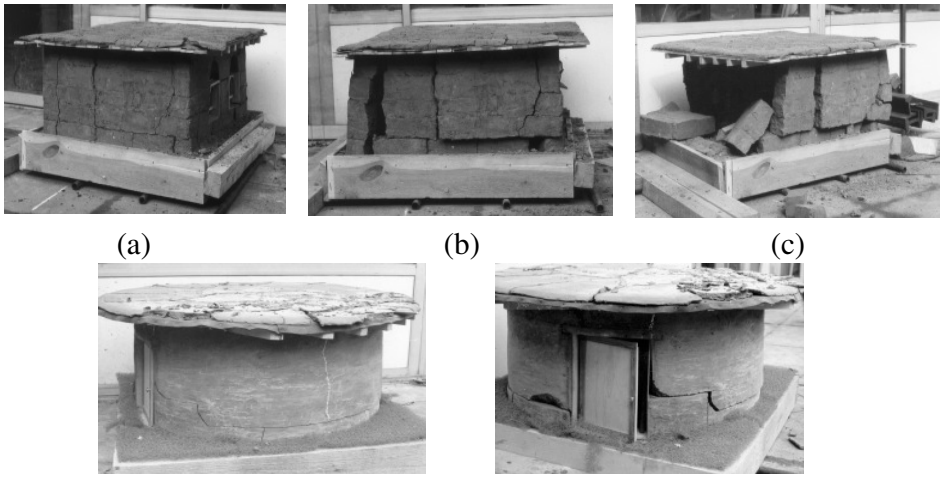

Figure (4.36): Earthquake Test Molds of Square and Circular Shape (Mink, Gernot, 2001).

4.5. Case Study (3): Lake Point Tower, Chicago, USA

Photo (4.2): Lake Point Tower, Chicago, Illinois, USA
1965-1968

Lake Point Tower is a high-rise residential building located just north of the Chicago River. The building was conceived and developed by William F. Hartnett, Jr., Chairman and Founder of Hartnett-Shaw Development Company. The building designers were John Heinrich and George Schipporeit. It was completed in 1968, is over 180*m* tall (70 stories), and was the highest apartment building in the world at that time.

It has a reinforced concrete structure and a triangular core of elevators. The building's plan is composed of three equal prongs extending from a central core, and alights atop a masonry podium. The exteriors of the prongs are gently curved, giving the

exterior of the building a rich, gleaming form. It is often described as having been inspired by a study model of a curvilinear high-rise building made by Van der Rohe during the early phase of his career, but is much taller than that proposed building, more regular in form, and its exterior glass curtain wall is tinted. The reputations of the architects of the building are associated very much with this structure.

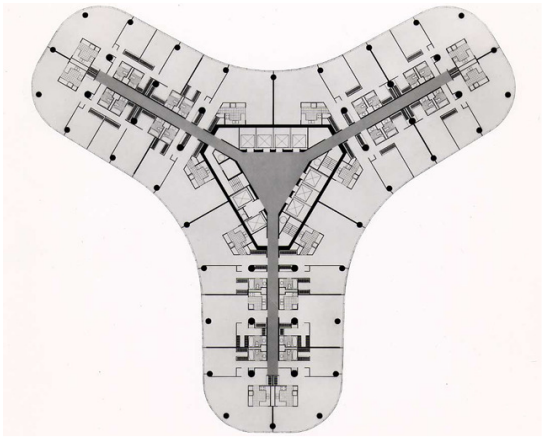

Figure (4.37): Lake Point Tower Actual Plan

Photo (4.3): Lake Point Tower, Aerial View

4.5.1. Lake Point Tower Layout Plans

The third case study to be considered is the Lake Point Tower. In this study three different structural systems have been used, one represents the actual case and two other hypothetical systems, as shown in Figure (4.38).

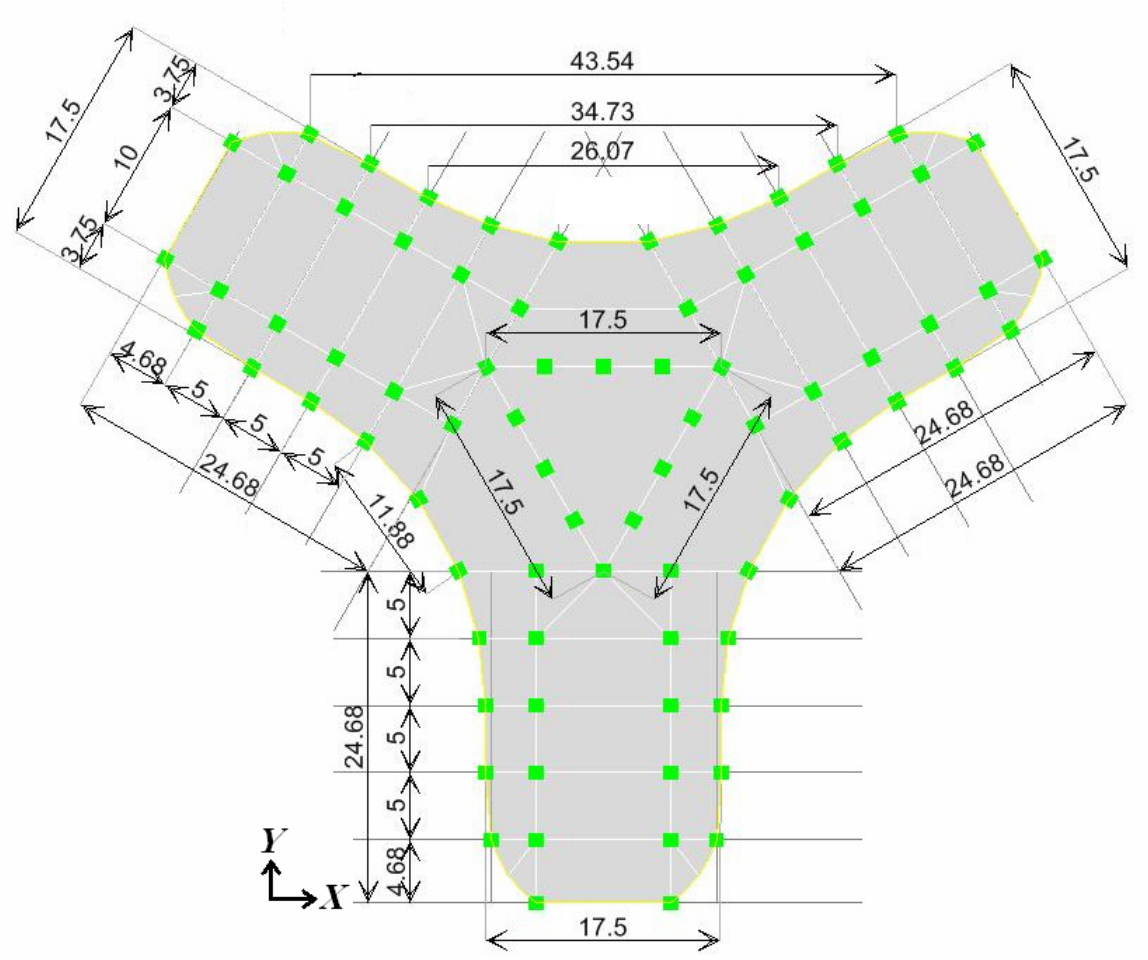

*All dimensions are in meter.

(a) Lake Point Tower Layout Plan, (*F*)

Figure (4.38 a): Lake Point Tower Plan Geometry

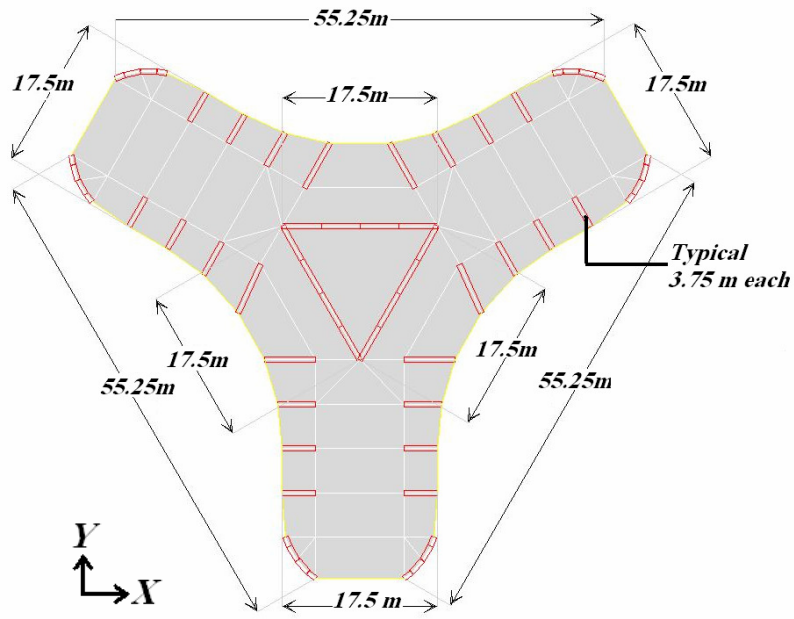

(b) Lake Point Tower Layout Plan, *(SW)*

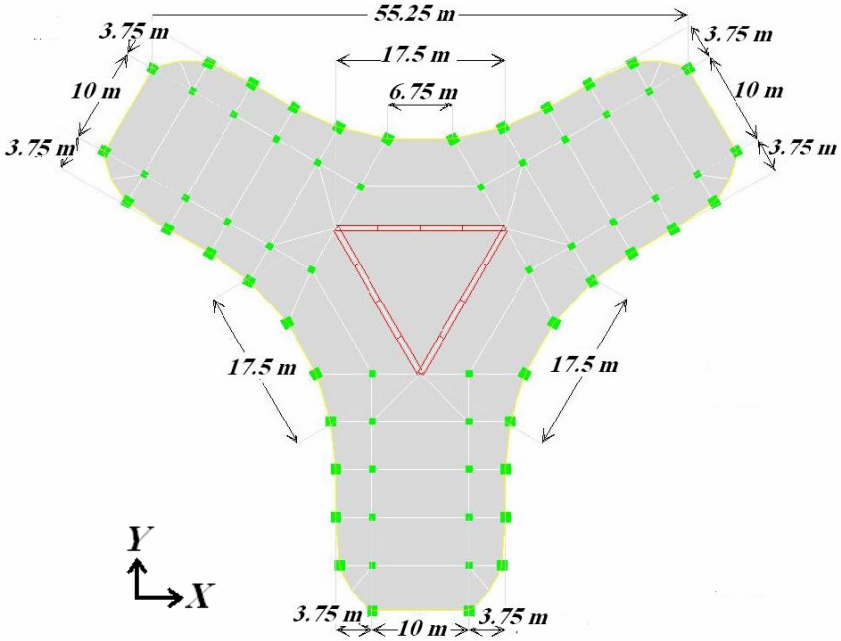

(c) Wall-Frame System, Same as Actual, *(DS)*

Figure (4.38 b,c): Lake Point Tower Plan Geometry

The 3D models have been generated using ETABS for each structural system as shown in Figure (4.39).

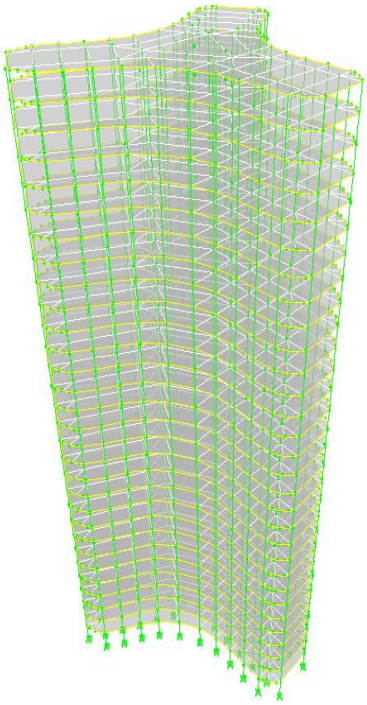

(a) 3D Lake Point Tower, (*F)*

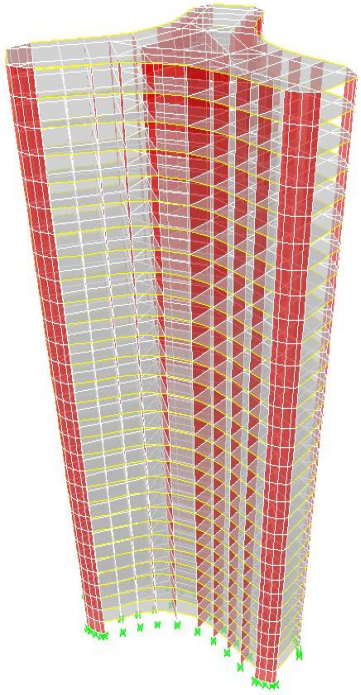

(b) 3D Lake Point Tower, (*SW*)

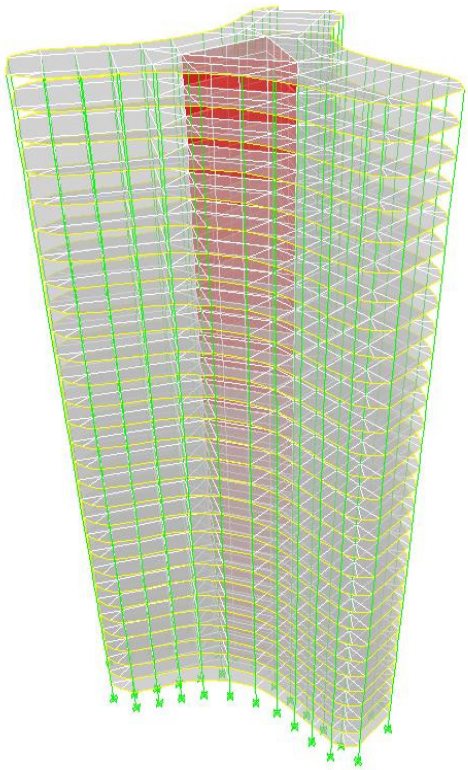

(c) 3D Lake Point Tower, *(DS)*

Figure (4.39): 3D-ETABS Generated Profiles of Lake Point Tower

4.5.2. Comparison Tables (only X-direction. has been considered)

4.5.2.1. Maximum Diaphragm Drift Ratio Due to Earthquake in X-direction.

Table [4.16]: Maximum Diaphragm Drift Ratio Due to E_X

		Frame (*F*)	Shear Wall (*SW*)	Wall-Frame (*DS*)
Story	**Point No.**	**Drift X (%)**	**Drift X (%)**	**Drift X (%)**
1	17	0.0637	0.0084	0.0137
2		0.1199	0.0190	0.0223
3		0.1358	0.0264	0.0258
4		0.1395	0.0319	0.0285
5		0.1393	0.0361	0.0306
6		0.1378	0.0393	0.0324
7		0.1357	0.0419	0.0338
8		0.1335	0.0438	0.0350
9		0.1312	0.0454	0.0358
10		0.1287	0.0467	0.0367
11		0.1291	0.0485	0.0388
12		0.1262	0.0496	0.0395
13		0.1233	0.0503	0.0397
14		0.1202	0.0507	0.0399
15		0.1169	0.0509	0.0400
16		0.1134	0.0510	0.0399
17		0.1097	0.0510	0.0398
18		0.1059	0.0509	0.0397
19		0.1019	0.0509	0.0395
20		0.0979	0.0510	0.0393
21		0.0974	0.0517	0.0402
22		0.0931	0.0516	0.0399
23		0.0882	0.0511	0.0393
24		0.0829	0.0503	0.0386
25		0.0770	0.0493	0.0377
26		0.0704	0.0480	0.0367
27		0.0629	0.0466	0.0355
28		0.0542	0.0450	0.0341
29		0.0445	0.0435	0.0326
30		0.0354	0.0422	0.0308

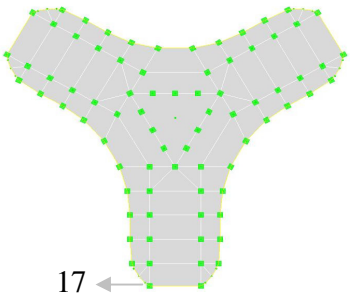

4.5.2.2. Diaphragm Center of Mass (*C.M.*) Displacement X Due to E_X

Table [4.17]: Diaphragm *C.M.* Displacement X Due to E_X

X-Displacement (cm)			
Story	**Frame (*F*)**	**Shear Wall (*SW*)**	**Wall-Frame (*DS*)**
1	0.17	0.02	0.02
2	0.50	0.07	0.06
3	0.87	0.14	0.12
4	1.25	0.22	0.18
5	1.63	0.31	0.26
6	2.01	0.42	0.34
7	2.38	0.53	0.43
8	2.75	0.65	0.53
9	3.11	0.77	0.63
10	3.46	0.91	0.74
11	3.81	1.04	0.85
12	4.15	1.19	0.96
13	4.49	1.33	1.08
14	4.81	1.48	1.20
15	5.13	1.63	1.32
16	5.44	1.78	1.44
17	5.74	1.93	1.56
18	6.02	2.08	1.68
19	6.30	2.24	1.80
20	6.56	2.39	1.92
21	6.82	2.55	2.05
22	7.06	2.70	2.17
23	7.30	2.86	2.29
24	7.51	3.01	2.41
25	7.71	3.17	2.53
26	7.90	3.32	2.65
27	8.06	3.47	2.77
28	8.21	3.61	2.88
29	8.33	3.76	2.99
30	8.44	3.90	3.10

4.5.2.3. Story Forces Due to E_X

Table [4.18]: Story Forces Due to E_X

Frame (*F*)				Shear Wall (*SW*)			Wall-Frame (*DS*)		
Story	V_X*10^3 (kN)	T_X*10^6 (kN.m)	M_Y*10^6 (kN.m)	V_X*10^3 (kN)	T_X*10^6 (kN.m)	M_Y*10^6 (kN.m)	V_X*10^3 (kN)	T_X*10^6 (kN.m)	M_Y*10^6 (kN.m)
1	18.2	0.310	1.250	23.8	0.386	1.360	16.5	0.280	0.910
2	18.0	0.305	1.180	23.6	0.382	1.290	16.3	0.276	0.860
3	17.6	0.298	1.130	23.3	0.376	1.220	15.9	0.269	0.810
4	17.2	0.289	1.070	22.8	0.367	1.150	15.5	0.261	0.770
5	16.7	0.279	1.010	22.1	0.356	1.080	14.9	0.252	0.730
6	16.3	0.269	0.960	21.3	0.343	1.020	14.3	0.241	0.690
7	15.8	0.259	0.900	20.4	0.329	0.960	13.6	0.231	0.650
8	15.4	0.250	0.850	19.5	0.314	0.910	13	0.220	0.620
9	15.0	0.241	0.800	18.5	0.299	0.860	12.3	0.209	0.580
10	14.6	0.232	0.750	17.5	0.283	0.820	11.7	0.198	0.550
11	14.2	0.224	0.700	16.6	0.268	0.770	11.2	0.188	0.530
12	13.9	0.216	0.650	15.8	0.254	0.730	10.7	0.179	0.500
13	13.5	0.208	0.610	15	0.241	0.690	10.2	0.170	0.470
14	13.1	0.200	0.560	14.3	0.228	0.650	9.8	0.162	0.450
15	12.7	0.192	0.520	13.8	0.217	0.610	9.5	0.155	0.420
16	12.3	0.183	0.470	13.3	0.207	0.570	9.2	0.148	0.400
17	11.9	0.175	0.430	12.9	0.197	0.530	9	0.141	0.370
18	11.4	0.166	0.390	12.7	0.189	0.490	8.7	0.135	0.340
19	11.0	0.157	0.350	12.4	0.181	0.450	8.6	0.129	0.320
20	10.5	0.148	0.310	12.3	0.175	0.410	8.4	0.124	0.290
21	10.1	0.140	0.270	12.1	0.168	0.360	8.3	0.119	0.260
22	9.6	0.131	0.240	11.9	0.162	0.320	8.1	0.114	0.230
23	9.1	0.123	0.200	11.6	0.155	0.270	7.9	0.108	0.200
24	8.6	0.113	0.160	11.2	0.146	0.230	7.7	0.102	0.170
25	7.9	0.103	0.130	10.6	0.136	0.180	7.3	0.096	0.140
26	7.1	0.092	0.100	9.7	0.123	0.140	6.8	0.087	0.110
27	6.2	0.079	0.070	8.5	0.108	0.100	6.1	0.077	0.080
28	5.0	0.063	0.050	7	0.088	0.060	5.1	0.064	0.050
29	3.6	0.045	0.020	5	0.063	0.030	3.7	0.047	0.030
30	1.8	0.023	0.010	2.5	0.032	0.010	2	0.024	0.010

*Where M_Y: moment around Y-axis, V_X: shear in X-direction and T_X: torsion due to E_X.

4.5.3. Graphical Presentation

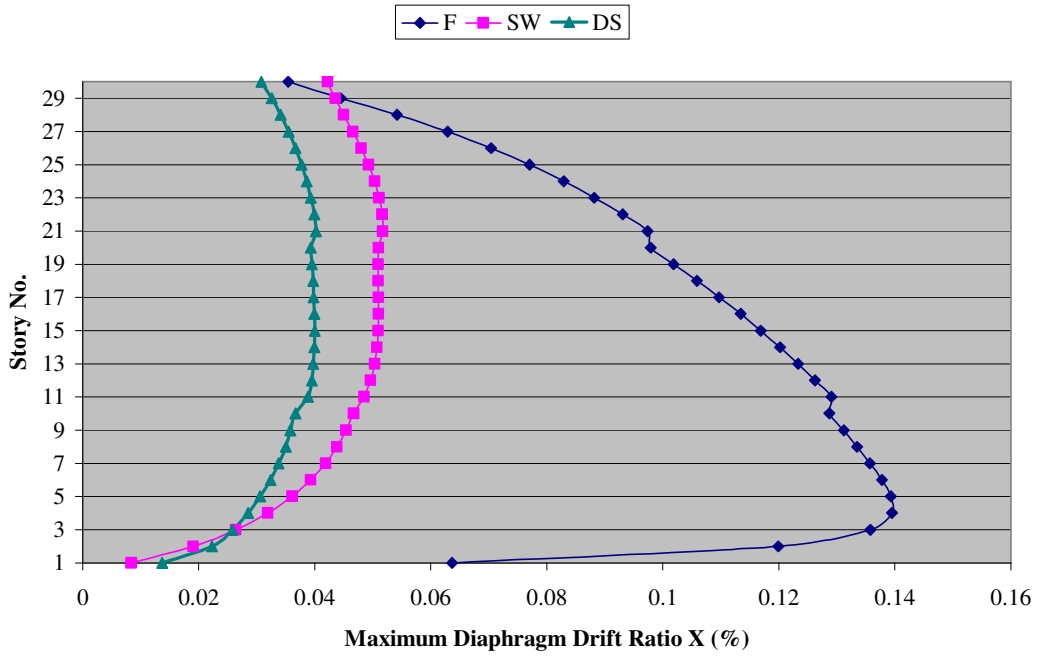

Figure (4.40): Lake Point Tower – Maximum Diaphragm Drift Ratio Due to E_X

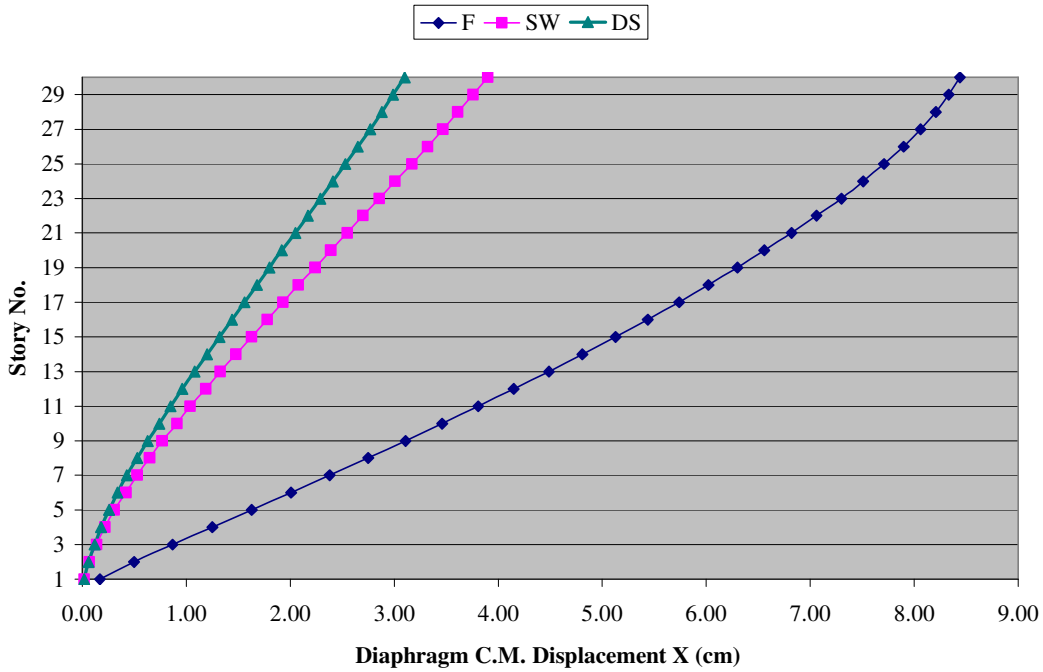

Figure (4.41): Lake Point Tower – Diaphragm *C.M.* Displacement X Due to E_X

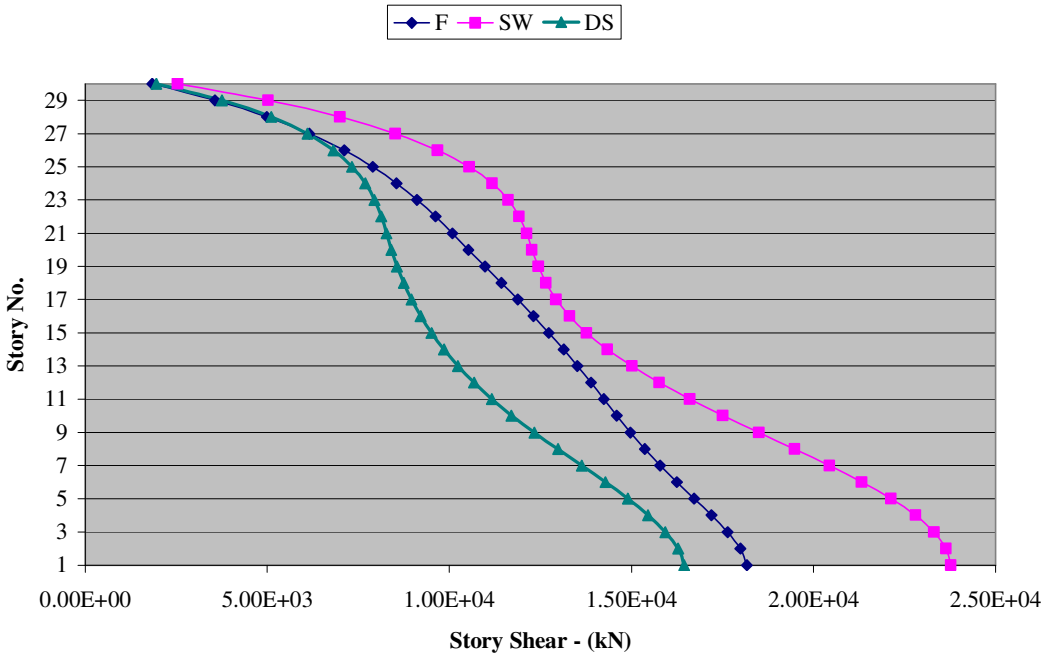

Figure (4.42): Lake Point Tower – Story Shear V_X Due to E_X

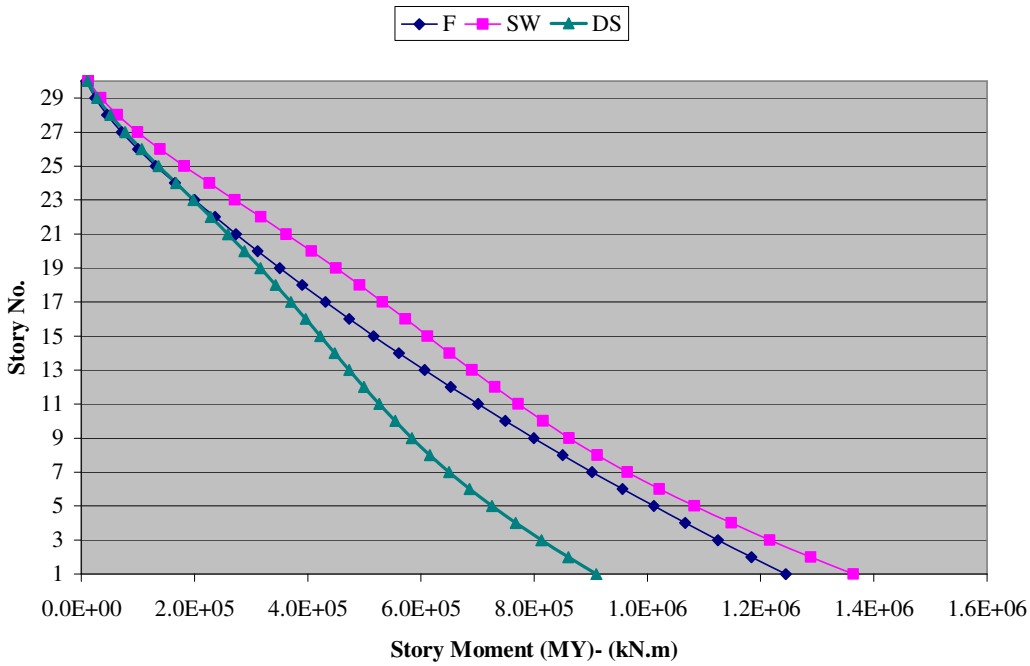

Figure (4.43): Lake Point Tower – Story Moment M_Y Due to E_X

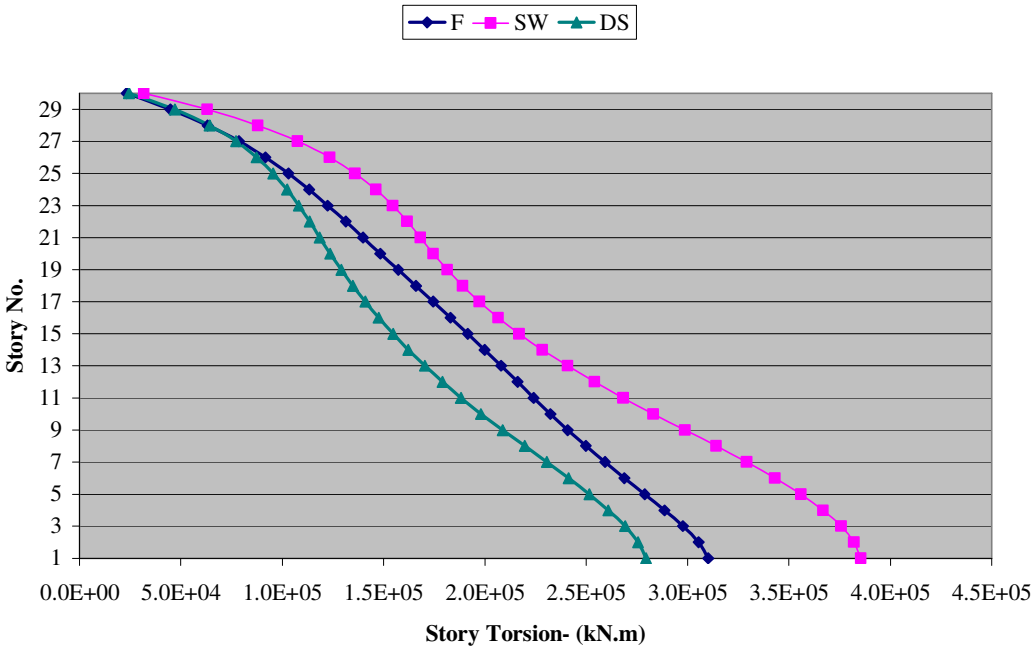

Figure (4.44): Lake Point Tower – Story Torsion (T_X) Due to E_X

4.5.4. Summary of Results for Lake Point Tower

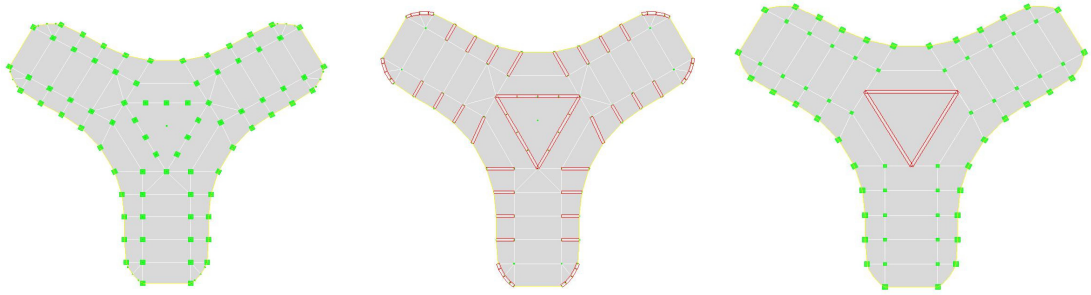

Figure (4.45): Lake Point Tower with Three Structural Systems

Table [4.19]: Summary of Results- Lake Point Tower

	F	***SW***	***DS***
Max. drift Ratio X- %	0.140	0.052	0.040
C.M. Absolute Max. displacement X-cm	8.44	3.9	3.1
Base shear-V_X- kN (10^3)	18.2	23.8	16.5
Base moment –M_Y- kN.m (10^6)	1.25	1.36	0.91
Base torsion-T_X- kN.m (10^6)	0.31	0.39	0.28
First mode shape period – sec.	3.14	2.10	2.12

Table [4.20]: Lake Point Tower Stiffness

	$K_X^{(1)}*10^6$
F	0.197
SW	0.430
DS	0.350

(1)K_X: Building Stiffness in X-direction, kN/m

4.5.5. Synthesis of Results: Remarks and Comments

- **Drift Ratio and Displacement Curves:** Refer to Figures (4.40) and (4.41).

  (1) Maximum drift ratio in the *(F)* system is 0.14% which is almost 2.5 times the other systems. Refer to Table [4.19].

(2) The *(SW)* system is stiffer than the other systems as indicated in Table [4.20]. Also, the *(DS)* system has the least displacement and drift values because of the unique behavior of frame-wall interaction where either one supports the other. It has to be noted that it is not necessary that *(DS)* system has always the least displacement as can be seen in case study (2), this depend on the level of horizontal interaction between frame and wall elements and the system's efficiency.

(3) The same trend for the deflected curves, as explained before, can be identified clearly for each system i.e. shear mode, flexural mode and a combination of the two modes. Figure (4.41)

- **Story Forces Curves:** Refer to Figures (4.42) to (4.43).

(1) The *(DS)* system still has the least base moment as explained in the previous case study.

(2) Due to the high overall stiffness of the *(SW)* system, the base shear observed is the largest in magnitude.

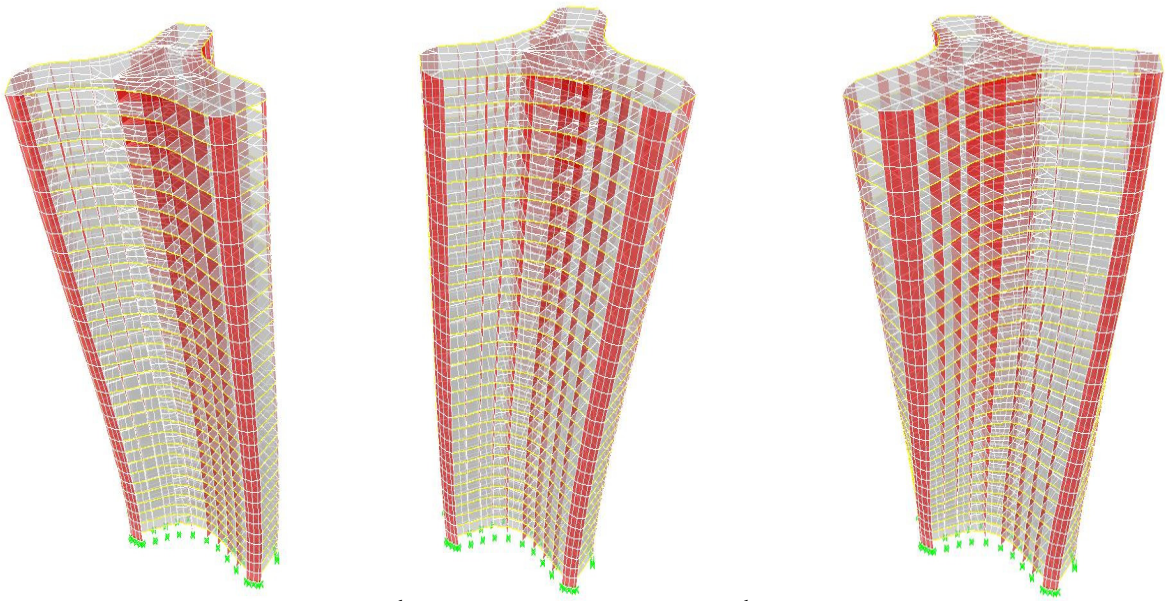

(a) 1st Mode, T=2.1 sec. (b) 2nd Mode, T=2.09 sec. (c) 3rd (Torsional Mode) T=1.66 sec.

Figure (4.46): The First Three Modes of Vibration for the (*SW)* System, Lake Point Tower

4.6. Case Study (4): Toronto City Hall, Canada.

Photo (4.4): Toronto City Hall, Canada, 1958-1965

The City Hall of Toronto, Ontario, Canada is one of the most distinctive landmarks of the city. Designed by Finnish architect Viljo Revell and engineered by Hannskarl Bandel, the building opened in 1965; its modernist architecture still impresses today. It was built to replace Old City Hall which was built in 1899.

While the building's base is rectangular, its two towers are curved in cross-section and rise to differing heights. The east tower is 27 stories (99.5*m*) tall and the west tower is 20 stories (79.4*m*). Between the towers is the saucer-like council chamber, and the overall arrangement is somewhat like two hands cradling the chamber. The outer concrete surfaces of the towers have been ribbed, to prevent collapse of the fabric as a result of the expansion of the exterior surfaces, and the tearing apart of the fabric as a result of differences in air pressure on the two sides of each wing-like tower during the high winds characteristic of the Great Lakes.

4.6.1. Toronto Layout Plans

The Last case study to be considered is the Toronto Tower. The actual building consists of two connected crescent-shaped towers. However, this study uses only one crescent shaped building with three different structural systems, as shown in Figure (4.47).

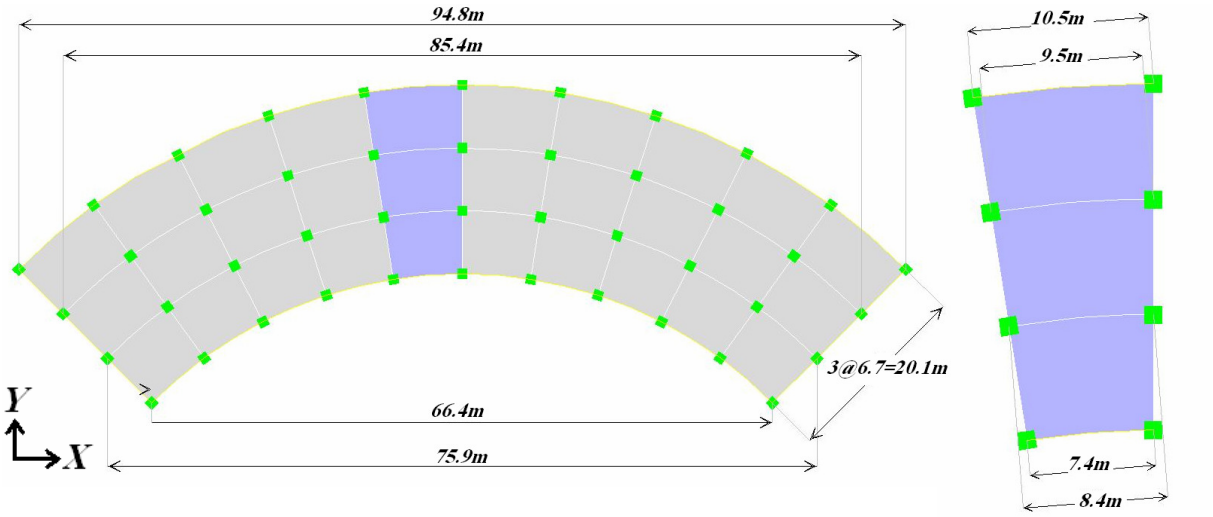

(a) Toronto Tower Layout Plan and Radial Segment in Floor Slab, *(F)* System

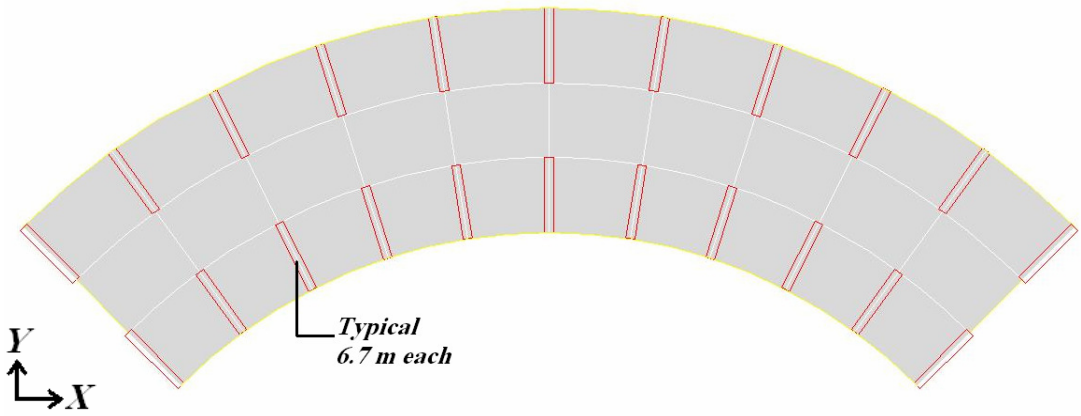

(b) Toronto Tower Layout Plan, *(SW)* System

Figure (4.47 a, b): Toronto Tower Plan Geometry

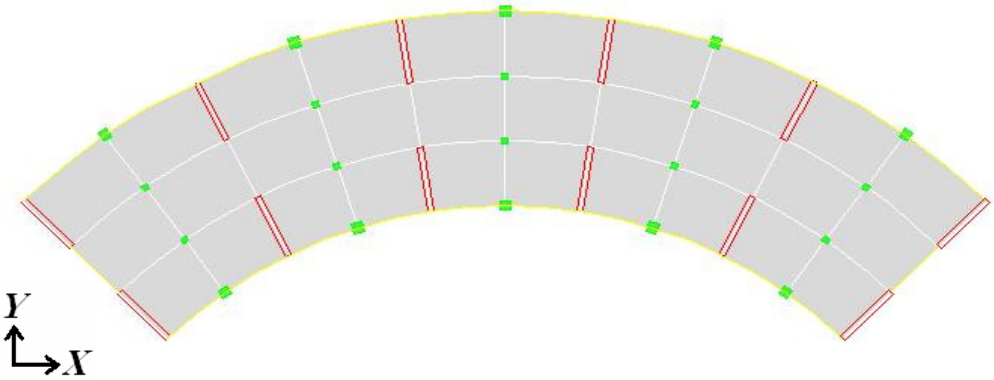

(c) Toronto Tower Layout Plan, *(DS)* System

Figure (4.47 c): Toronto Tower Plan Geometry

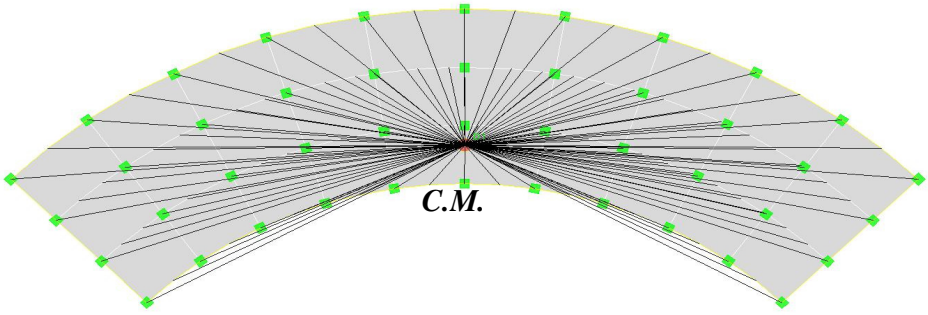

Figure (4.48): Toronto Tower Center of Mass Location

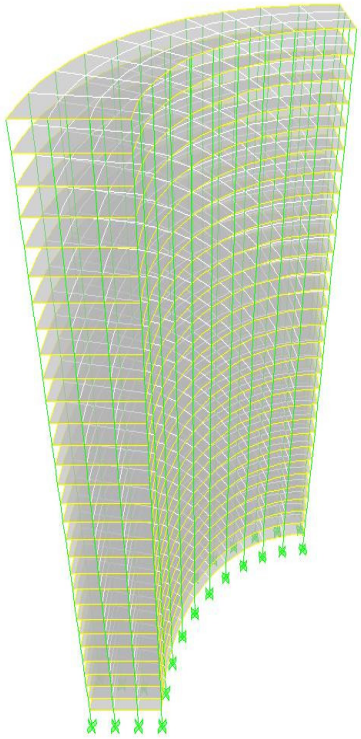

(a) 3D Toronto Tower, *(F)* System

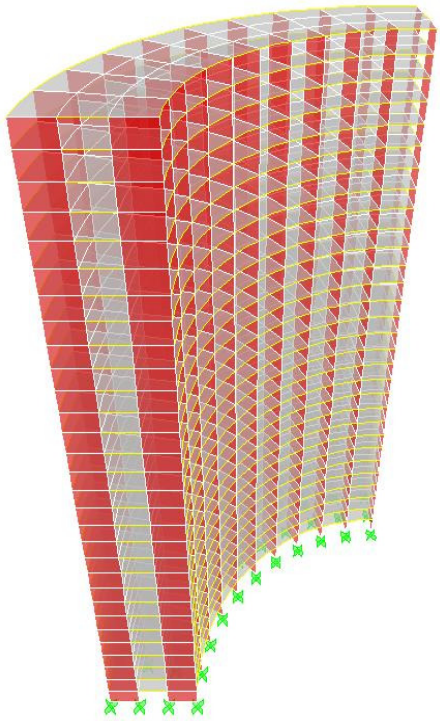

(b) 3D Toronto Tower, *(SW)* System

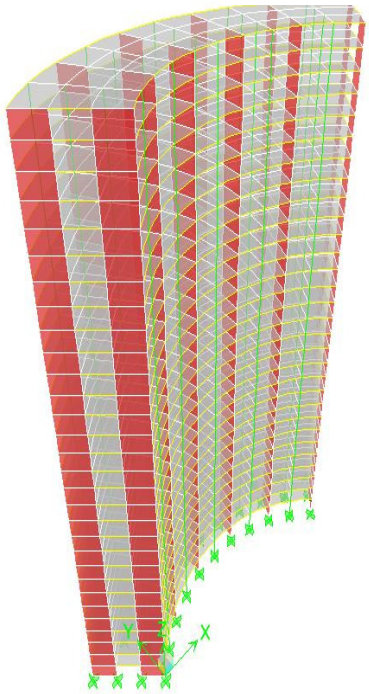

(c) 3D Toronto Tower, *(DS)* System

Figure (4.49): 3D-ETABS Generated Profiles of Toronto Tower

4.6.2. Comparison Tables

4.6.2.1. Maximum Diaphragm Drift Ratio Due to Earthquake in X-direction

Table [4.21]: Maximum Diaphragm Drift Ratio Due to E_X

Frame (*F*)			Shear Wall (*SW*)		Wall-Frame (*DS*)	
Story	**Point No.**	**Drift X (%)**	**Point No.**	**Drift X (%)**	**Point No.**	**Drift X (%)**
1	144	0.0660	144	0.0738	144	0.0823
2		0.1203		0.1631		0.1738
3		0.1329		0.2006		0.2067
4		0.1341		0.213		0.2145
5		0.1322		0.2136		0.212
6		0.1294		0.209		0.2056
7		0.1265		0.2024		0.1979
8		0.1236		0.1957		0.1903
9		0.1207		0.1897		0.1833
10	161	0.1177		0.1859		0.1778
11		0.1166		0.1907		0.1782
12		0.1139		0.1865		0.1719
13		0.1114		0.1797		0.1649
14		0.1088		0.1722		0.1577
15		0.1061		0.1644		0.1506
16		0.1032		0.1566		0.1436
17		0.1002		0.149		0.1367
18		0.0971		0.1419		0.1302
19		0.0938		0.1355		0.124
20		0.0903		0.1317		0.119
21		0.0883		0.1419		0.1227
22		0.0844		0.1374		0.1168
23		0.0802		0.1284		0.1091
24		0.0757		0.1185		0.1009
25		0.0705		0.108		0.0923
26		0.0646		0.0968		0.0829
27		0.0576		0.0846		0.0723
28		0.0493		0.071		0.0598
29		0.0397	161	0.0637	161	0.0553
30		0.0301		0.0612		0.0537

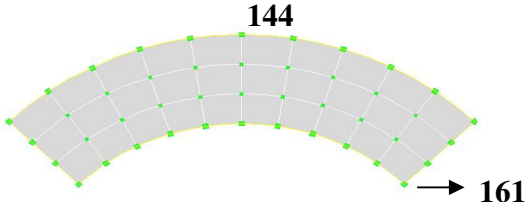

4.6.2.2. Maximum Diaphragm Drift Ratio Due to Earthquake in Y-direction

Table [4.22]: Maximum Diaphragm Drift Ratio Due to E_Y

Frame (*F*)			Shear Wall (*SW*)		Wall-Frame (*DS*)	
Story	**Point No.**	**Drift Y (%)**	**Point No.**	**Drift Y (%)**	**Point No.**	**Drift Y (%)**
1	164	0.1238	164	0.0154	121	0.0207
2		0.242		0.0378		0.0493
3		0.2796		0.0542		0.0694
4		0.2899		0.0667		0.0842
5		0.291		0.0765		0.0955
6		0.289		0.0842		0.1042
7		0.286		0.0904		0.1108
8		0.2825		0.0953		0.1158
9		0.2787		0.0992		0.1196
10		0.2744		0.1024		0.1224
11		0.2743		0.1062		0.1256
12		0.2693		0.1085		0.1273
13		0.2641		0.11		0.1282
14		0.2587		0.1109		0.1285
15		0.253		0.1113		0.1283
16		0.2472		0.1113		0.1277
17		0.2411		0.1111		0.1268
18		0.2347		0.1105		0.1256
19		0.228		0.1098		0.1241
20		0.2212		0.1091		0.1226
21		0.2194		0.1094		0.1218
22		0.2117		0.108		0.1194
23		0.2023		0.1061		0.1167
24		0.1921		0.104		0.1137
25		0.1809		0.1017		0.1105
26		0.1687		0.0992		0.1072
27		0.1548		0.0966		0.1037
28		0.1388		0.094		0.1001
29		0.1207		0.0914		0.0968
30		0.1033		0.0892		0.0938

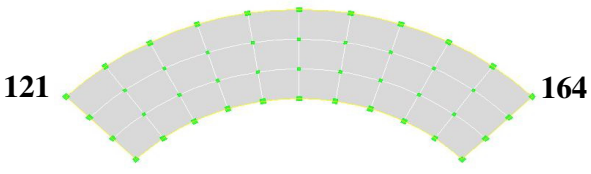

4.6.2.3. Diaphragm Center of Mass (*C.M.*) Displacement X Due to E_X

Table [4.23]: Diaphragm *C.M.* Displacement X Due to E_X

X-Displacement (cm)			
Story	**Frame (*F*)**	**Shear Wall (*SW*)**	**Wall-Frame (*DS*)**
1	0.23	0.21	0.24
2	0.65	0.68	0.74
3	1.12	1.25	1.32
4	1.59	1.85	1.91
5	2.05	2.43	2.49
6	2.50	2.99	3.03
7	2.94	3.53	3.55
8	3.37	4.03	4.03
9	3.78	4.51	4.49
10	4.19	4.98	4.93
11	4.58	5.46	5.37
12	4.97	5.91	5.78
13	5.34	6.35	6.17
14	5.70	6.76	6.54
15	6.04	7.14	6.89
16	6.37	7.50	7.21
17	6.69	7.84	7.52
18	6.99	8.15	7.81
19	7.28	8.45	8.08
20	7.55	8.74	8.34
21	7.81	9.05	8.61
22	8.05	9.34	8.85
23	8.27	9.60	9.07
24	8.48	9.82	9.26
25	8.66	10.02	9.42
26	8.83	10.18	9.56
27	8.97	10.31	9.67
28	9.10	10.41	9.75
29	9.19	10.48	9.80
30	9.26	10.55	9.86

4.6.2.4. Diaphragm Center of Mass (*C.M.*) Displacement Y Due to E_Y

Table [4.24]: Diaphragm *C.M.* Displacement Y Due to E_Y

Y-Displacement (cm)			
Story	**Frame (*F*)**	**Shear Wall (*SW*)**	**Wall-Frame (*DS*)**
1	0.29	0.03	0.04
2	0.88	0.10	0.14
3	1.57	0.21	0.28
4	2.3	0.35	0.47
5	3.04	0.52	0.68
6	3.77	0.71	0.93
7	4.49	0.92	1.19
8	5.2	1.15	1.47
9	5.91	1.39	1.77
10	6.61	1.64	2.07
11	7.3	1.90	2.39
12	7.99	2.16	2.70
13	8.66	2.43	3.03
14	9.32	2.71	3.35
15	9.97	2.99	3.68
16	10.6	3.27	4.00
17	11.21	3.55	4.33
18	11.81	3.83	4.65
19	12.39	4.11	4.97
20	12.95	4.39	5.29
21	13.51	4.67	5.60
22	14.05	4.95	5.91
23	14.56	5.22	6.21
24	15.05	5.49	6.50
25	15.51	5.75	6.79
26	15.93	6.01	7.07
27	16.33	6.27	7.35
28	16.68	6.53	7.62
29	17	6.78	7.88
30	17.29	7.03	8.15

4.6.2.5. Story Forces Due to E_X

Table [4.25]: Story Forces Due to E_X

	Frame (*F*)			Shear Wall (*SW*)			Wall-Frame (*DS*)		
Story	V_X*10^3 (kN)	T_X*10^6 (kN.m)	M_Y*10^6 (kN.m)	V_X*10^3 (kN)	T_X*10^6 (kN.m)	M_Y*10^6 (kN.m)	V_X*10^3 (kN)	T_X*10^6 (kN.m)	M_Y*10^6 (kN.m)
1	15.2	0.365	1.070	17.6	1.338	1.130	15.9	1.175	1.030
2	15.0	0.359	1.020	17.4	1.299	1.070	15.7	1.138	0.970
3	14.7	0.349	0.970	16.9	1.241	1.020	15.3	1.084	0.920
4	14.4	0.338	0.920	16.3	1.177	0.960	14.8	1.027	0.870
5	14.0	0.328	0.870	15.7	1.113	0.910	14.2	0.972	0.830
6	13.7	0.317	0.820	15.2	1.051	0.860	13.7	0.919	0.780
7	13.4	0.307	0.770	14.6	0.994	0.810	13.2	0.871	0.740
8	13.1	0.298	0.730	14.2	0.941	0.760	12.7	0.826	0.690
9	12.7	0.288	0.680	13.7	0.892	0.710	12.3	0.783	0.650
10	12.4	0.279	0.640	13.3	0.845	0.670	11.9	0.743	0.610
11	12.1	0.269	0.600	12.9	0.801	0.620	11.6	0.703	0.570
12	11.8	0.260	0.560	12.5	0.759	0.580	11.2	0.665	0.520
13	11.5	0.250	0.510	12.2	0.717	0.530	11	0.627	0.480
14	11.1	0.241	0.480	11.8	0.676	0.490	10.7	0.591	0.440
15	10.8	0.231	0.440	11.5	0.635	0.450	10.4	0.555	0.400
16	10.4	0.221	0.400	11.2	0.595	0.410	10.2	0.521	0.370
17	10.1	0.211	0.360	10.9	0.557	0.370	9.9	0.489	0.330
18	9.7	0.201	0.330	10.5	0.524	0.330	9.5	0.461	0.290
19	9.3	0.190	0.290	9.9	0.494	0.300	9	0.436	0.260
20	8.9	0.180	0.260	9.4	0.464	0.260	8.5	0.414	0.220
21	8.4	0.169	0.230	8.9	0.434	0.230	7.9	0.391	0.190
22	8.0	0.159	0.200	8.4	0.403	0.200	7.3	0.368	0.170
23	7.5	0.148	0.170	7.9	0.371	0.170	6.8	0.344	0.140
24	7.0	0.137	0.140	7.4	0.339	0.140	6.2	0.319	0.110
25	6.5	0.125	0.110	6.9	0.306	0.110	5.7	0.291	0.090
26	5.8	0.112	0.080	6.2	0.272	0.080	5.1	0.261	0.070
27	5.0	0.097	0.060	5.4	0.235	0.060	4.4	0.225	0.050
28	4.1	0.079	0.040	4.4	0.205	0.040	3.7	0.183	0.030
29	2.9	0.057	0.020	3.2	0.150	0.020	2.7	0.132	0.020
30	1.5	0.031	0.010	1.7	0.080	0.010	1.5	0.069	0.010

*Where M_Y: moment around Y-axis, V_X: shear in X-direction and T_X: torsion due to E_X

4.6.2.6. Story Forces Due to E_Y

Table [4.26]: Story Forces Due to E_Y

Story	Frame (*F*)			Shear Wall (*SW*)			Wall-Frame (*DS*)		
	V_Y*10^3 (kN)	T_Y*10^6 (kN.m)	M_X*10^6 (kN.m)	V_Y*10^3 (kN)	T_Y*10^6 (kN.m)	M_X*10^6 (kN.m)	V_Y*10^3 (kN)	T_Y*10^6 (kN.m)	M_X*10^6 (kN.m)
1	13.7	0.669	0.910	17.6	0.779	0.980	15.7	0.719	0.900
2	13.5	0.655	0.860	17.5	0.771	0.920	15.6	0.711	0.850
3	13.1	0.635	0.820	17.2	0.757	0.870	15.3	0.696	0.810
4	12.7	0.613	0.780	16.7	0.736	0.820	14.8	0.675	0.760
5	12.3	0.592	0.740	16.1	0.709	0.780	14.2	0.649	0.720
6	12.0	0.572	0.700	15.4	0.679	0.730	13.6	0.622	0.680
7	11.7	0.554	0.660	14.7	0.648	0.690	13	0.593	0.640
8	11.4	0.537	0.620	13.9	0.617	0.660	12.4	0.566	0.610
9	11.1	0.519	0.580	13.3	0.586	0.620	11.8	0.540	0.580
10	10.8	0.502	0.550	12.6	0.558	0.590	11.3	0.516	0.540
11	10.6	0.485	0.510	12.1	0.532	0.550	10.9	0.496	0.510
12	10.3	0.468	0.480	11.6	0.510	0.520	10.6	0.477	0.480
13	10.0	0.451	0.450	11.2	0.489	0.490	10.3	0.461	0.460
14	9.7	0.435	0.410	10.8	0.470	0.470	10	0.445	0.430
15	9.4	0.419	0.380	10.5	0.453	0.440	9.8	0.430	0.400
16	9.2	0.403	0.350	10.2	0.437	0.410	9.5	0.415	0.370
17	8.9	0.387	0.320	9.9	0.421	0.380	9.3	0.400	0.350
18	8.6	0.371	0.290	9.7	0.405	0.350	9	0.384	0.320
19	8.3	0.355	0.260	9.4	0.390	0.320	8.7	0.369	0.290
20	8.0	0.338	0.230	9.2	0.376	0.300	8.4	0.353	0.270
21	7.7	0.320	0.200	8.9	0.362	0.270	8.2	0.338	0.240
22	7.3	0.302	0.180	8.7	0.349	0.240	8	0.324	0.210
23	6.9	0.283	0.150	8.5	0.335	0.210	7.7	0.310	0.190
24	6.5	0.263	0.130	8.2	0.321	0.180	7.5	0.295	0.160
25	6.1	0.242	0.100	7.9	0.303	0.140	7.2	0.279	0.130
26	5.6	0.219	0.080	7.4	0.282	0.110	6.8	0.260	0.100
27	5.0	0.194	0.060	6.8	0.255	0.080	6.2	0.235	0.080
28	4.2	0.162	0.040	5.8	0.217	0.060	5.3	0.201	0.050
29	3.2	0.121	0.020	4.4	0.164	0.030	4.1	0.154	0.030
30	1.8	0.068	0.010	2.4	0.089	0.010	2.3	0.085	0.010

*Where M_X: moment around X-axis, V_Y: shear in Y-direction and T_Y: torsion due to E_Y.

4.6.3. Graphical Presentation

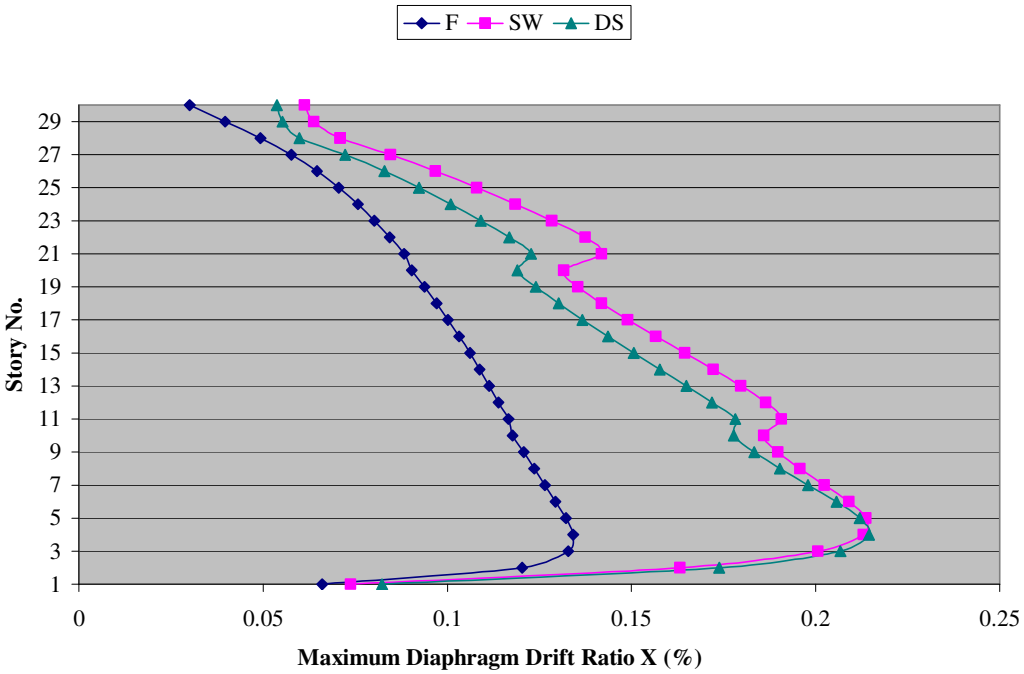

Figure (4.50): Toronto Tower – Maximum Diaphragm Drift Ratio Due to E_X

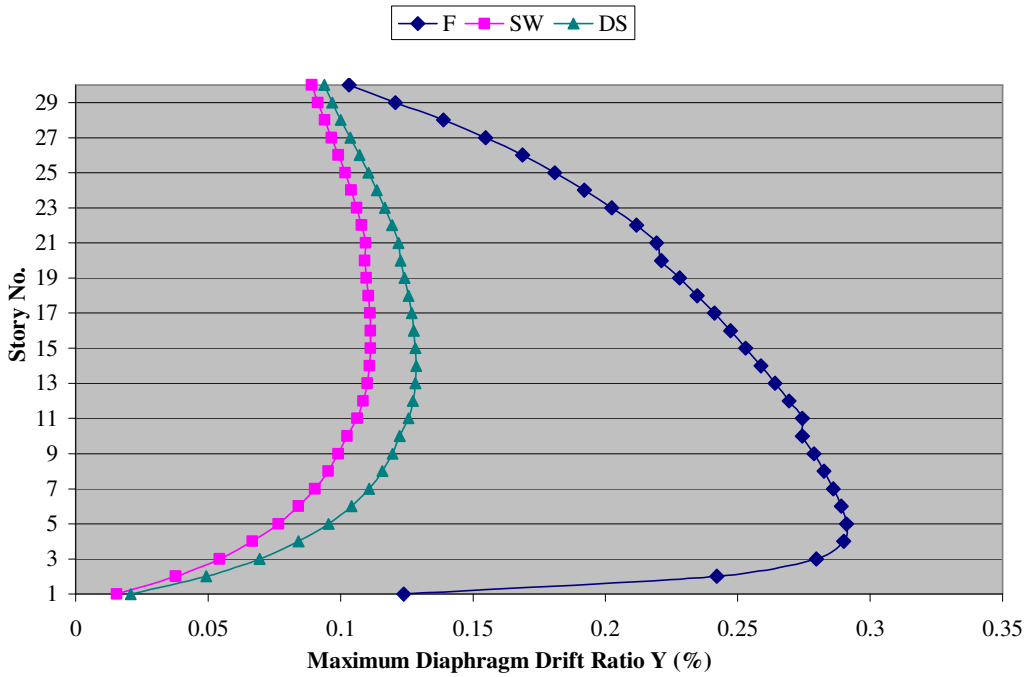

Figure (4.51): Toronto Tower – Maximum Diaphragm Drift Ratio Due to E_Y

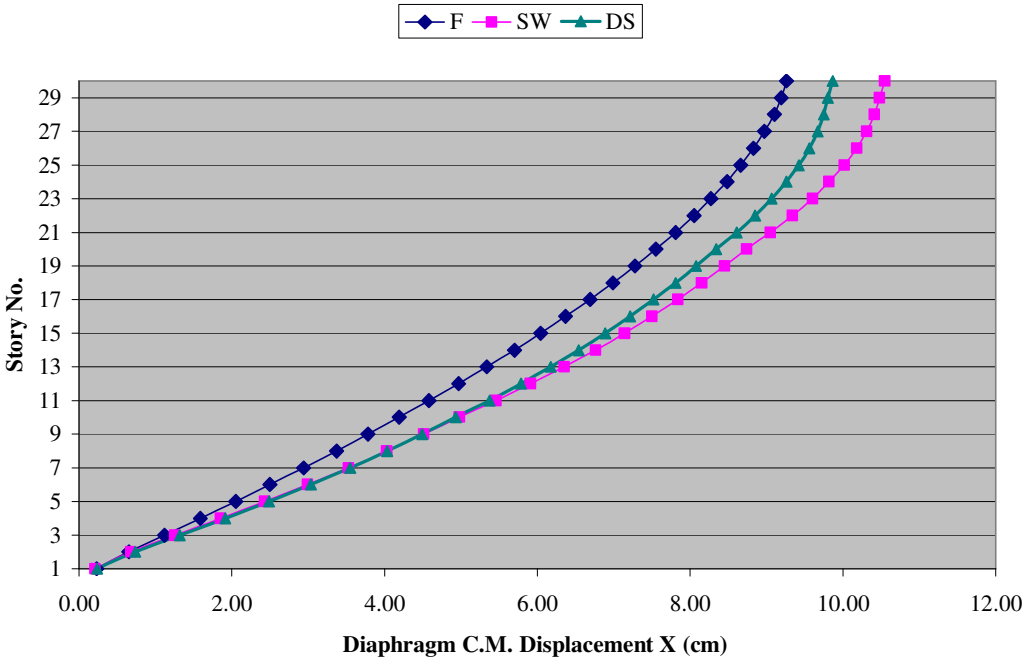

Figure (4.52): Toronto Tower – Diaphragm *C.M.* Displacement X Due to E_X

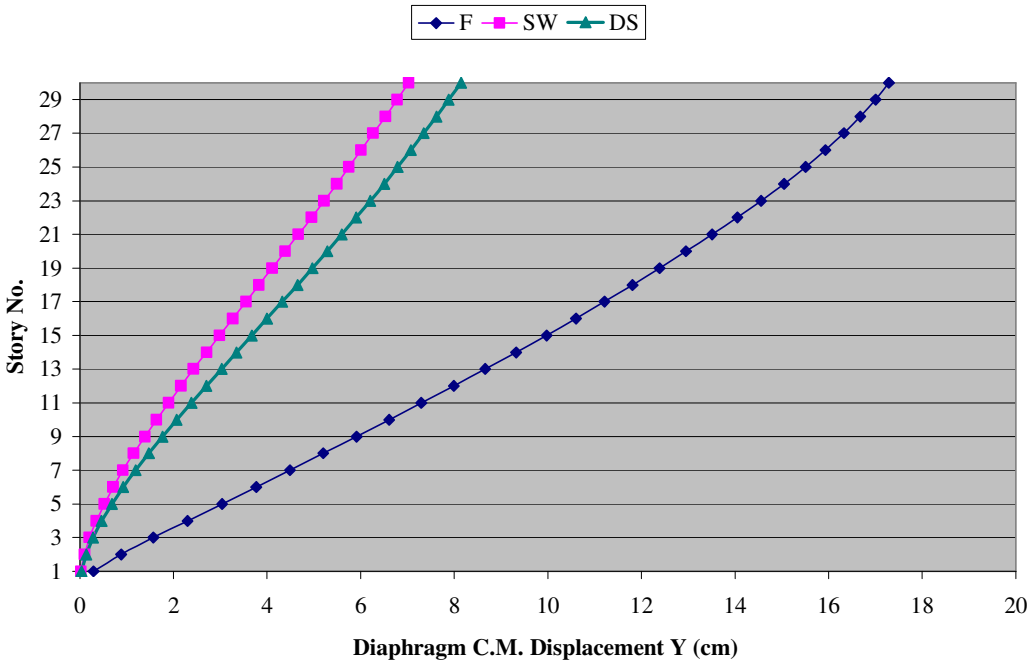

Figure (4.53): Toronto Tower – Diaphragm *C.M.* Displacement Y Due to E_Y

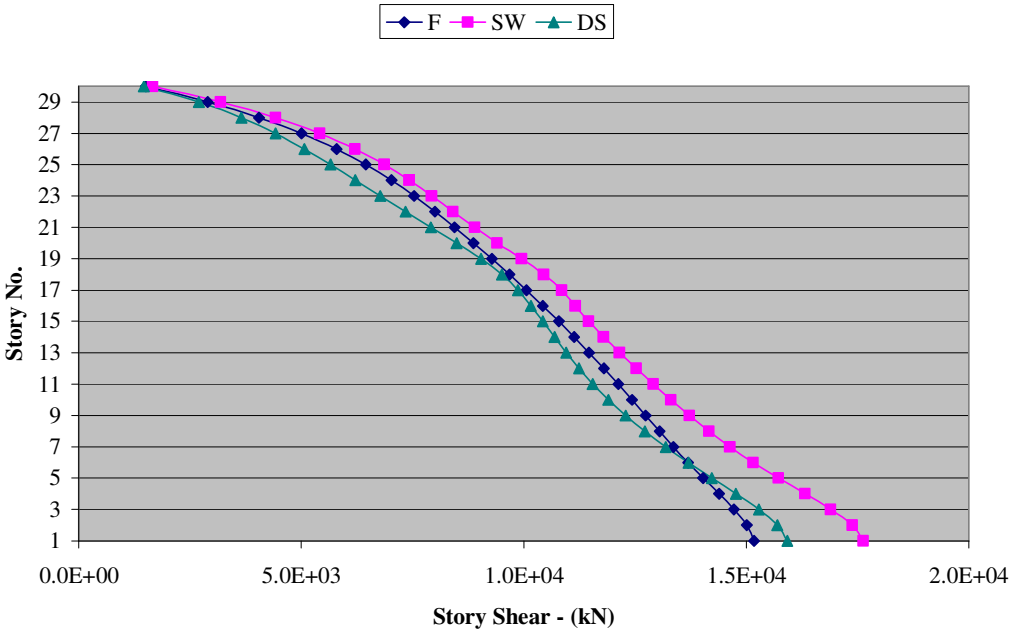

Figure (4.54): Toronto Tower – Story Shear V_X Due to E_X

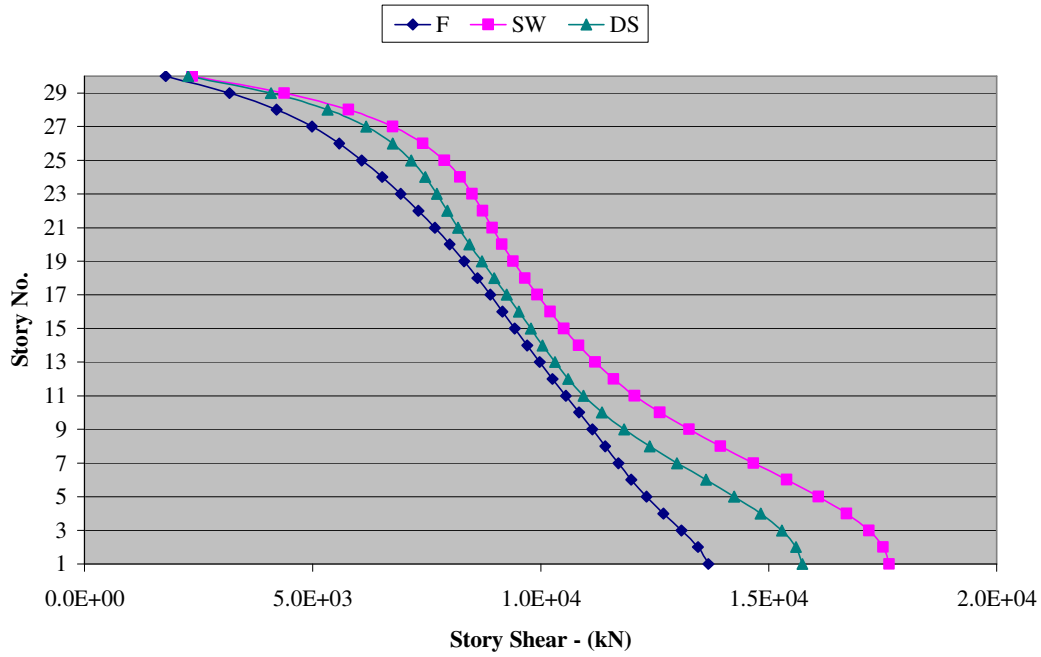

Figure (4.55): Toronto Tower – Story Shear V_Y Due to E_Y

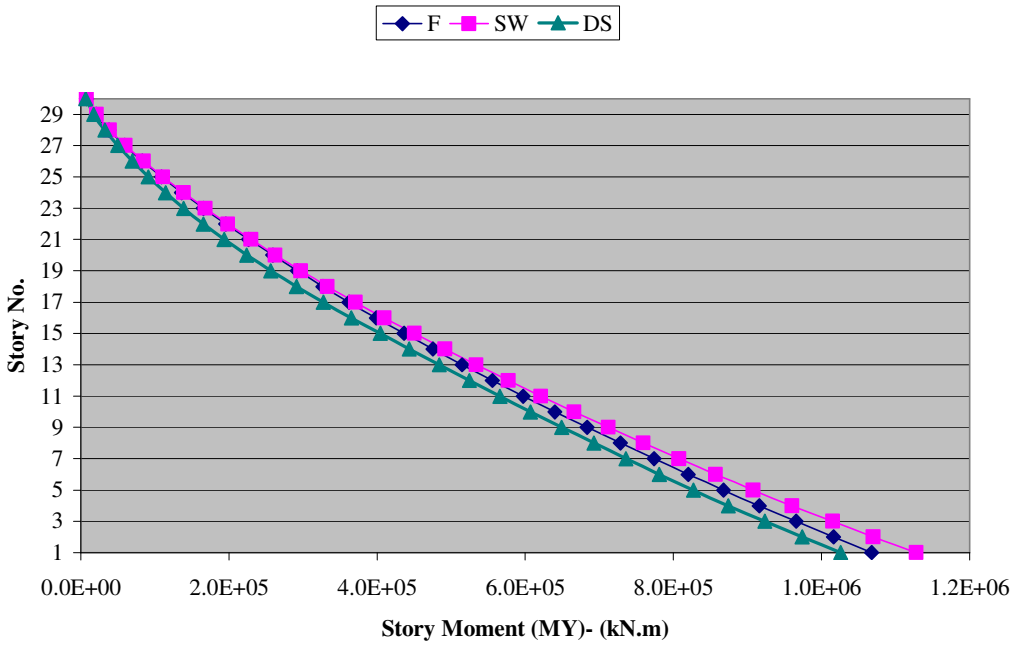

Figure (4.56): Toronto Tower – Story Moment M_Y Due to E_X

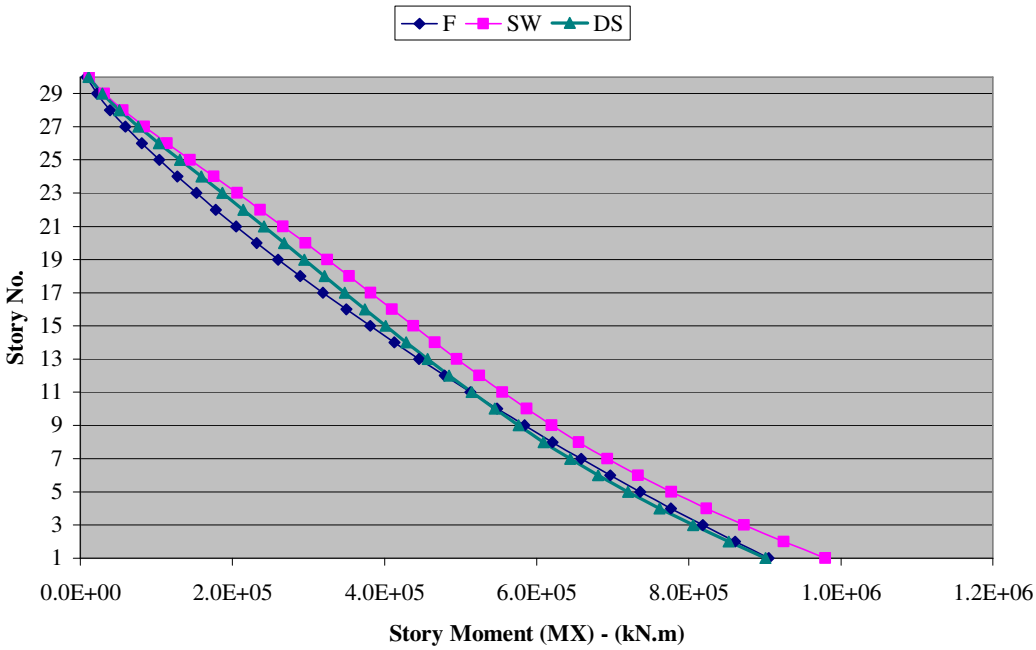

Figure (4.57): Toronto Tower – Story Moment M_X Due to E_Y

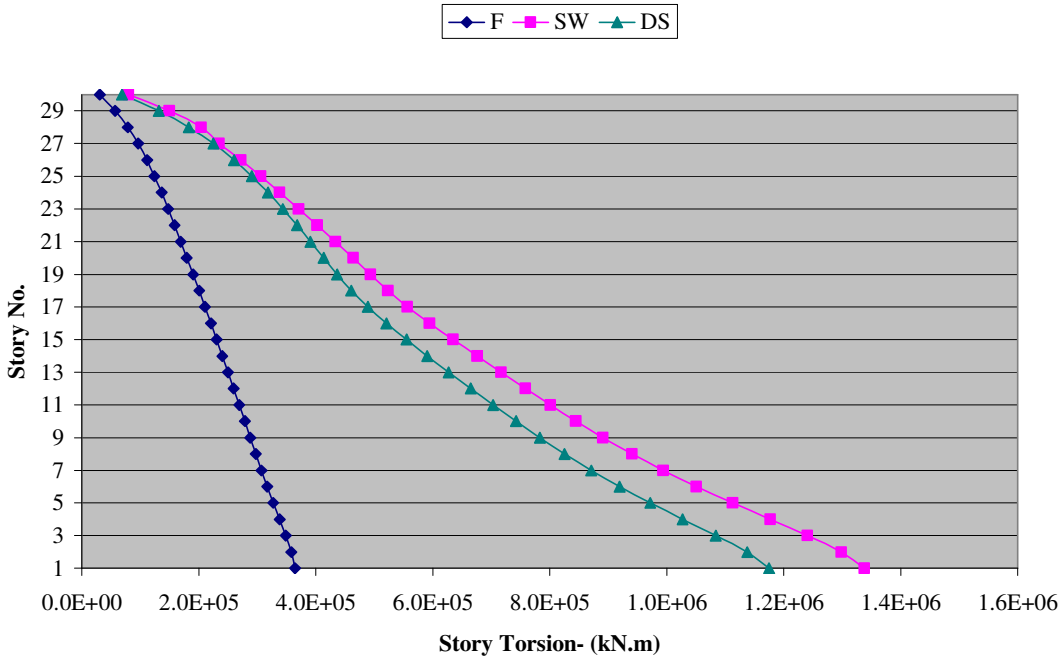

Figure (4.58): Toronto Tower – Story Torsion (T_X) Due to E_X

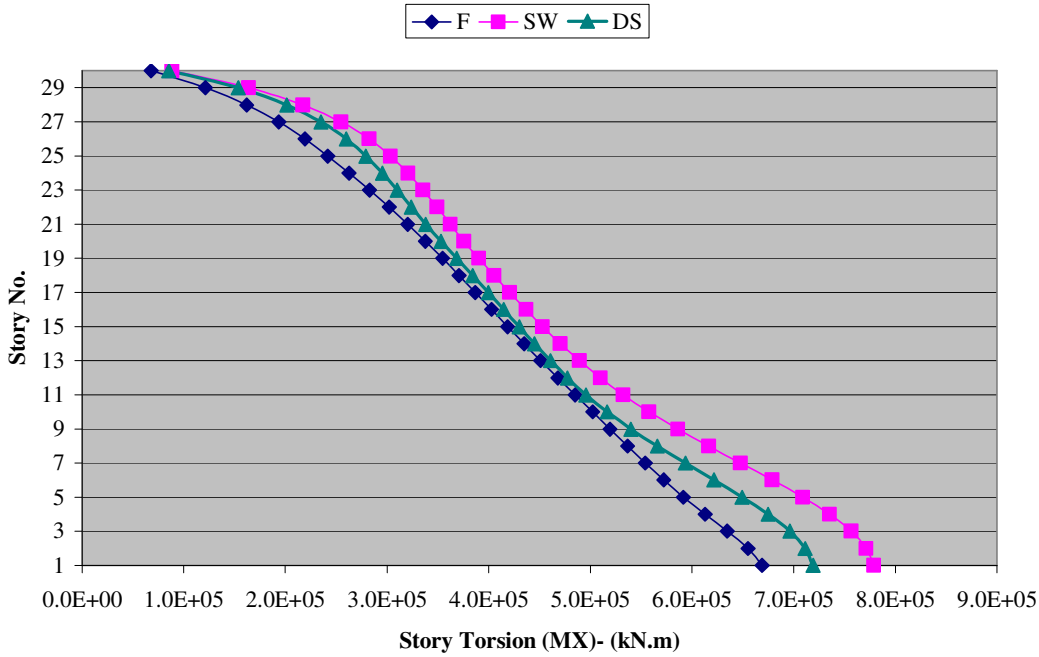

Figure (4.59): Toronto Tower – Story Torsion (T_Y) Due to E_Y

4.6.4. Summary of Results for Toronto Tower

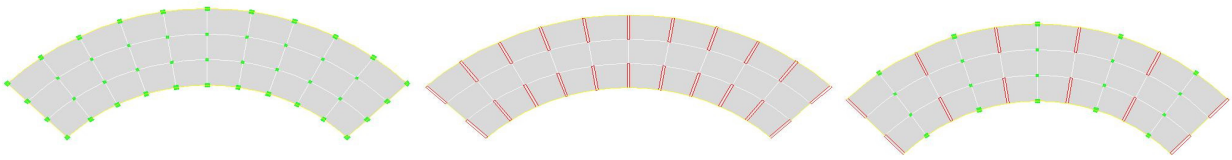

Figure (4.60): Toronto Tower with Three Structural Systems

Table [4.27]: Summary of Results- Toronto Tower

	F	***SW***	***DS***
Max. drift Ratio X- %	0.134	0.214	0.215
Max. drift Ratio Y- %	0.291	0.111	0.129
C.M. Absolute Max. displacement X-cm	9.3	10.6	9.9
C.M. Absolute Max. displacement Y-cm	17.3	7.0	8.1
Base shear-V_X- kN (10^3)	15.2	17.6	15.9
Base shear $-V_Y$- kN (10^3)	13.7	17.6	15.7
Base moment-M_Y- kN (10^6)	1.07	1.013	1.03
Base moment $-M_X$- kN.m (10^6)	0.905	0.979	0.901
Base torsion-T_X- kN.m (10^6)	0.365	1.34	1.18
Base torsion-T_Y- kN.m (10^6)	0.669	0.779	0.719
First mode shape period – sec.	5.09	3.69	3.62

Table [4.28]: Toronto Building Stiffness

	$K_X^{(1)*}10^6$	$K_Y^{(2)*}10^6$	K_X/K_Y
F	0.111	0.049	2.30
SW	0.112	0.125	0.90
DS	0.108	0.101	1.07

(1)K_X: Building Stiffness in X-direction, kN/m
(2)K_Y: Building Stiffness in Y-direction, kN/m

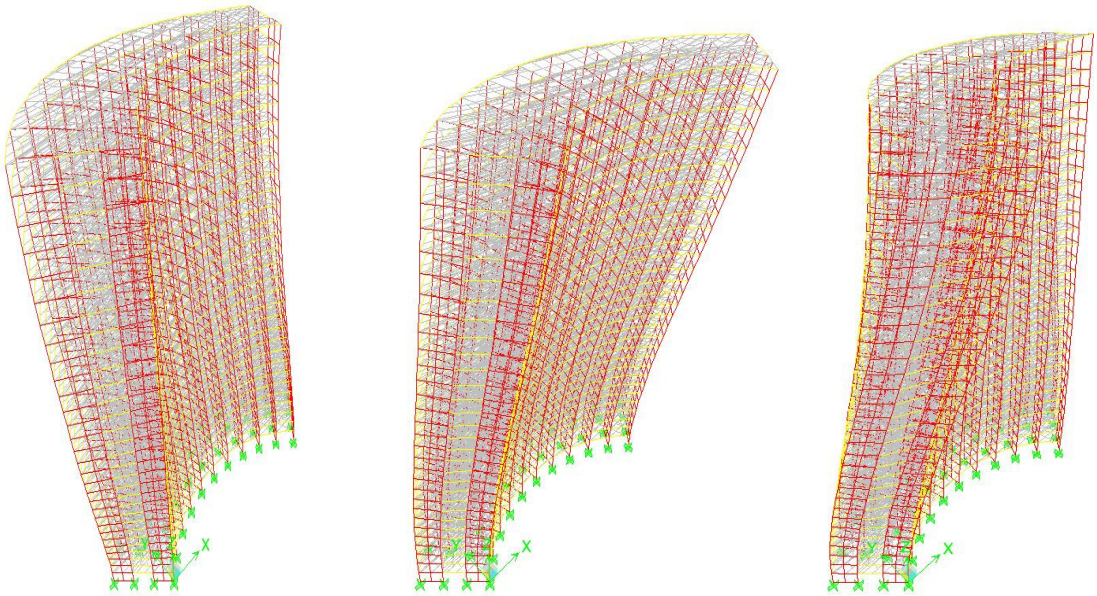

(a) 1st Mode, T=3.69sec. (b) 2nd Mode, T=3.25sec. (c) 3rd T=2.45 sec.

Figure (4.61): The First Three Modes of Vibration for *(SW)* System Toronto Tower

4.6.5. Synthesis of Results: Remarks and Comments

- **Drift Ratio and Displacement Curves:**

(1) The drift curves in the X-direction, Figure (4.50), differ from all other shapes presented in the previous case studies, where the *(F)* system has the least drift values and the *(SW)* system has the largest ones. However, in the Y-direction the results match with what has been discussed earlier. The reason for this behavior can be explained by the inefficient arrangement of shear wall elements in the (*SW*) system, where all the inertia of the vertical elements is located in only one radial direction. Therefore, the structural stiffness in X-direction becomes small enough to approach that of the *(F)* system stiffness, refer to Table [4.28].

(2) Stiffness values are almost similar for each system in the X-direction, which in turn renders displacement and drift values closer to each other for the three systems, see Table [4.27].

(3) The wall elements of the *(SW)* system do not resist seismic force efficiently in the X-direction because none of these walls is parallel to this direction, also the center of rigidity and center of mass do not coincide as in all the previous shapes. The distribution of walls in this system in radial forms is not serving the X-direction in resisting seismic loads.

(4) Figure (4.52) indicates that both *(SW)* and *(DS)* systems behave similarly to *(F)* system in the X-direction, which is clearly observed by the shear mode deflected curves. This illustrates that the *(DS)* system is not working properly or the axial forces between walls and frames are not enough to create a well interacted behavior. Therefore, walls are not able to restrain the frames at the base, and the frames are unable to restrain the walls at the top.

- **Story Forces Curves:**

(1) The base shears are proportioned in accordance with the calculated stiffness of Table [4.28]

(2) The base shear values in both directions for both (*DS)* and (*SW)* systems are shared equally because K_X/K_Y value almost equals 1.0. See Table [4.28].

(3) The curvilinear shape induces a large torsional moment in the X-direction for both (*DS)* and (*SW)* systems. The reason as stated before is the extremely large eccentricity between the center of mass and the center of twist or rigidity.

A clear graphical presentation for the location of center of mass *(C.M.)* and center of rigidity *(C.R.)* for the curvilinear shape in shown in Figure (4.62).

It can be observed from these figures that the (*SW)* system produces much more eccentricity than the (*F)* system, as shown below.

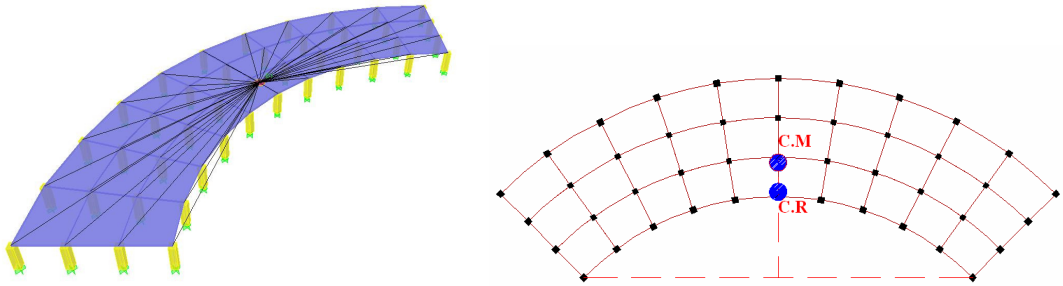

(a) Frame System, *(F)*

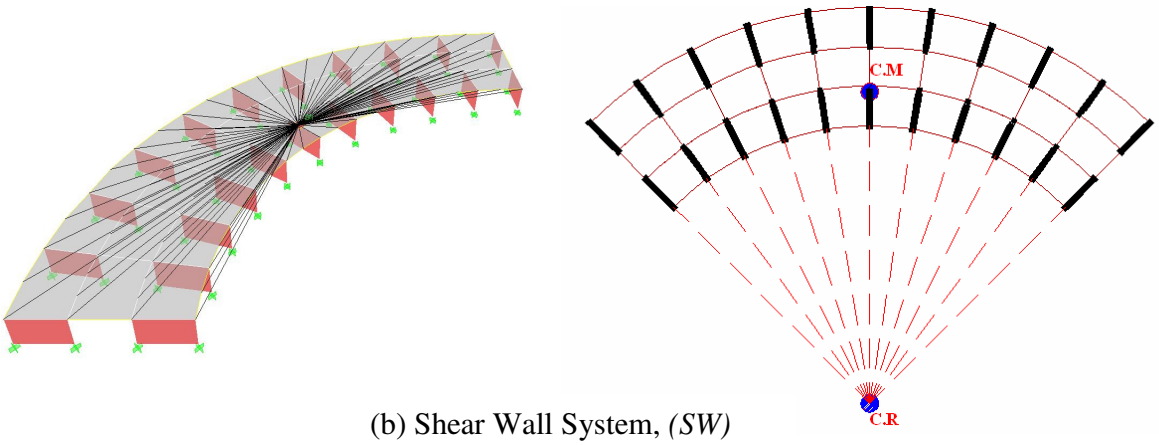

(b) Shear Wall System, *(SW)*

Figure (4.62): *C.M.* vs *C.R.* in Curvilinear Shape

ETABS evaluates the center of rigidity at a particular diaphragm; the structure is analyzed for three load cases. The loads are applied at the center of mass (or any arbitrary point). Load case 1 has a unit load applied in the global X direction and results in a diaphragm rotation of Rzx. Load case 2 has a unit load applied in the global Y direction and results in a diaphragm rotation of Rzy. Load case 3 has a unit moment applied about

the global Z-axis, giving a diaphragm rotation of Rzz. The center of rigidity relative to the center of mass (or the arbitrary point) is then given by the coordinates (X, Y), where X = -Rzy / Rzz and Y = Rzx / Rzz. This point is a function of the structural properties and is independent of any loading.

It should be noted that eccentricity increases when the surface elements are assigned as membrane, because it can only resist forces through its plan, on the contrary to shell elements which resist forces in both in-plane and out-of-plane plate bending. Also ETABS adds the slab's stiffness, if assigned as a shell element, to the overall stiffness when calculating the center of rigidity.

4.6.6. Proposed New *(SW)* and *(DS)* Plans Configurations

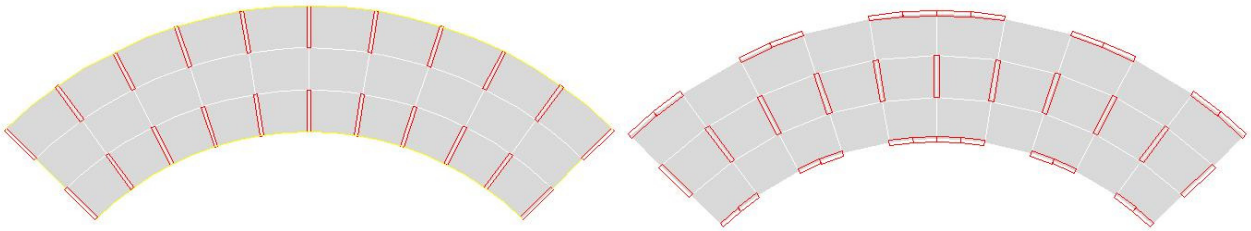

(a) Original Wall Configuration (b) New Wall Configuration

Figure (4.63): Curvilinear Shape, *(SW)* System Layout Plans

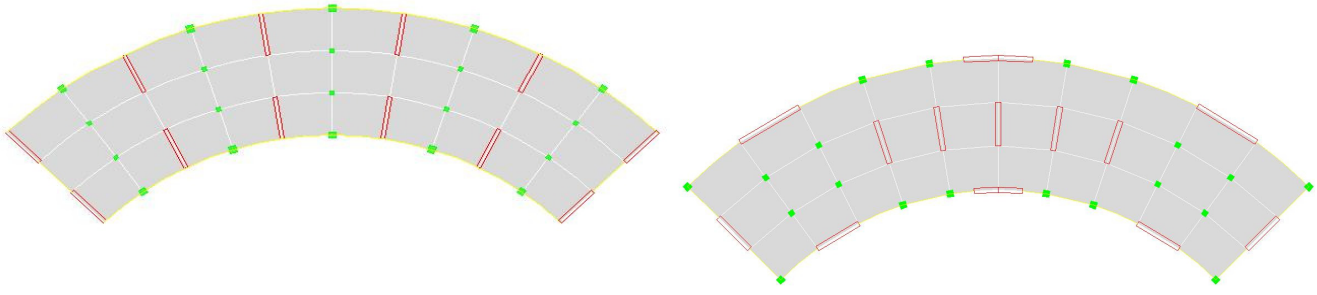

(a) Original Wall-Frame Configuration (b) New Wall-Frame Configuration

Figure (4.64): Curvilinear Shape, *(DS)* System Layout Plans

Table [4.29]: Proposed New *(SW)* and *(DS)* Configurations-Comparison Table

	$K_{X\ Original} * 10^6$	$K_{XNEW} * 10^6$	$T^{(1)}_{Original}$	T_{New}
SW	0.112	0.557	3.69	2.88
DS	0.108	0.295	3.62	3.40

(1) *T*: First Mode Period, sec.

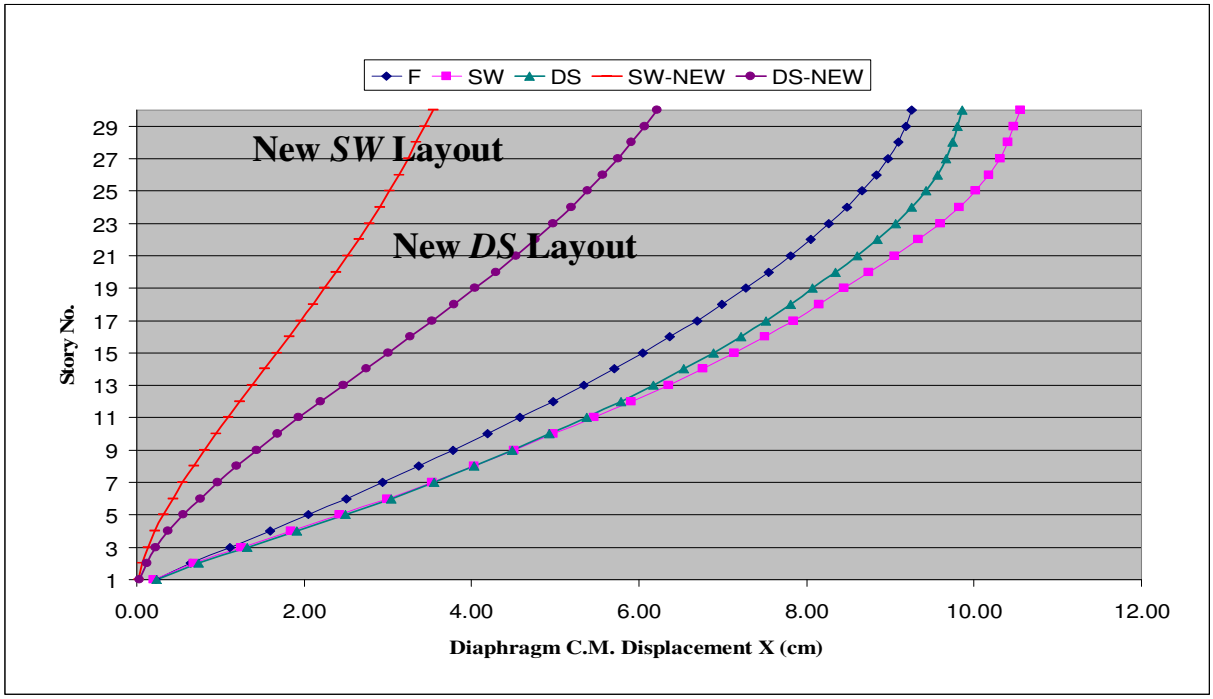

Figure (4.65): Diaphragm *C.M.* Displacement X Due to E_X with the New Layout Plans

The efficiency of these systems can be traced by the displacement curves shown in Figure (4.65). The new deflected shape for the *(SW)* system appears with its expected flexural mode shape and the *(DS)* system with its two curvatures.

It can be noted that the displacement curves can serve as a good indication of how the structure behaves under lateral loads.

The new modified *(SW)* system layout plan shows the necessity for the structural engineer to understand thoroughly the importance of arranging and locating the vertical

elements in any structure during the design phase, and emphasizes how the new arrangement of walls changes the location of *C.R.* dramatically, as shown in Figure (4.66).

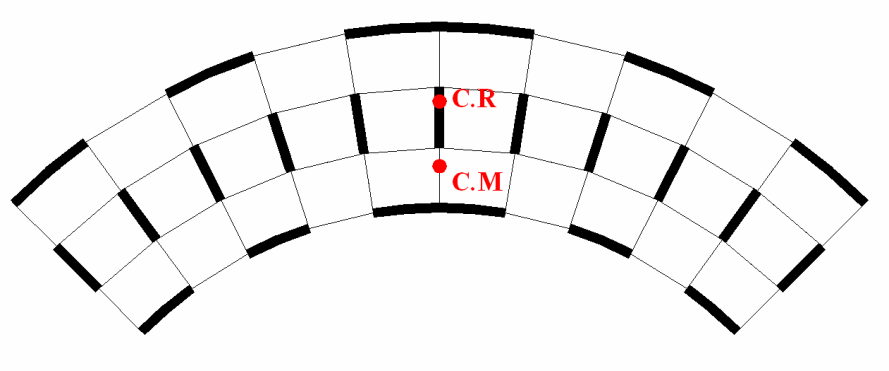

Figure (4.66): Location of the Center of Rigidity in the New (*SW*) System

CHAPTER FIVE

THE INTERACTION BETWEEN BUILDING SHAPE, OVERALL STIFFNESS, AND STRUCTURAL SYSTEM

5.1. General

Once a given building plan (and shape) is selected, it is inherently embedded that a number of structural systems are better suited for this plan than for other buildings plans (and shapes). Thus, in a way, a given building plan dictates a few particular structural systems, which also indicates that the overall stiffness of the building, a function of the structural system, is indirectly related to the building plan.

A comparison of the stiffnesses of the four buildings is forthtelling, particularly when the buildings are so designed to have the same mass by proportioning all four buildings to have the same floor area each. Other similarities for the models that have been considered in this study are:

(1) Story height.

(2) Number of stories.

(3) Gravity loading.

(4) Response spectrum and seismic data.

(5) Material and element sections.

(6) Supports condition.

The comparison plots between the four building shapes using the same structural system represent the variation due to the only factor which is the overall geometry that is the combined effect of the shape and the structural stiffness together.

The building stiffness, as mentioned earlier, has been calculated for comparison purposes by placing the static seismic forces according to the IBC equivalent force procedure at the center of mass (*C.M.*) for each story distributed vertically in a power distribution applied in the needed direction. Then the stiffness is simply calculated by dividing the total base shear force over the calculated maximum top displacement in that direction.

5.2. Comparison of Different-Plan Buildings with Frame (*F*) System

Moment-resisting frames carry lateral loads primarily by flexure in the members and joints. Joints are designed and constructed so they are theoretically completely rigid, and therefore any lateral deflection of the frame occurs from the bending of columns and beams.

The IBC differentiates between three types of moment resisting frames: first, special moment-resisting frames that must be specifically detailed to provide ductile behavior to meet the inelastic displacement demand the structure undergoes. Second, the intermediate moment-resisting frame, which is a concrete frame with less restrictive requirements than special moment-resisting frames. The third type is the ordinary moment-resisting frame. To be kept in mind, is an awareness that code assigned limitations in the selection of systems depend on building height and seismic design category (a classification assigned to a structure based on its seismic use group and the severity of the design earthquake ground motion at the site). However, these limitations are differ from code to another but mainly for example, ordinary moment-resisting frame is used in low seismic area.

Figure (5.1) shows frame systems for the different building layouts. Also the period and stiffness for each system in the X-direction have been calculated and plotted as shown in Figures (5.2) and (5.3), respectively.

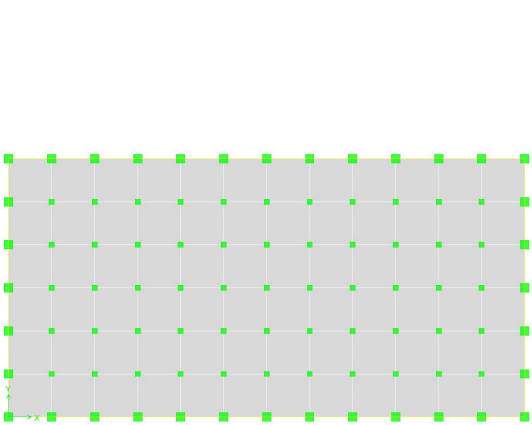

(a) Rectangular Building

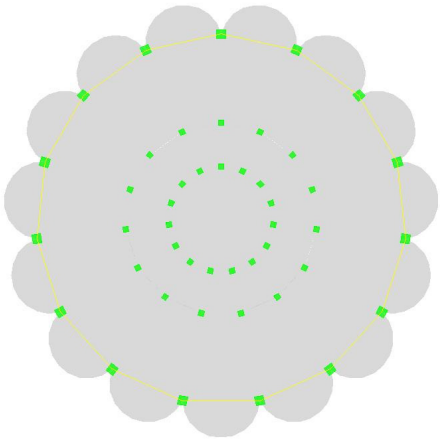

(b) Marina Tower

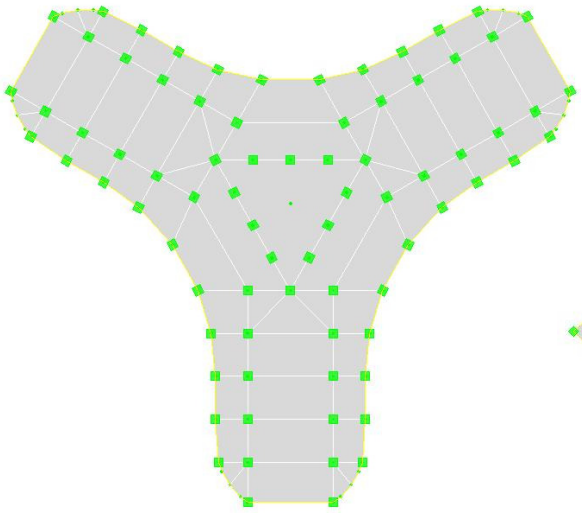

(c) Lake Point Tower

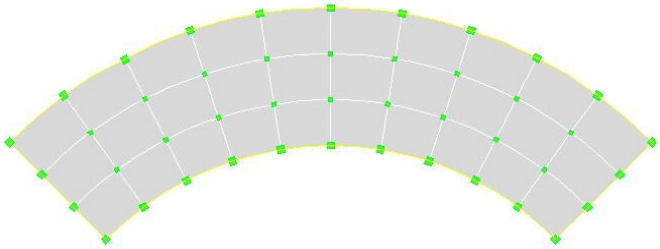

(d) Toronto Tower

Figure (5.1): Frame System for Different-Plan Buildings

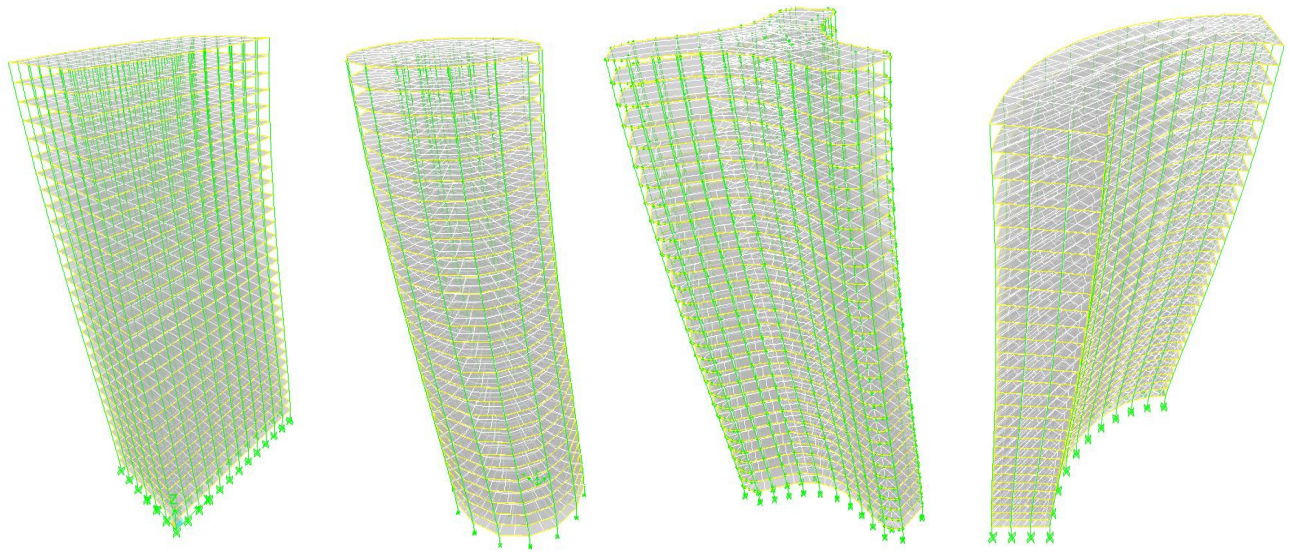

(a) *T*=3.14sec. (b) T= 4.24sec. (c) T= 3.15sec (d) T=4.09 sec.

Figure (5.2): Period, First mode of vibration, *(F)* System Different-Plans

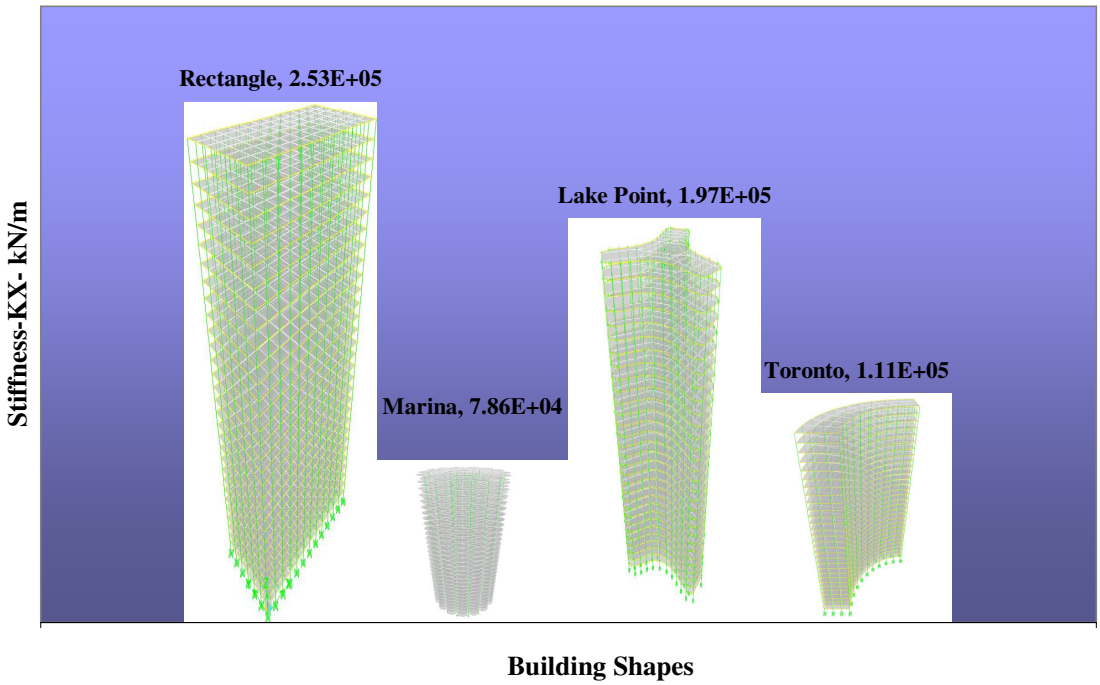

Figure (5.3): Stiffness (K_X) Comparison for Different Shapes with Frame System *(F)*

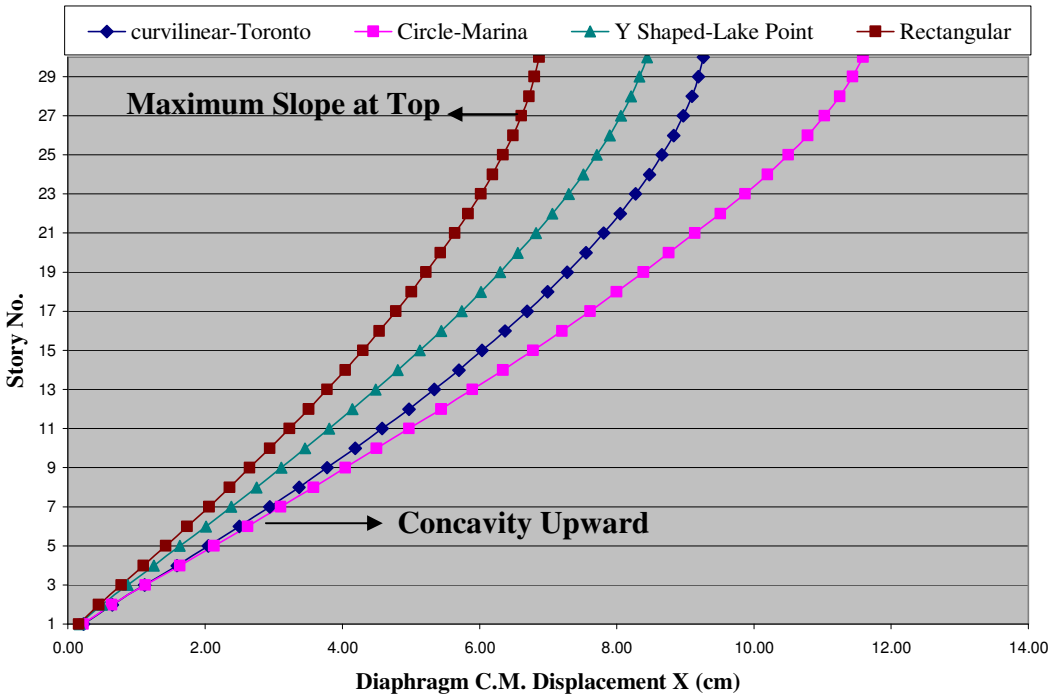

Figure (5.4): Diaphragm *C.M.* Displacement X Due to E_X for Different Building Shapes with Frame Systems

Figure (5.4) indicates clearly how the stiffness of a structure plays a major role in determining the deflected shape behavior, it can be observed that:

Displacements in ⟶ Rectangular building < Lake Point < Toronto < Marina

This is inversely proportional to stiffness as shown in Figure (5.3).

Stiffness in ⟶ Rectangular building > Lake Point > Toronto > Marina.

The horizontal stiffness of a rigid frame is governed mainly by the bending resistance of girders, the columns, and their connections while in a tall building this is done mainly by the axial rigidity of the column i.e. (*AE/L*) in the elastic range, where *A*: cross-sectional area, *L*: length of column, and *E*: modulus of elasticity.

The accumulated horizontal shear above any story of a rigid frame is resisted by shear in the columns in that story. The shear causes the story columns to bend in double

curvature with points of contraflexure at approximately mid-story height levels. The moments applied to a joint from the columns above and below a given floor are resisted by the attached girders, which bend in double curvature, with points of contraflexure at approximately mid span, refer to Figure (5.5).

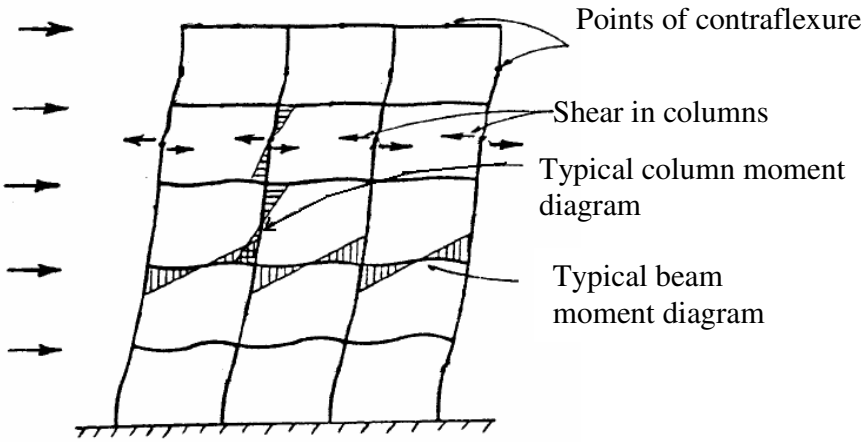

Figure (5.5): Forces and Deformations Caused by External Shear

These deformations of the columns and girders allow racking of the frame and horizontal deflection in each story. The overall deflected shape of a rigid frame structure due to racking has a shear configuration mode with a maximum inclination at the top as shown in all frame models of this thesis whatever the structural stiffness of the model is as shown in Figure (5.4).

The overall moment of the external horizontal load is resisted in each story level by coupled forces resulting from the axial tensile and compressive forces in the columns on opposite sides of the structure, Figure (5.6).

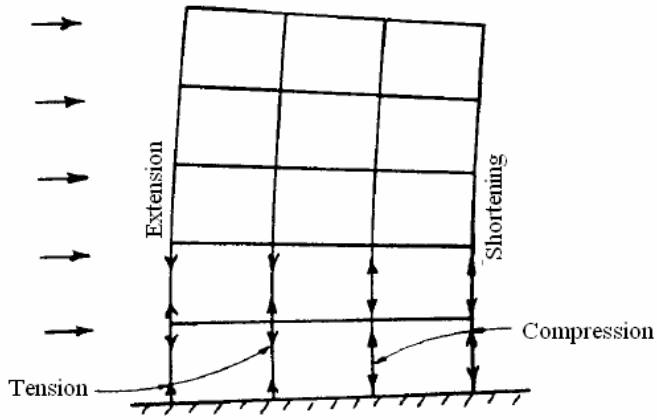

Figure (5.6): Forces and Deformations Caused by External Moment

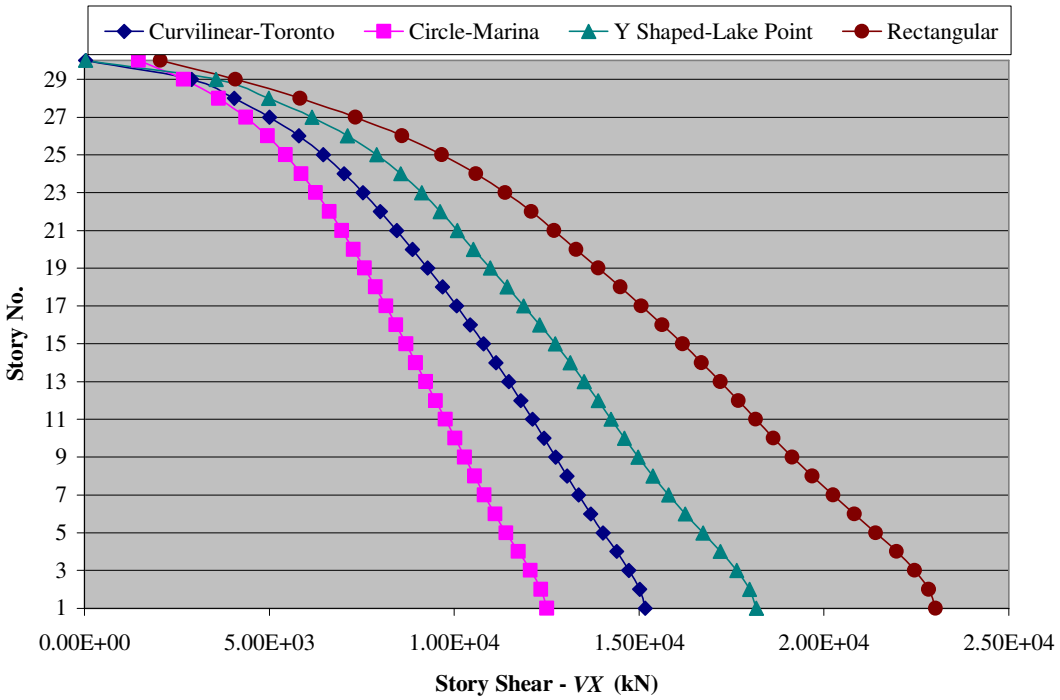

Figure (5.7): Story Shear V_X Due to E_X for Building Shapes with Different Frame Systems

It is noted also that the stiffer the system the more force it attracts, from Figure (5.7), and the shorter the period the stiffer the structure, hence spectral acceleration approaches peak ground acceleration. On the other hand, for very long period systems, the spectral displacement approaches peak ground displacement. This behavior is depicted in Figure (5.8).

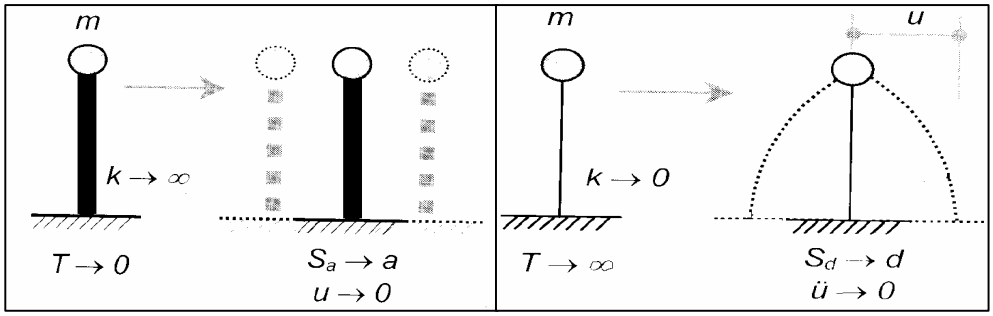

Figure (5.8): Stiff (Left) and Flexible (Right) Structure's Response, (Armouti, 2004).

5.3. Comparison of Different-Plan Buildings with (*SW*) System

A shear wall building is in some way a misnomer because walls deform predominantly in flexure, as will be illustrated in the next paragraphs.

In the four models of this study, the shear wall systems is said to be a proportionate system in which the ratio of the flexural rigidities of the walls remain constant throughout their height, as shown in Figure (5.9 a).

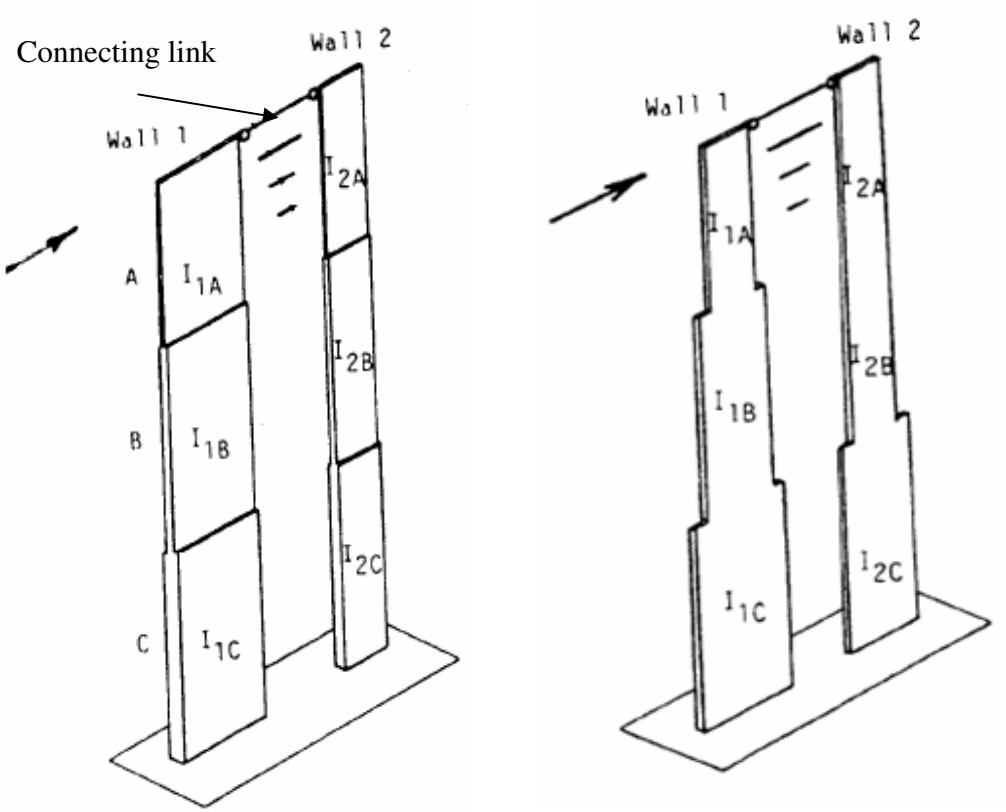

$$\frac{I_{1A}}{I_{2A}} = \frac{I_{1B}}{I_{2B}} = \frac{I_{1C}}{I_{2C}}$$

$$\frac{I_{1A}}{I_{2A}} \neq \frac{I_{1B}}{I_{2B}} \neq \frac{I_{1C}}{I_{2C}} \quad (\textit{not equal})$$

(a) Proportionate Shear Walls (b) Non-Proportionate Shear Walls

Figure (5.9): Proportionate and Non-Proportionate Shear Walls
(Coull, A. and Smith, B., 1991)

Figure (5.10) shows shear wall systems for the different building layouts. Also the stiffness for each system in the X-direction has been calculated and plotted as shown in Figures (5.11).

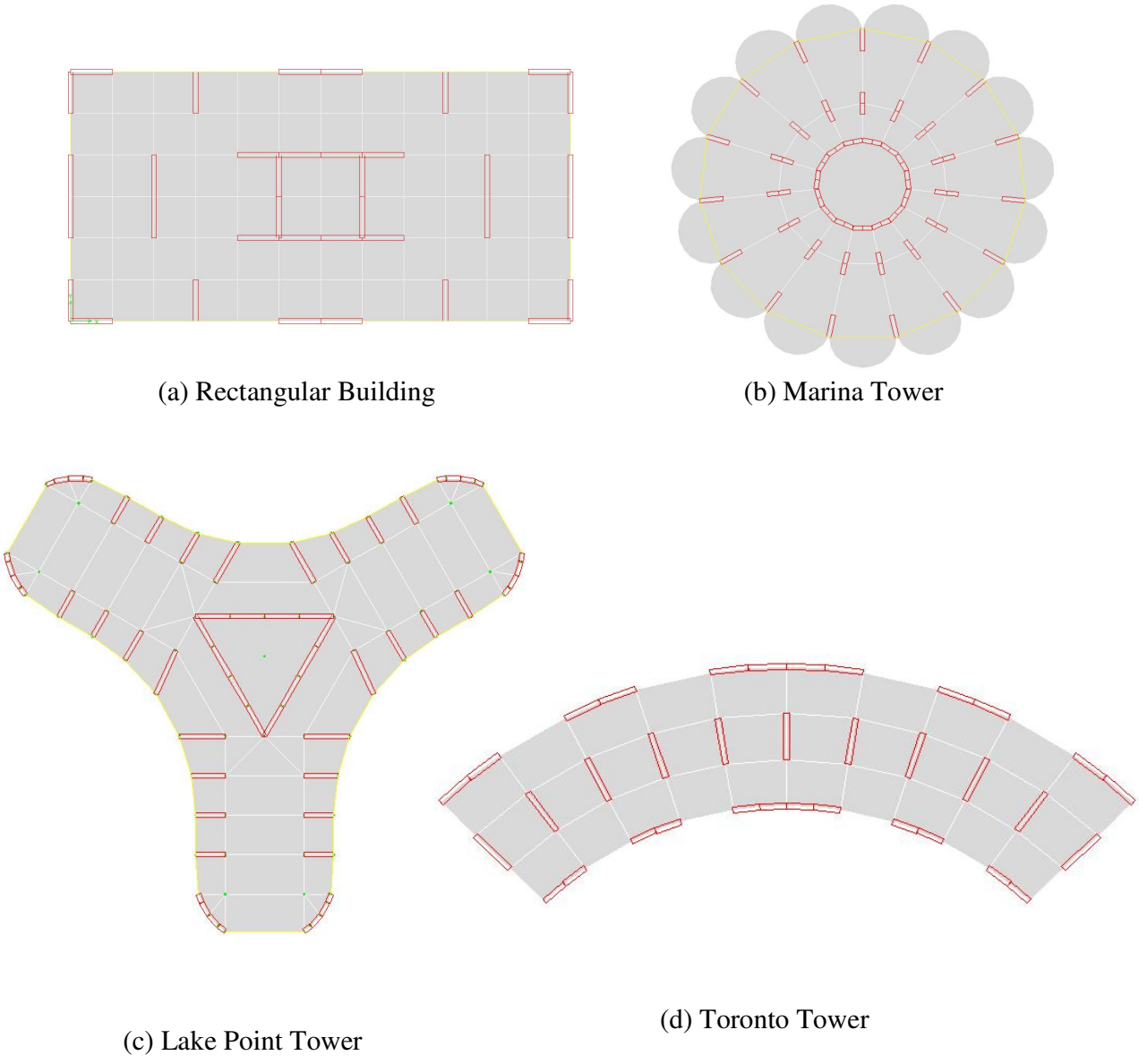

(a) Rectangular Building

(b) Marina Tower

(c) Lake Point Tower

(d) Toronto Tower

Figure (5.10): Shear Wall System for Different-Plan Building

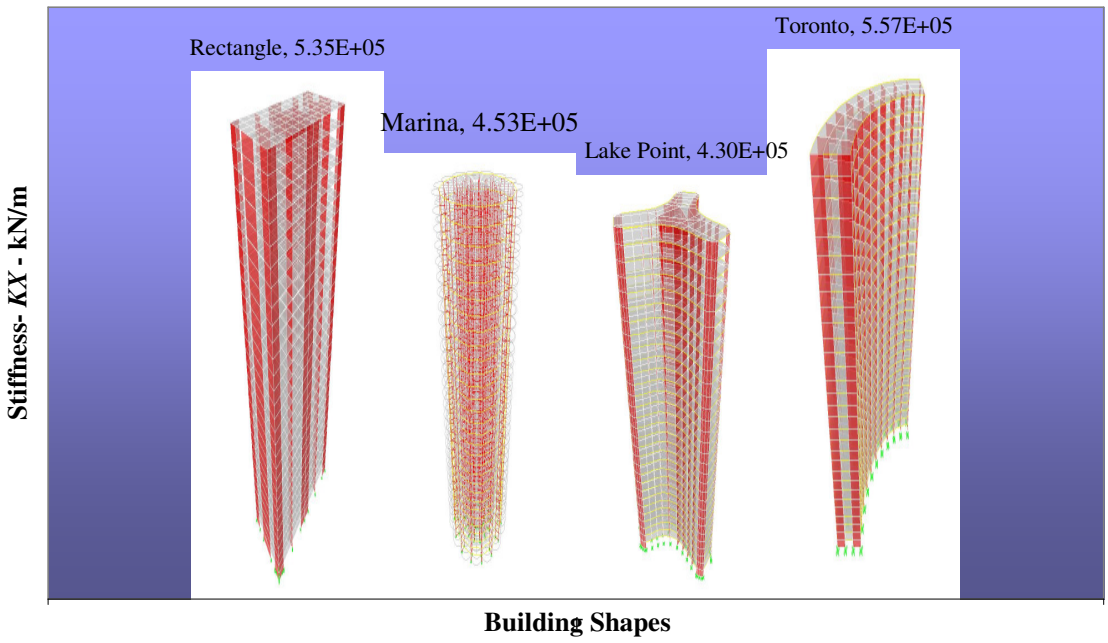

Figure (5.11): Stiffness Comparison for Different Shapes with Shear Wall System

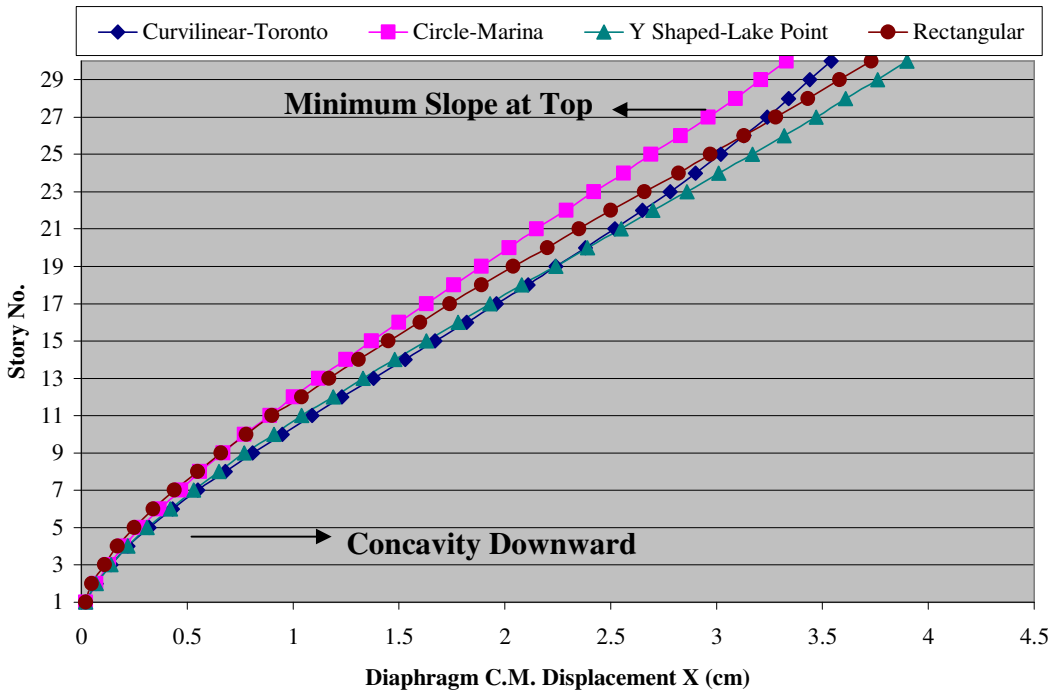

Figure (5.12): Diaphragm *C.M.* Displacement X Due to E_X for Different Building Shapes with Shear wall Systems

The shape of the graphs in Figure (5.12) indicates again that shear wall system deflects in a flexural mode whatever the arrangement of walls is within the layout plan.

The rectangular building, Marina Tower and Lake Point shear wall systems are considered non-twisting structures, where the *C.M.* and *C.R.* coincide. So at any level *i*, the total external shear V_i, will be distributed between the walls in the ratio of their flexural rigidities. The resulting shear in a wall *j* at level i can be expressed as:

$$V_{ji} = V_i * \frac{(EI)_{ji}}{\sum (EI)_i} \tag{5.1}$$

Where; $(EI)_{ji}$ is the flexural rigidity of wall j at level i and $\sum(EI)_i$ represents the summation of the flexural rigidities of all the walls at level *i*.

On the other hand Toronto curvilinear Tower is a type of proportionate twisting structure under lateral earthquake in the X-direction, so the horizontal displacement of any floor is a combination of a translation and a rotation of the floor about a center of twist or center of flexural rigidity of the walls.

It can be seen that the stiffness values in Figure (5.11) are close which illustrates why the displacement curves for all shapes in the X-direction are adjacent to each other.

This leads to say that whatever the shape of the building is, seismic forces induced depend primarily on the stiffness of the structure. The effect of the plan shape on the results has therefore an indirect, rather than direct, bearing.

5.4. Wall Deflection Components

Walls, when subjected to in-plane lateral loads, undergo deflection. This deflection is a result of the wall behaving both in a flexural mode and a shear mode. The prime behavioral mode is dependent on height to length ratios. Most walls behave neither in pure

flexural mode, nor in pure shear mode. Their overall behavior is normally a combination of the two modes. However, shear walls in the study models behave in a flexural mode predominantly. The reason for this is, presented in the subsequent paragraphs.

Wall rigidity is the amount of force required to deflect the wall by one unit. Strictly speaking, rigidity is the reciprocal of deflection. Calculation of rigidity primarily serves two purposes:

(1) Distribution of lateral loads to various lateral load-resisting elements.

(2) Calculation of the overall deflection (drift) of the system.

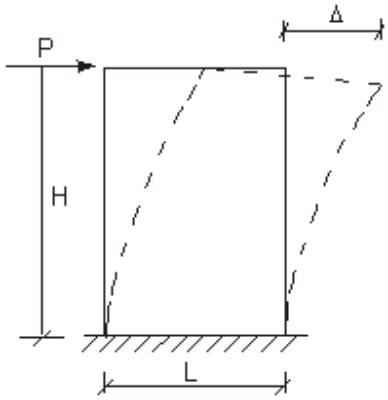

Figure (5.13): Shear Wall Deflection

A cantilever shear wall subjected to lateral load will deflect "Δ" as shown in Figure (5.13). Considering flexural and shear deformations, Δ of a unit lateral load can be calculated by:

$$\Delta = \frac{H^3}{3EI} + \frac{1.2H}{GA} \qquad (5.2)$$

Where; $A = t \times L$

$I = \frac{tL^3}{12}$ for uncracked section

t = thickness of wall

G = shear modulus = $0.4\,E$

H = height of shear wall

Substituting these values in the previous equation yields:

$$\Delta = \left[\frac{4H^3}{EtL^3}\right] + \left[\frac{3H}{EtL}\right] = \frac{1}{Et}\left[4\left(\frac{H}{L}\right)^3 + 3\left(\frac{H}{L}\right)\right] \qquad (5.3)$$

Flexural deformation Component

Shear deformation Component

Similarly for "piers" or walls with top and bottom edges fixed against rotation, " Δ " is given by:

$$\Delta = \frac{1}{Et}\left[\left(\frac{H}{L}\right)^3 + 3\left(\frac{H}{L}\right)\right] \qquad (5.4)$$

Whether flexural deformation governs or shear deformation governs, is dependent on the (*H/L*) ratio. For a given wall, rigidity = (*1/Δ*), therefore, the lesser the deflection, the more rigid the wall. This can be intuitively seen by imagining trying to deflect a wall in its own plane. A higher (*H/L*) ratio will require less force to deflect the wall than a wall with a lower (*H/L*) ratio by the same amount.

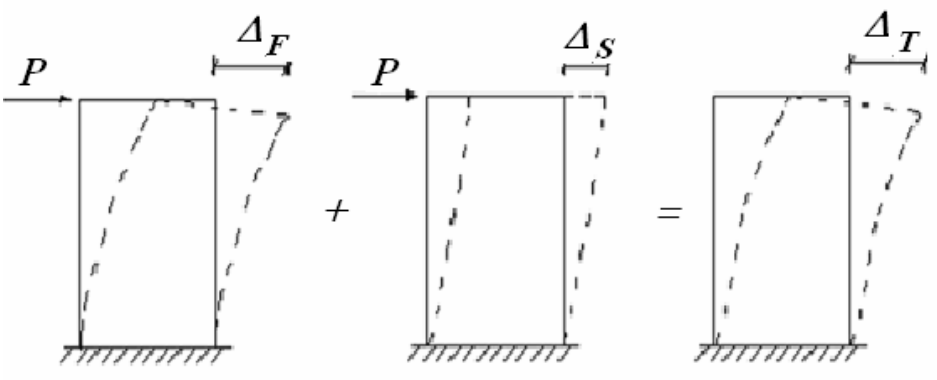

Flexural Deformation + Shear Deformation = Total Deformation

Figure (5.14): Modes of Deformation

Schematically, the modes of deformation are shown in Figure (5.14):

$$\Delta_F + \Delta_S = \Delta_T \tag{5.5}$$

where; Δ_F is the flexural deformation.

Δ_S is the shear deformation.

Δ_T is the total deformation.

As shown in Table [5.1], even for short walls, i.e. $H/L \approx 1.0$, flexural deformation is 57% of the total deflection, whereas with H/L ratio of 2.5, which is not uncommon in 2-3 story buildings, flexural deformation is almost 90% of the total deformation. The purpose of Table [5.1] is to show the deformation multiplier, and this explains why shear walls usually deflect in a flexural mode. Table [5.1] is for cantilever walls; a similar table could be developed for other boundary end conditions.

Table [5.1]: Cantilever Wall Deformation Components

			% of Total "Δ"	
H/L	**4 (H/L)^3**	**3 (H/L)**	**Flexural**	**Shear**
0.25	0.1	0.8	8	92
0.50	0.5	1.5	25	75
1.00	4.0	3.0	57	43
1.50	13.5	4.5	75	25
2.00	32.0	6.0	84	16
2.50	62.5	7.5	89	11
3.00	108.0	9.0	92	8
5.00	500.0	15.0	97	3
8.00	2,048.0	24.0	99	1

Although failure in shear is undesirable as it is considered non-ductile (brittle), the behavior of the wall due to its geometry cannot be changed. A well designed and detailed wall for anticipated shear demand should perform well.

5.5. Comparison of Different-Plan Buildings with (*DS*) System

When a wall-frame structure is loaded laterally, the different free deflected forms of the walls and the frame cause them to interact horizontally through the floor slabs.

The potential advantages of a wall-frame structure depend on the amount of horizontal interaction, which is governed by the relative stiffness of the walls and frames, and the height of the structure. The taller the building and, in typically, proportionate structures as in the study-case models, the stiffer the frames, the greater the interaction.

The principal advantages of accounting for the horizontal interaction in designing a wall-frame structure are as follows:

(1) The estimated drift may be significantly less than if the walls alone were considered to resist the horizontal loading. This was demonstrated clearly in the case-study buildings discussed in Chapter Four.

(2) The estimated bending moments in the walls or cores will be less than if they were considered to act alone.

(3) The columns of the frames may be designed as fully braced.

Figure (5.15) shows frame-shear wall *(DS)* systems for the different building layouts. Also the stiffness for each system in the X-direction has been calculated and plotted as shown in Figures (5.16).

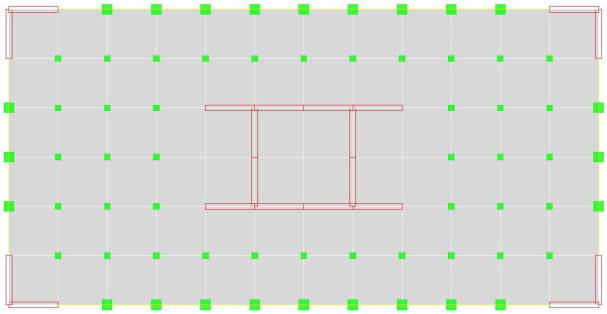

(a) Rectangular Building

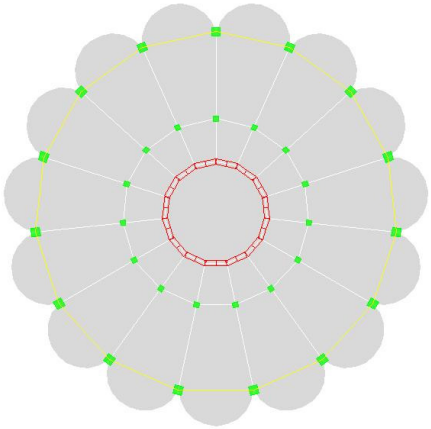

(b) Marina Tower

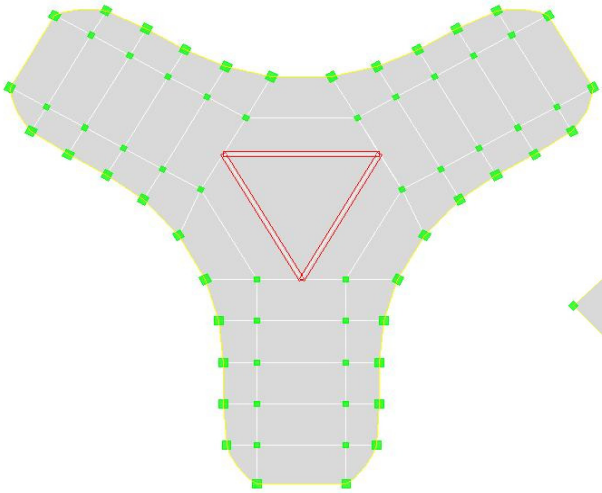

(c) Lake Point Tower

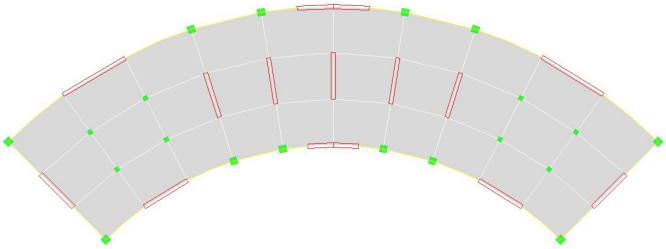

(d) Toronto Tower

Figure (5.15): Frame-Shear Wall (DS) System for Different-Plan Buildings

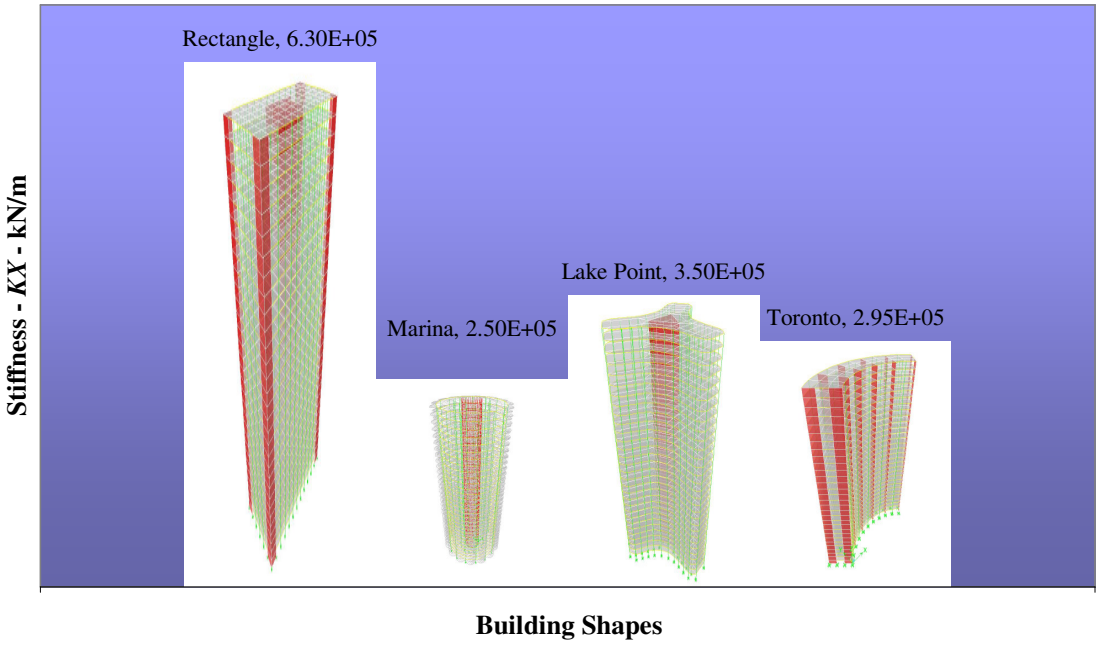

Figure (5.16): Stiffness Comparison for Different Shapes with Frame-Wall System

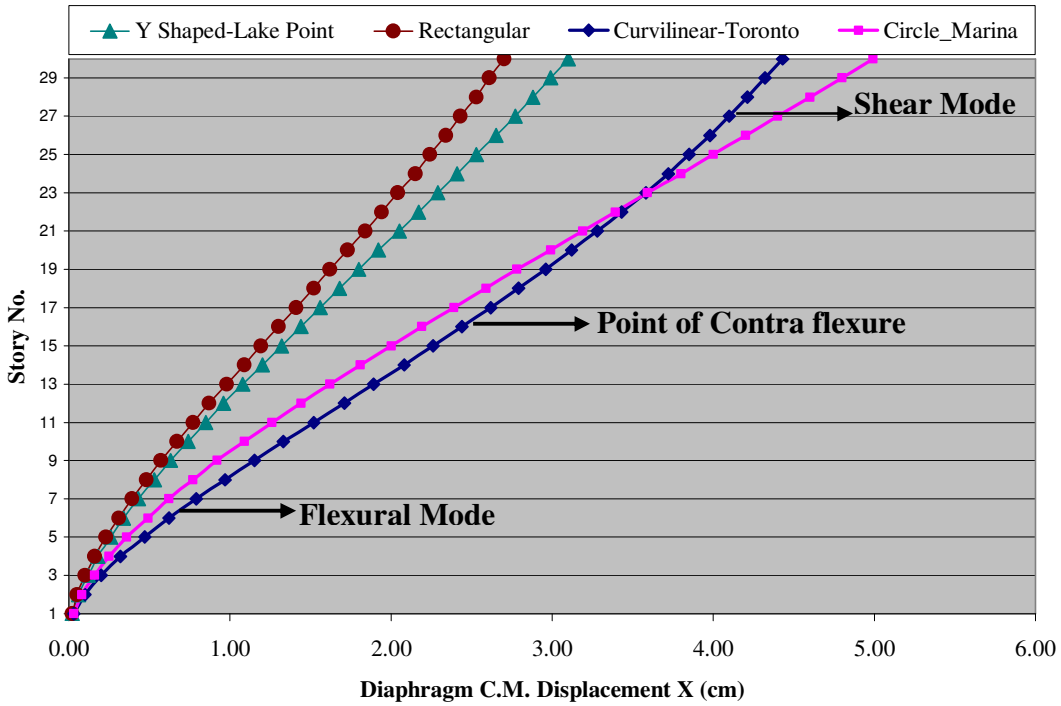

Figure (5.17): Diaphragm *C.M.* Displacement X Due to EX for Different *DS* System

Figures (5.16) and (5.17) show that the stiffer the system the less displacement can be achieved. When the wall and frame are combined together in the presence of horizontal loading, the deflected shape of the composite structure has a flexural profile in the lower part and a shear profile in the upper part as shown in Figure (5.17).

The interaction force between the two systems could be increased simply by increasing the shear rigidity (GA) of the frame where, A: cross-sectional area, G: shear modulus.

Increasing shear rigidity could be achieved in practice by increasing the inertias of the beams and columns in the story of the frame adjacent to the top of wall. Particular attention must be given to designing the frames, and members connecting the wall to the frames, due to the locally high forces associated with the interaction.

5.6. Building Interaction Factors: Graphical Summary

The building configuration and geometry properties can be defined as the size, shape and proportions of the three-dimensional form of the building as well as the type of structural elements and their locations as shown in Figure (5.18).

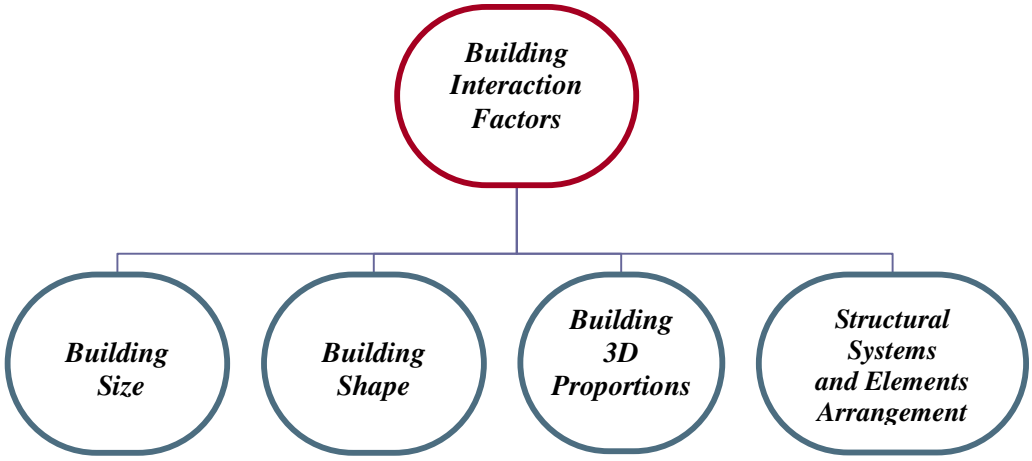

Figure (5.18): Building Interaction Factors

As stated before, it is inherently embedded that a number of structural systems are more suited for some building shapes than for other shapes. Therefore, the overall stiffness of the building and the building structural system are directly related because it is known that stiffness is a function of structural system, while stiffness and building plan shape have indirect relation, refer to Figure (5.19).

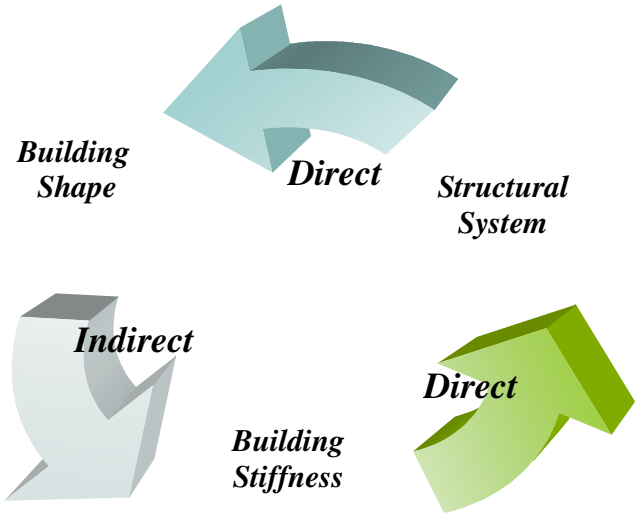

Figure (5.19): The Relationship between Building Shape, Structural System, and Building Stiffness

CHAPTER SIX

CONCLUSIONS AND RECOMMENDATIONS

6.1. Summary

This study aims to urge the structural engineer to produce creative and original design, also to have a better understanding for the manner in which a structure responds to load. That means to acquire a comprehensive knowledge in the way which the structure deflects under given load combinations. Besides, to have a sense and an order of magnitude of internal forces using different structural configurations and different plan geometries.

This study focuses on the behavior of concrete structures; specifically the behavior of tall concrete structures under the presence of seismic loading. Four building shapes have been chosen for this study, these plans are:

(1) Rectangular building proposed as a hypothetical model.

(2) Marina City, a twin tower in Chicago, USA.

(3) Lake Point Tower, an existing building in Chicago, USA.

(4) Toronto City Hall, is an existing structure composed of two curved buildings in Toronto, Canada.

Each shape has been examined using three different systems: a frame system, a shear wall system and a dual system.

Analysis has been carried out by modeling a three dimensional structure for each case with the assistance of ETABS software (Extended three dimensional analysis of building systems).The models have been subjected to gravity and lateral loads. The seismic

loads have been calculated using the International Building Code (IBC-2003) approach. Inelastic dynamic analysis have been performed using ETABS.

6.2. Recommended Structural Systems

In general, good seismic design is achieved through simplicity in structural systems and structural forms. Some building configurations that perform well when resisting earthquake loading include the following aspects:

(1) Simple plan layouts: structures with square or circular shapes are preferred.

(2) Compact shapes: structures with long extended wings should be avoided.

(3) Symmetrical layouts with large torsional resistance are preferred.

(4) Systems with vertical uniformity and continuity are preferred. Structures with sudden changes in mass and stiffness should be avoided.

(5) Systems with low slenderness ratio are preferred.

(6) Systems with diaphragm continuity are also preferred.

6.3. Conclusions

On the basis of this study the following conclusions may be drawn:

- It is apparent from the study cases that the overall deflected shape of a rigid frame structure has a shear configuration mode with a maximum slope at the top and minimum at the bottom. In comparison, shear wall system behaves in a distinct flexural mode with a maximum slope at the bottom and minimum at the top.
- Frame-shear wall system has a flexural profile in the lower part and a shear profile in the upper part. This causes the walls to push back the frames near the base and the frames to pull back the walls at the top.
- It is inherently embedded that a number of structural systems are better suited for a

specific building plans or shapes. Thus, in a way, a given building plan dictates a few particular structural systems, which also indicates that the overall stiffness of the building, a function of the structural system, is indirectly related to the building plan.

- The building configuration and geometry properties can be defined as the size, shape and proportions of the three-dimensional form of the building as well as the type of structural elements and their locations.
- Support conditions for the vertical elements have a significant influence on drift, displacement, and values of forces, particularly in the lower stories.
- The maximum drift and displacement values for a frame system may exceed two times the other systems.
- The more horizontal interaction exists between frame and wall in dual system, the more efficient the system is in providing a sense of human comfort during seismic motion by reducing the values of drift and displacement.
- The principal advantages of accounting for the horizontal interaction in designing a wall-frame structure is that the estimated drift may be significantly less than if the walls alone were considered to resist the horizontal loading. The estimated bending moments in the walls or cores will be also less than if they were considered to act alone. This was demonstrated clearly in the study cases.
- What is very important to remember is that displacement curves can serve as a good indication of structural behavior under lateral loads and also provide a clear vision about structural system performance and efficiency.

- It has to be noted that it is not merely the stiffness of building in one direction which contributes to the overall behavior of high-rise building under seismic loads, but it is the ratio of the overall stiffness in the two directions that makes the difference.
- The fundamental period of vibration is a good indication of its structural stiffness. Also, first mode of vibration tends to deflect in the least stiffness direction.
- The more flexible the structure is, the less ground acceleration is absorbed by the structure, which in turn decreases the base shear force. This reduction in forces happens at the expense of increasing the displacement values. However, the structure can survive earthquake excitation as long as the maximum displacement demand doesn't reach the ultimate displacement capacity of the structure. Therefore, such displacements impose additional structural requirements in term of ductility and energy dissipation.
- Shear wall cores are efficient structural systems for tall buildings that provide stiffness and stability against lateral loads. This influence can be observed when tracking the reduction in stiffness and subsequent increase in displacement in one of the study cases, when the shear wall was replaced entirely by a frame system.
- The structural designer should understand thoroughly the importance of arranging and locating the vertical elements in any structure during the design phase, taking into consideration the location of both center of mass and center of rigidity to minimize torsion as much as possible because torsion has proven to be a major cause of distress and failure in tall buildings.
- The more slender a building, the worse the overturning effects of an earthquake and the greater the earthquake stresses in the outer columns.

- It has been shown that as the building becomes more symmetrical; its tendency to suffer torsion and stress concentration will reduce providing better performance under seismic forces. The effects of symmetry refer not only to the overall building shape, but also to structural layout plan. It is possible to have a building which is geometrically symmetrical in exterior form, but highly asymmetrical in the arrangement of its structural systems.
- Some building shapes have inherent stiffness in their geometrical form. They provide higher structural efficiency or allow greater building height at a low cost. For example, cylindrical building similar to Marina Tower provides true tubular geometry and true three-dimensional response to lateral loading.

REFERENCES

Arbabian, H., (2000). **The Role of Architects in Seismic Design**. International Conference on the Seismic Performance of Traditional Buildings, Istanbul, Turkey.

Armouti, Nazzal S., (2004). **Earthquake Engineering, Theory and Implementation.** First Edition, Jordan.

Charles H. T, Udom H, Leonard M. J, (1997). **Design of the world's tallest buildings - Petronas Twin Towers at Kuala Lumpur City Centre**. Journal of structural design of tall buildings, 6 (4), 245-263.

Chopra, A. (1995). **Dynamics of Structures, Theory and Applications to Earthquake Engineering.** Prentice Hall International, Inc.

Clough, R.,W., and Penzien, J.,(1995). **Dynamics of Structures**. Third Edition, Computers and Structures, Inc., Berkeley, USA.

Coull, A., and Smith, B., (1991). **Tall Building Structures: Analysis and Design,** Third Edition. John Willy and Sons, Inc., New York.

CSI, Structural Analysis Program, **ETABS Non-Linear Version 9.07**, Computer and Structures, Inc., Berkeley, 2006.

Farzad Naeim, (2001). **The Seismic Design Handbook**, Second Edition, USA. Kluwer Academic Publishers.

Fisher, David (1995).The shape of tall buildings. In: Council on Tall Buildings and Urban Habitat, Cognition, **Structural Systems for Tall Buildings**, (39-70).

International Code Council**, International Building Codes 2000-2003 (IBC 2003)**, Joint UBC, BOCA, SBCCI, Whittier, CA.

International Conference of Building Officials, **Uniform Building Code, (UBC 1997)**, Vol. 2, ICBO, Whittier, CA.

Lindeburg, M., (1996). **Seismic Design of Building Structures**, Seventh Edition, Belmont, CA, Professional Publications.

Mark Fintel, (1974). **Handbook of Concrete Engineering.** Van Nostrand Reinhold, New York,

Mink, Gernot, (2001). **Construction Manual for Earthquake-Resistant Houses Built of Earth.** Gate-Basin (Building Advisory Service and Information Network)

Nilson, Darwin, and Dolan, (2003). **Design of Concrete Structures**. Thirteen Edition, McGraw Hill.

Sev, A., Ozgen, A., (2000). **The Relationship Between Tall Building Configuration and Seismic Behaviour**. Yapi , Magazine of Building and Industry Center, Istanbul.

Thomas C. Kavanagh, Fazlur Khan, Edwin H, Emilio Rosenbueth, (1972), **Tall Building Criteria and Loading**. American Society of Civil Engineers, USA.

Wolfgang Schueller, (1977). **High-Rise Building Structure.** First Edition, John Willy and Sons, Inc., New York, USA.

تأثير شكل المقطع الأفقي والنظام الإنشائي على تصرف المباني العالية

إعداد
مهند يعقوب فاخوري

المشرف
الأستاذ الدكتور رائد محمود السمرة

ملخص

تهدف هذه الدراسة إلى حضّ المهندس الإنشائي على إنتاج تصميم مبدع وأصيل، أيضاً ليحظى بفهم أفضل للطريقة التي يتجاوب بها المنشأ مع الأحمال. هذا يعني اكتساب معرفة شاملة بالطريقة التي يتحرّك بها المنشأ تحت تجميعات أحمال معينة. إضافة إلى هذا، امتلاك حِسّ ونظام قيم تقريبية للقوى الداخلية باستخدام تشكيلات إنشائية مختلفة ومقاطع أفقية مختلفة.

تركز هذه الدراسة على تصرف المنشآت الخرسانية، وبخاصة تصرف المباني الخرسانية العالية بوجود الأحمال الزلزالية. تم اختيار أربعة أشكال من الأبنية في هذه الدراسة، وتم فحص كل من هذه الأشكال باستخدام ثلاثة أنظمة إنشائية مختلفة هي: نظام الهياكل الانشائية، ونظام جدران القص، والنظام الإنشائي المزدوج، بارتفاع كلي مقداره 120م، وارتفاع طابقي مقداره 4م.
أشكال المباني هذه هي: (1) بناية مستطيلة اقتُرحتْ كنموذج إفتراضي. (2) "مارينا سيتي"، وهو منشأ موجود في شيكاغو، الولايات المتحدة الأمريكية. (3) "لاك بوينت تور" في شيكاغو، الولايات المتحدة الأمريكية. (4) "تورنتو سيتي" في تورنتو كندا.

استخلصت أنماط الإزاحة الفعلية وتمت مناقشتها لكل نظام إنشائي بإسهاب. وتُظهر هذه الدراسة أيضاً كيف أن تشكيل وترتيب المقطع الكلي والأفقي للمنشأ يحدد بصورة واسعة الطرق التي تتوزع بها القوى الزلزالية داخل المبنى وأيضاً تؤثر في القيم النسبية لهذه القوى كنتيجة لذلك.

علاوة على هذا، يأخذ هذا البحث بعين الاعتبار قضايا تصميمية أخرى كتأثير اللي لأشكال المقاطع الأفقية المتماثلة وغير المتماثلة، ومنظور الكود لمقاطع المباني غير المنتظمة وبعض الحلول لهذه المشاكل، وقضايا الجساءة وتأثيراتها، ومعايير الإزاحة.

تم عمل التحليل الإنشائي من خلال مباني ثلاثية الأبعاد لكل حالة بواسطة برنامج ETABS (تحليل واسع ثلاثيّ الأبعاد لأنظمة المباني)، وتعريضها لأحمال زلزلية محسوبة بناءاً على كود البناء العالمي 2003. لمثل هذه المباني، تم استخدام التحليل الديناميكي غير المرن.

أظهرت هذه الدراسة بأنّ التصميم الزلزالي الجيد يتحقق من خلال البساطةِ في الأنظمةِ والأشكالِ الإنشائية.

ومِنْ الواضح من حالاتِ الدراسة أن شكلَ الإزاحة العامَّ لنظام الهياكل الإنشائية له شكل إزاحة قصّي ، ولنظام جدران القص له شكل إزاحة منحنٍ، وأما النظام الثنائي فهو مجموع من كلا النمطين. يساعد هذا السلوك التفاعليّ على تخفيض قِيَم الانجرافِ والإزاحةِ.

أظهرت هذه الدراسةِ أيضاً بأنّ منحنيات الإزاحةِ يُمْكِنُ أنْ تخدم كمؤشر جيد للسلوكِ الإنشائي تحت الأحمال الجانبية، وتُزوّدُ أيضاً برؤية أوضح حول الأداءِ وكفاءةِ النظام الإنشائي.

تركّز هذه الدراسة أيضاً على ضرورة أن يفهم المصمّم الإنشائي بعمق أهمية تَرتيب وتَحديد مكان العناصر الإنشائية العموديةِ في أثناء مرحلةِ التصميم.

كما أظهرت هذه الدراسةِ التأثيرَ غير المباشر لشكلِ المبنى على سلوكِ المباني العالية.